Improving the size selectivity of trawl codends for northern shrimp (*Pandalus borealis*) and redfish (*Sebastes* spp.) fisheries in the North Atlantic

by © Zhaohai Cheng

A dissertation submitted to the School of Graduate Studies in partial fulfillment of the requirements for the degree of

Doctor of Philosophy

Environmental Science Programme

Faculty of Science

Memorial University of Newfoundland

May 2020

St. John’s, Newfoundland and Labrador

Abstract

A bottom trawl is a towed fishing gear that is designed to catch commercially important species that live in close proximity to the seafloor. In the Northwest Atlantic, bottom trawls are widely used to harvest shrimp, redfish, and various groundfish species. Coastal fishing fleets in both Canada and Iceland have been using bottom trawls to harvest northern shrimp (*Pandalus borealis*) and redfish (*Sebastes* spp.) for several decades. The codend of these fishing gears plays an important role in reducing unintended bycatch of non-targeted species and sizes of animals. Careful design and engineering of these codends is a necessary step in the fishing gear development cycle.

In this thesis, I conducted different experiments, including laboratory and field work, to improve the size selectivity of codends for northern shrimp and redfish in the North Atlantic. In my first experiment, I compared the performance of different codends on the size selectivity of shrimp in the coastal fishery of Iceland. I compared codends of same nominal mesh size (42 mm) constructed using netting in the traditional orientation (T0, two-panel) against experimental codends constructed using netting rotated 45^{o} (T45, two-panel) and 90^{o} (T90, four-panel). My results revealed that the T90 codend retained significantly less shrimp between 9 and 19 mm carapace length than the T0 codend, and between 15 and 19 mm than the T45 codend. Since discarding of undersized shrimp is prohibited in Iceland, using the T90 codend would enable fishers to use their quotas more efficiently. In my second experiment, I compared the performance of two different codends on the size selectivity of redfish in a commercial fishery off the south coast of Iceland. The codends varied in their design, mesh size (inside-knots measurement), and

construction (i.e., knotted vs. knotless). My results showed that there was no significant difference in size selectivity between the codends at lengths greater than 29 cm for *S. norvegicus* and 19 cm for *S. viviparous*. At smaller lengths, size selectivity was undetermined due to small catches at those sizes. In my third experiment, I compared the performance of four different codends on the size selectivity of redfish in eastern Canada (Unit 1, Gulf of St. Lawrence). I evaluated a traditional diamond mesh codend with a nominal mesh size of 90 mm and three experimental T90 codends of different nominal mesh sizes (90, 100, 110 mm). My results demonstrated that the traditional codend was not size selective, catching greater than 97% of redfish over all of the length classes observed. Overall, my results reveal that T90 codends improve size selectivity in which large proportions of undersized fish are successfully released. In my final experiment, I examined the hydrodynamic performance of full-scale T0 and T90 codends with and without a cover net using the flume tank located at the Fisheries and Marine Institute. I measured flow velocity, mesh shape, mesh opening, and drag at various towing velocities. The results showed that the flow velocity inside each codend was lower than the towing velocity. T90 codends had higher flow velocity and better mesh opening than the T0 near the terminal end of the codend. The total drag of each T90 codend was significantly higher than the T0. With the cover net, the flow velocity in the area between codend and the cover did not change significantly for the T0 codend, but was significantly different for the T90 (90 mm) codend.

In summary, the findings from this thesis confirm the importance of codend design on the size selectivity of bottom trawls. Changes in mesh size and mesh orientation in particular, were shown to significantly affect the size selectivity of northern shrimp (Iceland) and redfish (Iceland and Canada). These results could prove helpful in the pursuit of sustainable fisheries, whereby smaller undesirable or non-targeted animals can be released from codends during towing operations, preventing their unnecessary capture and mortality.

Acknowledgments

Firstly, I would like to express my sincere gratitude to my supervisor Dr. Paul Winger for the consistent encouragement, valuable guidance and scholarly inputs throughout my research. I appreciate all his contributions of time, ideas, and funding to make my PhD experience productive and stimulating. I could not have imagined having a better supervisor for my PhD study. I am also grateful to my co-supervisor Dr. Shannon Bayse for his academic support, insightful comments and inspiring discussion, but also for the hard questions which encouraged me to improve my research. I would like to thank the rest of my supervisor committee: Dr. Scott Grant and Dr. Pingguo He for their great support and invaluable advice that widened my research from various perspectives.

My sincere thanks also go to Haraldur Arnar Einarsson at the Marine and Freshwater Research Institute of Iceland, who provided me opportunities to conduct sea trials in Iceland as well as access to research data. I am grateful to Bent Herrmann, Stephen Walsh, and Michael Pol for reviewing my manuscripts, providing valuable suggestions for the tank testing and sea trials, and for support in statistical data analysis.

I thank the many staff at the Centre for Sustainable Aquatic Resources (CSAR), including Harold DeLouche, Craig Hollett, George Legge, Mark Santos, Meghan Donovan, Roy Gibbons, and Kelly Moret for their unconditional help during the flume tank and comparative fishing experiments. Special thanks to Harold who taught me so much about fishing gear and helped me carry out the flume tank testing. Also I thank my fellow lab-mates Tomás Araya-Schmidt, Gebremeskel Kebede, Vang Nguyen, Maggie Folkins, Jessica Wood, and Khanh Nguyen. Thank you very much to all the staff and students at CSAR whom I had the pleasure of working with.

Thanks are also due to the Ocean Frontier Institute (Sustainable Fisheries Theme, Module H), Research and Development Corporation (RDC) of Newfoundland and Labrador (Ocean Industries Student Research Awards), Marine and Freshwater Research Institute of Iceland, Fisheries and Oceans Canada (DFO), and the Fish Food & Allied Workers Union (FFAW) for their financial support and cooperation at various phases of my PhD research.

I am grateful to my industrial collaborators Hampidjan Canada Ltd. and Hampidjan Iceland for their technical support and for providing me with great opportunities to test various fishing gears. I also wish to extend my gratitude to vessel crews of the *F/V Lisa M, Helga Maria AK-16, Bjarni Sæmundsson RE-30* and *Guðbjörg Sigurðardóttir ÍS-508* for their professional assistance during the comparative fishing experiments at sea.

Finally, I would like to express my deepest gratitude to my family and friends. This thesis would not have been possible without their warm love, continued patience, and endless support.

Table of Contents

List of Tables

List of Figures

CHAPTER 1. Introduction

1.1 Life History and Ecology of Northern Shrimp and Redfish

Pandalus is a genus of cold-water shrimp with more than 20 species around the world (Komai, 1999). One of the species, *Pandalus borealis*, known as northern shrimp, is distributed throughout the northern waters of the Atlantic, Pacific, and Arctic Oceans (Holthuis, 1980). In the North Atlantic Ocean, this species can be found from northern Europe in the eastern Atlantic, and in the western Atlantic from Greenland to about 40° (N) (Squires, 1990). The distribution of northern shrimp in the northern hemisphere is shown in Figure 1.1. Northern shrimp mainly occupy soft and muddy seafloor habitats. They can be found at depths from 20 to 1,330 m, thriving in low water temperatures between 2 to 6 ^{o}C (Holthuis, 1980). Northern shrimp have a life history known as protandrous hermaphroditism (Bergström, 1992). Individuals begin as males and then change to females at about 4 to 7 years of age. They can grow to a total length of 15 cm and live for more than eight years (Shumway et al., 1985). The gender can be detected by the shape of the inner flap of the first pair of swimmers (Shumway et al., 1985). They migrate horizontally and vertically for spawning or in search of small pelagic crustaceans or krill.

The species plays an important role in ocean ecology. It is a major food source for Atlantic cod (*Gadus morhua*), silver hake (*Merluccius bilinearis*), redfish (*Sebastes* spp.) and Atlantic halibut (*Hippoglossus hippoglossus*) (Shumway et al., 1985). While other lesser known species of shrimp exist in the North Atlantic, northern shrimp is by far the dominant species with commercial exploitation by several countries (DFO, 2018).

The redfish, genus *Sebastes*, is the largest genus in the family *Scorpaenidae* with more than 100 species worldwide (Nelson et al., 2016). Four species inhabit in the North Atlantic Ocean, *Sebastes fasciatus* (Acadian redfish), *S. norvegicus* (golden redfish), *S. mentella* (deepwater redfish) and *S. viviparus* (Norway redfish) (Scott and Scott, 1988; Froese and Pauly, 2017). *S. norvegicus*, *S. viviparus*, and *S. mentella* are present in Icelandic waters while *S. norvegicus*, *S. fasciatus,* and *S. mentella* are found along the east coast of Canada (Scott and Scott, 1988). Figure 1.2 shows the distribution of *S. fasciatus* and *S. mentella* in the Northwest Atlantic.

Redfish in the Northwest Atlantic are typically slow growing and long-lived (DFO, 2016). On average, it takes redfish (*S. fasciatus* and *S. mentella*) 6 to 8 years to reach the size of sexual maturity (approx. 22 cm) (DFO, 2016). Both species are ovoviviparous: fertilization is internal, and the eggs develop into larvae within the female body (Pikanowski, 1999). Their distribution throughout the water depth varies by species, but are most common in areas deeper than 100 m. Redfish routinely swim off the bottom to prey at night with no obvious horizontal migration known (Pikanowski, 1999). Adult redfish feed on small crustaceans as well as other bathypelagic fish and young redfish. They are known to prey on Atlantic cod (*Gadus morhua*), pollock (*Pollachius virens*), wolffish (*Anarhichas lupus*), and Greenland halibut (*Reinhardtius hippoglossoides*) (Pikanowski, 1999).

The different species of redfish are difficult to differentiate due to their similar morphological characteristics (Pampoulie and Daníelsdóttir, 2008; Christensen et al., 2018). Methods to differentiate these species exist, however most of the approaches at the present time require skilled technicians and/or analytical laboratory techniques (Misra and Ni, 1983; Kenchington, 1986; Pampoulie and Daníelsdóttir, 2008). In many cases, redfish fisheries are simply managed as a mixed stock complex called "redfish" without precise knowledge on the exploitation rate for specific species (Scott and Scott, 1988).

1.2 Iceland's Northern Shrimp Fishery

Northern shrimp is an important commercial fishery species of the North Atlantic (Holthuis, 1980). It is the most important crustacean species commercially harvested in Iceland (ISF, 2018). The shrimp fishery includes inshore and offshore components with regard to fishing grounds (ISF, 2018). Inshore fishing started in 1924, was commercialized in 1935, and then expanded around the periphery of Iceland (Garcia, 2007). The inshore landings were between 2500 and 7800 t from 1969 to 1984, increasing to approximately 12,000 t in 1996 (Skúladóttir and Sigurjónsson, 2003). The inshore landings decreased and fluctuated around 2,500 t between 2010 and 2013 (SFP, 2016). The offshore shrimp fishery started in the mid-1970s, and by the end of the 1990s catches reached nearly 70,000 t. Over the subsequent decade, the offshore shrimp landings declined dramatically, and then fluctuated around 5,000-7,000 t from 2010 to 2015 (SFP, 2019).

The northern shrimp fishery in Iceland is managed by the Ministry of Fisheries and Agriculture (MFA). The Marine and Freshwater Research Institute (MFRI) of Iceland conducts resource assessments and provides management advice to the MFA. Management regulations for the inshore and offshore shrimp fisheries include limited entry (i.e., licenses), mandatory logbooks of catches, minimum landing size (MLS) of carapace length (CL), CL>15 mm for the inshore and CL>13 mm for the offshore fishery, a quota system based on Total Allowable Catch (TAC), and individual transferable quota (ITQ). The minimum mesh size (inside-knots measurement) of codends are 36 mm and 45 mm for the inshore and offshore fisheries, respectively. Discarding of small shrimps is prohibited. If 30% or more of the catch (by number) is under the MLS, the fishing area is closed. The use of sorting grids for excluding bycatch is mandatory in the offshore shrimp fishery but voluntary in the inshore fishery (MFRI, 2018a,b).

Like most of the world's shrimp fisheries, bycatch can be a concern in Iceland's shrimp fisheries due to the use of small-mesh codends. Bycatch refers to the capture of non-targeted species or undersized of targeted species whether disposed of or retained (Alverson et al., 1994; Kelleher, 2005). The bottom trawl (Figure 1.3) is the main fishing gear used to catch northern shrimp in the North Atlantic Ocean, and is often associated with high amounts of bycatch (Howell and Langan, 1992). The capture and disposal of this bycatch increases the fishery-induced mortality of these species and should be avoided as a conservation measure to promote fishery sustainability (Harrington et al., 2005). Although management measures discussed above have been implemented to help address the problem, further research to improve the size selectivity of bottom trawls for northern shrimp, in particular reducing the capture of undersized shrimp, has been encouraged (H. Einarsson, pers. comm.).

1.3 Redfish Fisheries in Iceland and Canada

Large amounts of redfish were found by steam trawlers in the North Atlantic in the 1920s (George et al., 1972). Compared with species such as Atlantic cod (*Gadus morhua*), haddock (*Melanogrammus aeglefinus*), and herring (*Clupea harengus*), there was little demand for redfish which were caught as bycatch and discarded (George et al., 1972). However, when freezing techniques were improved in the 1930s, American and German trawlers began to land redfish in the North Atlantic (George et al., 1972). Redfish fishing began in the Gulf of Maine and moved eastward to the banks off Nova Scotia, the Gulf of St. Lawrence, and the Grand Bank (George et al., 1972; Goetting, 2008). Atlantic Canadian provinces entered into the redfish fishery since its beginning. Newfoundland and Labrador and Nova Scotia became the major provinces harvesting redfish due to their locational advantage (George et al., 1972).

In Icelandic waters, *S. norvegicus* and *S. mentella* are important commercial species while *S. viviparus* is generally regarded as bycatch due to its small size (MFRI, 2018c,d). Redfish can be captured with longlines, Danish seine nets, gillnets, handlines, and bottom trawls. Bottom trawls are the predominant fishing gear for the commercial fishery (ICES, 2017). The total catch by Icelandic vessels from all fishing areas was around 60,000 t in 1979, growing to above 120,000 t in 1996. After that, the catch gradually decreased to 60,000 t in 2009 and has fluctuated around 60,000 t every year since 2010 (Statistics Iceland, 2018).

The Iceland redfish fishery is under the management of MFA based on scientific advice by the MFRI (Marchal et al., 2016). Fishery management measures include time/area closures, quotas, annual TAC, and ITQ. There is no MLS for golden redfish in some fishing areas of Iceland, however the minimum reference size (MRS) is 33 cm. If more than 20% of catch is below the MRS, the fishing area is closed. Discarding is prohibited. The legal minimum mesh size of trawl codends using traditional diamond netting is 135 mm (Ciccia et al., 2015). The bycatch of undersized redfish can be problematic for fishers that cannot discard the small fish. Catch of juvenile redfish harms the population sustainability considering the slow growing and late maturing nature of the species. Additionally, when the relatively small *S. viviparous* (rarely > 30 cm) are present together with the larger or targeted species, it can lead to further bycatch. Improving the size selectivity of Icelandic trawls is necessary to prevent the capture of small redfish.

In Newfoundland and Labrador (NL), the redfish fishery started in the early 1950s and was characterized by three periods of high exploitation (DFO, 2016). The first peak was in the middle of 1950s, with a record landing of 50,000 t in 1955. Annual landings reached an average of 46,000 t from 1960 to 1969, and this figure increased to 82,000 t between 1970 and 1976. From 1977 to 1994, the average annual landings decreased to 37,000 t (DFO, 2016). The fishery was closed in 1995 due to low stock abundance and lack of recruitment. After the fishery was closed, an index fishery began in 1998 with a total allowable catch (TAC) of 2,000 t/year. An experimental fishery was also recently established with an additional TAC of 2,500 t for 2018-2019 and 3,950 t for 2019-2020. Both fisheries have resulted in annual landings of less than 1,000 t/year to date (DFO, 2020).

The commercial redfish species in NL waters are *S. mentella* and *S. fasciatus*. These two species are managed as one single stock under the management of Fisheries and Oceans Canada (DFO, 2016). Besides TAC, the development and management of a sustainable redfish fishery involves a combination of measures, such as dockside monitoring, gear specifications, time/area closures, and protection of spawning and nursery areas (DFO, 2016). Fishing practices are monitored through dockside monitoring, radio reports (i.e., hailing) upon arrival/departure of the vessel, and onboard observers. The minimum codend mesh size is 90 mm. The MLS is 22 cm, although most processors prefer fish >25 cm around NL waters. Fishing is prohibited outside the area between longitudes 59° and 65° (W) and is closed in the fall and spring seasons to protect redfish mating and larval extrusion (DFO, 2016; Brassard et al., 2017).

According to the most recent stock assessment for Unit 1 and 2, the stock prospect is positive for the Gulf of St Lawrence (DFO, 2020). The population of juvenile redfish is dominated by *S. mentella* and have been increasing since 2013. The 2011 cohort of *S. mentella* has contributed significantly to the current population in the Gulf of St Lawrence. The modal size is currently 23 cm and if anticipated growth continues, 62% of the biomass should be larger than 25 cm by 2020 (DFO, 2020). For the healthy exploitation of this redfish resource, it is essential to protect the juvenile individuals for the next several years. Minimizing the bycatch of juveniles and improving the size selection properties of the fishing gears is important for the sustainability of this fishery.

1.4 Selectivity in Northern Shrimp and Redfish Fisheries

Several studies have documented the benefits of mechanical sorting devices (e.g., grids) inside trawls as method to reduce non-targeted bycatch (e.g., Isaksen et al., 1992; He and Balzano, 2007; Aydın and Tosunoğlu, 2012; Larsen et al., 2018). However, the use of a grid is not mandatory in Iceland's inshore shrimp fisheries (Mamie et al., 2008). The grid was often found to be clogged with seaweeds causing substantial loss of marketable shrimp and was less effective when the catch rate was high (>1 ton/10 min) which was common in the fjord fishing areas (ICES, 2017). Thus, in the absence of a sorting grid, other alternative methods must be found to decrease bycatch and improve size selectivity (e.g., Ingólfsson and Jørgensen, 2019).

The selectivity of a trawl can be improved by various modifications to the trawl (Wileman et al., 1996), especially the codend. Changing the mesh size, twine size, or mesh orientation of a codend can improve the selectivity (e.g., He, 2007; Herrmann et al., 2013; Pol et al., 2016). One of the simplest and most convenient ways is to change the orientation of the mesh. Traditional codends are typically made using diamond mesh (mesh in standard net orientation, T0) while the square-mesh codend (T45) is constructed using standard diamond netting turned 45° (Robertson and Stewart, 1988). Research conducted in Iceland and Canada reported significant decreases in the bycatch of undersized shrimp (Thorsteinsson, 1992). Deval et al. (2009) compared the size selectivity of T45 and T0 codends made of different netting material and found that the T0 codend had poor size selectivity for deepwater crustaceans including several shrimp species. The authors reported that using the T45 codend with appropriate mesh size could improve the selectivity. A similar finding was reported by Sala et al. (2008), who documented that changing mesh orientation from T0 to T45 improved the size selectivity for deepwater rose shrimp (*P. longirostris*) and several other species, and the catch of immature and small individuals was reduced. A study by Thorsteinsson (1992) showed codends made from T45 netting reduced the catch of small individuals and improved the size selectivity in Icelandic shrimp fisheries compared with T0 codends. T45 codends have also been reported to improve selectivity for many fish species, especially the roundfish (e.g. Campos and Fonseca, 2003; Broadhurst et al., 2004; Kaykaç et al., 2009; Sala et al., 2015).

Compared with T0 codends, the netting of T90 codends is turned 90° (Moderhak, 1997). Recent experiments have shown that T90 codends have the potential to improve size selectivity properties compared with a T0 codend made of similar netting (Herrmann et al., 2013; Tokaç et al., 2014; Deval et al., 2016; Sola and Maynou, 2018). An experiment reported by Deval et al. (2016) indicated that changing the codends from traditional T0 to T90 significantly increased size selectivity for four commercial shrimp species. The mesh of T0 codend tends to close under tension while T45 or T90 allows the mesh to remain open (Herrmann et al., 2007; Madsen et al., 2012). The open meshes increase the opportunity for escape and are effective at improving the size selectivity for several roundfish species (e.g., Wienbeck et al., 2014; Tokaç et al., 2014; Bayse et al., 2016). It is speculated that T45 or T90 codends may be effective at reducing bycatch and improving size selectivity in northern shrimp or redfish fisheries in the North Atlantic Ocean.

Knotless codends have also been tested as a means to reduce the capture of undersized fish below minimum landing sizes (Bohl, 1961). Bohl (1961) compared a 122 mm knotless codend and several knotted codends in the East Greenland redfish fishery and found that knotless codends had a narrower selection range than knotted codends. Compared to traditional knotted netting, knotless netting may have better mesh shape and opening. It is possible that undersized fish escape easier from knotless codends compared to knotted codends. Fish escaping through knotted netting may also suffer from abrasion or damage due to contact with knots, which decreases the survival rate (see Coles and Butterworth, 1976). The use of knotless netting has not been tested for redfish in Icelandic waters and could prove effective at improving selectivity of bottom trawls in the region.

Studies on redfish size selectivity were recently reviewed by Herrmann et al. (2012). Icelandic and Greenland redfish fisheries have had mesh selectivity studies dating as far back as the 1960s (Bohl, 1961). Research conducted in Iceland during 1972-1976 were reviewed by Thorsteinsson et al. (1980) in which the selective characteristics of T0 codends for redfish was described. See Table 1.1 for a complete list of all redfish size selectivity studies. The selectivity of T0 codends with and without shortened lastridge ropes was compared in the Newfoundland redfish fishery (Hickey et al., 1995) and the results showed that codends with shortened lastridge ropes reduced the capture of small redfish. According to Lisovsky et al. (2005), the size selectivity in redfish fishery can be affected by the mesh size; decreasing the mesh size from 130 mm to 90-100 mm was recommended. Most recently, Pol et al. (2016) compared the size selectivity of three T0 codends with different mesh sizes for redfish (*S. fasciatus*) in the Gulf of Maine. The authors reported lengths at 50% capture (L_{50}) of 22.3 cm, 29.2 cm, and 33.6 cm for nominal mesh sizes of 114 mm, 139 mm, and 165 mm, respectively. Despite the aforementioned studies, the size selectivity of redfish has not been evaluated using T90 codends. Application of T90 codends in the redfish fishery of eastern Canada may improve the size selectivity, reducing the bycatch of undersized fish.

1.5 Objectives of the Research

This thesis aims to improve the size selectivity of trawl codends used in northern shrimp and redfish fisheries in North Atlantic waters. The research areas include Iceland's northern shrimp and redfish fishing grounds, and Canada's redfish fishing grounds in the Gulf of St. Lawrence. It is intended that the research findings will contribute to the development and application of selective fishing techniques and the development of management measures to reduce bycatch in these fisheries. The research also intends to explore how net design affects the hydrodynamic performance of the codends and to explain the selection properties in relation to the performance.

1.6 Chapter Outline

This thesis is comprised of six chapters:

Chapter 1 provides an introduction and overview of the thesis, including the life history and ecology of northern shrimp and redfish, an introduction to Iceland's northern shrimp fishery, an introduction to the redfish fisheries in Iceland and Canada, and finally a review of previous size selectivity research for shrimp and redfish.

Chapter 2 describes an experiment at sea to evaluate the size selectivity of traditional and experimental codends used in Iceland's northern shrimp fishery.

Chapter 3 describes an experiment at sea to evaluate the size selectivity of traditional and experimental codends in Iceland's redfish fishery.

Chapter 4 describes an experiment at sea to evaluate and compare the size selection properties of traditional and experimental codends for redfish in the Gulf of St. Lawrence, Canada.

Chapter 5 describes a laboratory-based flume-tank experiment to evaluate the hydrodynamic performance (mesh opening, flow velocity and drag) of T0 and T90 codends (tested in Chapter 4) with and without a codend cover.

Chapter 6 is the final chapter of the thesis. It synthesizes the main conclusions of the experiments and discusses the limitations of the research. Recommendations to improve the size selectivity of bottom trawls and fishery sustainability in the future are discussed.

1.7 Co-Authorship Statement

I am the major intellectual contributor and principal author of all chapters presented in this thesis. I contributed to all practical aspects of the research, including design of the experiments, data collection and analysis, interpretation of results, and subsequent manuscript preparation. However, my studies could not have been completed without the excellent supervision and invaluable guidance of my supervisor Dr. Paul Winger, great support and direction from the supervisory committee members (Dr. Shannon Bayse, Dr. Scott Grant, Dr. Pingguo He), and the collaborative contribution of many individuals, especially Dr. Haraldur Einarsson. I prepared and revised the manuscripts based on the advice and comments from my co-authors. Their contribution and involvement are recognized here.

Chief collaborators for Chapter 2 were Haraldur Einarsson, Shannon Bayse, Bent Herrmann and Paul Winger. Dr. Haraldur Einarsson designed the field work, gathered the data, and provided editorial reviews of the manuscript. Dr. Shannon Bayse provided support during data analysis and editorial reviews of the manuscript. Dr. Bent Herrmann contributed to the software and editing the manuscript. Dr. Paul Winger provided financial support and comprehensive editorial reviews of the manuscript.

Chief collaborators for Chapter 3 were Haraldur Einarsson, Shannon Bayse, Bent Herrmann and Paul Winger. Dr. Haraldur Einarsson contributed to the research proposal, planned the study, gathered the data and provided reviews of the manuscript. Dr. Shannon Bayse contributed to the data analysis, interpretation of results, and editorial reviews of the manuscript. Dr. Bent Herrmann contributed to statistical methods and editing of the manuscript. Dr. Paul Winger provided comprehensive editorial reviews of the manuscript.

Chief collaborators for Chapter 4 were Paul Winger, Shannon Bayse, Gebremeskel Kebede, Harold DeLouche, Haraldur Einarsson, Michael Pol, David Kelly, and Stephen Walsh. Dr. Paul Winger contributed to the research proposal, the experimental design, field work arrangement, supervision, and advice throughout the study and provided editorial reviews of the manuscript. Dr. Shannon Bayse contributed to the experimental design, field work, supervision, interpretation of results, and editorial reviews of the manuscript. Dr. Gebremeskel Kebede assisted with the field experiment and participated in the design of the study. Harold DeLouche contributed to the design of the experiment. Dr. Haraldur Einarsson contributed to the research proposal and the experimental design, and provided editorial reviews of the manuscript. Dr. Michael Pol assisted with the experimental design and provided editorial reviews of the manuscript. David Kelly assisted with fishing gear design and preparation for the field work. Dr. Stephen Walsh contributed to the research proposal, the experimental design, and provided editorial reviews of the manuscript.

Chief collaborators for Chapter 5 were Paul Winger, Shannon Bayse, Gebremeskel Kebede, and David Kelly. Dr. Paul Winger contributed to the research proposal, experimental design, and provided editorial reviews of the manuscript. Dr. Shannon Bayse contributed to the interpretation of results and editorial reviews of the manuscript. Dr. Gebremeskel Kebede participated in the design of the study and assisted with the laboratory experiment. David Kelly contributed to the experimental design and assisted with fishing gear design.

1.8 Dissemination of Research

Chapter 2 is accepted with revisions to the journal *Aquaculture and Fisheries.* Dr. Haraldur Einarsson and I are the primary authors (equal authorship). Dr. Shannon Bayse, Dr. Bent Herrmann and Dr. Paul Winger are the second, third, fourth, and fifth author, respectively.

Chapter 3 has been published in the journal *Fisheries Research* in 2019 (216: 138-144). Dr. Haraldur Einarsson and I are the primary authors (equal authorship). Dr. Shannon Bayse, Dr. Bent Herrmann and Dr. Paul Winger are the second, third, fourth, and fifth author, respectively.

Chapter 4 has been submitted to the journal *Canadian Journal of Fisheries and Aquatic Sciences*.

Chapter 5 is currently in preparation for submission to the journal *Fisheries Research*.

1.9 References

Alverson, D.L., Freeberg, M.H., Murawski, S.A., Pope, J.G., 1994. A global assessment of fisheries bycatch and discards. FAO Fish. Tech. Pap., 339p.

Aydın, C., Tosunoğlu, Z., 2012. Evaluation of sorting grids for deepwater rose shrimp (*Parapenaeus longirostris*) in the Eastern Mediterranean demersal trawl fishery. J. Appl. Ichthyol., 28, 102-106.

Bayse, S.M., Herrmann, B., Lenoir, H., Depestele, J., Polet, H., Vanderperren, E. Verschueren, B., 2016. Could a T90 mesh codend improve selectivity in the Belgian beam trawl fishery? Fish. Res., 174, 201-209.

Bergström, B.I., 1992. Demography and sex change in pandalid shrimps. PhD thesis. Göteborg University, Faculty of Natural Sciences, Göteborg.

Bohl, H., 1961. German mesh selection experiments on redfish. Coun. Meet. ICES, Comp. Fish. Comm., Doc. Nr., 88, 1991.

Broadhurst, M.K., Millar, R.B., Kennelly, S.J., Macbeth, W.G., Young, D.J., Gray, C.A., 2004. Selectivity of conventional diamond-and novel square-mesh codends in an Australian estuarine penaeid-trawl fishery. Fish. Res., 67, 183-194.

Brassard, C., Bourdages, H., Duplisea, D., Gauthier, J., Valentin, A., 2017. The status of the redfish stocks (*Sebastes fasciatus* and *S. mentella*) in Unit 1 (Gulf of St. Lawrence) in 2015. DFO Can. Sci. Advis. Sec. Res. Doc., 2017/023. 53 p.

Campos, A., Fonseca, P., Henriques, V., 2003. Size selectivity for four fish species of the deep groundfish assemblage off the Portuguese southwest coast: evidence of mesh size, mesh configuration and cod end catch effects. Fish. Res., 63, 213-233.

Christensen, H.T., Rigét, F., Backe, M.B., Saha, A., Johansen, T., Hedeholm, R.B., 2018.

Comparison of three methods for identification of redfish (*Sebastes mentella* and *S. norvegicus*) from the Greenland east coast. Fish. Res., 201, 11-17.

Ciccia, R.V., Assessor Dankert Skagen, L., Geraldine, C.A., 2015. FAO-Based Icelandic Responsible Fisheries Management Redfish Surveillance Report, ICE/RED/001.1/2015. Available from: https://www.responsiblefisheries.is/media/1/fao-irfm-redfish-1st-surveillance-report-june2015-final.pdf

Coles, T.F., Butterworth, A.J., 1976. The use of knotless netting in fisheries research, Fish. Manag., 7, 53-56.

Deval, M.C., Bök, T., Ateş, C., Ulutürk, T., Tosunoğlu, Z., 2009. Comparison of the size selectivity of diamond (PA) and square (PE) mesh codends for deepwater crustacean species in the Antalya Bay, eastern Mediterranean. J. Appl. Ichthyol., 25, 372-380.

Deval, M.C., Özgen, G., Özbilgin, H., 2016. Selectivity of 50 mm T0 and T90 codends for commercial shrimp species in the Turkish deepwater trawl fishery, Eastern Mediterranean. J. Appl. Ichthyol., 32, 1041-1057.

DFO, 2016. Assessment of Redfish Stocks (*Sebastes fasciatus* and *S. mentella*) in Units 1 and 2 in 2015. DFO Can. Sci. Advis. Sec. Sci. Advis. Rep., 2016/047.

DFO, 2018. Northern shrimp and striped shrimp – Shrimp fishing areas 0, 1, 4-7, the Eastern and Western Assessment Zones and North Atlantic Fisheries Organization (NAFO) Division 3M. DFO Can. Sci. Advis. Sec. Sci. Advis. Rep., 2018.

DFO, 2020. Redfish (*Sebastes mentella* and *S. fasciatus*) stocks assessment in Unit 1 in 2019. DFO Can. Sci. Advis. Sec. Sci. Advis. Rep. 2020/000.

Froese, R., Pauly, D., 2017. FishBase. Available from: http://www.fishbase.org/summary/Sebastes-viviparus.html

Garcia, E.G., 2007. The northern shrimp (*Pandalus borealis*) offshore fishery in the Northeast Atlantic. Adv. Mar. Biol., 52, 148-266.

Gascon, D., 2003. Redfish multidisciplinary research zonal program (1995-1998): Final Report. Can. Tech. Rep. Fish. Aquat. Sci., 2462, 139 p.

George F.K., Paul M.E., John D.K., Fred E.L., Henry R.M., Ernest, D.M., 1972. Fishery Facts - Redfish. NMFS Extension Publication, 1972, 18p

Goetting, K., 2008. Is fisheries diversification a sustainable strategy? The case of the Newfoundland redfish fishery. M.Sc. Thesis, Memorial University, St. John's, NL.

Gorchinsky, K.V., Lisovsky, S.F., Sadokhin, M.K., 1993. Selectivity of bottom trawls during the fishery for redfish on the Flemish Cap Bank. NAFO SCR. Doc., 93/100, N2293, 9 p

Harrington, J.M., Myers, R.A., Rosenberg, A.A., 2005. Wasted resources: bycatch and discards in US fisheries. Fish Fish., 6, 350-361

He, P., 2007. Selectivity of large mesh trawl codends in the Gulf of Maine I: Comparison of square and diamond mesh. Fish. Res., 83, 44-59.

He, P., Balzano, V., 2007. Reducing the catch of small shrimps in the Gulf of Maine pink shrimp fishery with a size-sorting grid device. ICES J. Mar. Sci., 64, 1551-1557.

Herrmann, B., Priour, D., Krag, L.A., 2007. Simulation-based study of the combined effect on cod-end size selection for round fish of turning mesh 90 degrees and of reducing the number of meshes in the circumference. Fish. Res., 84, 222-232.

Herrmann, B., Sistiaga, M.B., Nielsen, K.N., Larsen, R.B., 2012. Understanding the size selectivity of redfish (*Sebastes* spp.) in North Atlantic trawl codends. J. Northwest Atl. Fish. Sci., 44, 1-13.

Herrmann, B., Wienbeck, H., Moderhak, W., Stepputtis, D., Krag, L.A., 2013. The influence of twine thickness, twine number and netting orientation on codend selectivity. Fish. Res., 145, 22-36.

Hickey, W.M., Boulos, D.L., Brothers G., 1995. A Study of the influence of lastridge ropes on redfish selectivity in a bottom trawler. Can. Tech. Rep. Fish. Aquat. Sci., 2076: vii+25

Holthuis, L.B., 1980. FAO species catalogue: Vol. 1. Shrimps and prawns of the world. An annotated catalogue of species of interest to fisheries. FAO Fisheries Synopsis, No 125.

Howell, W.H., Langan, R., 1992. Discarding of commercial groundfish species in the Gulf of Maine shrimp fishery. N. Am. J. Fish. Manage., 12, 568-580.

ICES, 2017. Report of the North Western Working Group (NWWG), 27 April - 4 May 2017, Copenhagen, Denmark. ICES CM 2017/ACOM:08. 642 pp.

Ingólfsson, Ó.A., Jørgensen, T., 2019. Shorter trawls improve size selection of northern shrimp. Can. J. Fish. Aquat. Sci., 999, 1-10.

Isaksen, B., Valdemarsen, J.W., Larsen, R.B., Karlsen, L., 1992. Reduction of fish by-catch in shrimp trawl using a rigid separator grid in the aft belly. Fish. Res., 13, 335-352.

ISF, 2018. Initial assessment of the ISF Iceland northern shrimp fishery (inshore and offshore). Icelandic Sustainable Fisheries, Grandagarður, 16, 101 Reykjavík

Kaykaç, H., Tokaç, A., Özbilgin, H., 2009. Selectivity of commercial, larger mesh and square mesh trawl codends for deep water rose shrimp Parapenaeus longirostris (Lucas, 1846) in the Aegean Sea. Sci. Mar., 73, 597-604.

Kelleher, K., 2005. Discards in the World's Marine Fisheries. An Update. FAO Fisheries Technical Paper 470. UN Food and Agriculture Organization, Rome, Italy, 131 pp.

Kenchington, T.J., 1986. Morphological comparison of two Northwest Atlantic redfishes, *Sebastes fasciatus* and *S. mentella*, and techniques for their identification. Can. J. Fish.

Aquat. Sci., 43, 781-787.

Komai, T., 1999. A revision of the genus Pandalus (Crustacea: Decapoda: Caridea: Pandalidae). J. Nat. Hist., 33, 1265-1372.

Larsen, R.B., Herrmann, B., Sistiaga, M., Brinkhof, J., Grimaldo, E., 2018. Bycatch reduction in the Norwegian Deep-water Shrimp (*Pandalus borealis*) fishery with a double grid selection system. Fish. Res., 208, 267-273.

Lisovsky, S.F., Pavlenko, A.A., Vaskov, A.A., 2005. On the minimal trawl codend mesh size in the fishery of redfish species in division 3O of the NAFO regulation area. NAFO SCR Doc, 5, 18p.

Madsen, N., Herrmann, B., Frandsen, R.P., Krag, L.A., 2012. Comparing selectivity of a standard and turned mesh T90 codend during towing and haul-back. Aquat. Living Resour., 25, 231-240.

Mamie, J.C.J., Leone, S., Valtýsson, H.Þ., Ármannsson H., 2008. Stock assessment of shrimp *Pandalus borealis* (KRØYER 1838). United Nations University, Reykjavik. Available at: http://www.unuftp.is/static/fellows/document/josephus08prf.pdf.

Marchal, P., Andersen, J.L., Aranda, M., Fitzpatrick, M., Goti, L., Guyader, O., Haraldsson, G., Hatcher, A., Hegland, T.J., Le Floc'h, P., Macher, C., Malvarosa, L., Maravelias, C.D., Mardle, S., Murillas, A., Nielsen, J.R., Sabatella, R., Smith, A.D.M., Stokes, K., Thoegersen, T., Ulrich, C., 2016. A comparative review of fisheries management experiences in the European Union and in other countries worldwide: Iceland, Australia, and New Zealand. Fish Fish., 17, 803-824.

MFRI, 2018a. Assessment Reports 2018, Offshore northern shrimp. Technical Report. Marine and Freshwater Research Institute, Reykjavik, Iceland.

MFRI, 2018b. Assessment Reports 2018, Shrimp in Ísafjarðardjúp. Technical Report. Marine and Freshwater Research Institute, Reykjavik, Iceland.

MFRI, 2018c. MFRI Assessment Reports 2018 on Golden redfish, Technical Report. Marine and Freshwater Research Institute, Reykjavik, Iceland.

MFRI, 2018d. MFRI Assessment Reports 2018 on Norway redfish, Technical Report. Marine and Freshwater Research Institute, Reykjavik, Iceland.

Misra, R.K., Ni I.H., 1983. Distinguishing beaked redfishes (Deepwater redfish, *Sebastes mentella* and Labrador redfish, *S. fasciatus*) by discriminant analysis (with covariance) and multivariate analysis of covariance. Can. J. Fish. Aquat. Sci., 40, 1507-1511.

Moderhak, W., 1997. Determination of selectivity of cod codends made of netting turned through 90. Bull. Sea Fish. Inst., 140, 1-14.

Montgomerie, M., 2015. Basic Fishing Methods – A comprehensive guide to commercial fishing methods. SeaFish. Available from: http://marine.gov.scot/data/basic-fishing-methods-comprehensive-guide-commercial-fishing-methods-seafish-2015.

Nelson, J.S., Grande, T.C., Wilson, M.V., 2016. Fishes of the World. John Wiley & Sons, NY.

Pampoulie, C., Daníelsdóttir, A.K., 2008. Resolving species identification problems in the genus Sebastes using nuclear genetic markers. Fish. Res., 93, 54-63.

Pikanowski, R.A., 1999. Essential fish habitat source document Redfish, *Sebastes* spp., life history and habitat characteristics. NOAA Technical Memorandum NMFS-NE-132, 19 pp.

Pol, M.V., Herrmann, B., Rillahan, C., He, P., 2016. Impact of codend mesh sizes on selectivity and retention of Acadian redfish Sebastes fasciatus in the Gulf of Maine trawl fishery. Fish. Res., 184, 54-63.

Robertson, J.H.B., Stewart, P.A.M., 1988. A comparison of size selection of haddock and whiting by square and diamond mesh codends. ICES J. Mar. Sci., 44, 148-161.

Sala, A., Lucchetti, A., Piccinetti, C., Ferretti, M., 2008. Size selection by diamond-and square-mesh codends in multi-species Mediterranean demersal trawl fisheries. Fish. Res., 93, 8-21.

Sala, A., Lucchetti, A., Perdichizzi, A., Herrmann, B., Rinelli, P., 2015. Is square-mesh better selective than larger mesh? A perspective on the management for Mediterranean trawl fisheries. Fish. Res., 161, 182-190.

Scott, W.B., Scott, M.G., 1988. Atlantic fishes of Canada. Can. B. Fish. Aquat. Sci, 219, 731 pp.

Shumway, S.E., Perkins, H.C., Schick, D.F., Stickney, A.P., 1985. Synopsis of biological data on the pink shrimp, *Pandalus borealis* Krøyer, 1838. FAO Fisheries Synopsis, 144, 1-47.

Skúladóttir, U., Sigurjónsson, J., 2003. Pandalus stocks in Icelandic waters: biology, exploitation and management. Marine and Freshwater Research Institute, Reykjavik, Iceland. Available from: https://imr.brage.unit.no/imr-xmlui/bitstream/handle/11250/107787/Shrimp-Iceland.pdf?sequence=16&isAllowed=y

SFP, 2016. Northern prawn Icelandic inshore. FishSource profile. In: FishSource. Available from: https://www.fishsource.org/stock_page/109.

SFP, 2019. Northern prawn Icelandic offshore. FishSource profile. In: FishSource. Available from: https://www.fishsource.org/stock_page/1100.

Sola, I., Maynou, F., 2018. Assessment of the relative catch performance of hake, red mullet and striped red mullet in a modified trawl extension with T90 netting. Sci. Mar., 82, 19-26,

Squires, H.J., 1990. Decapod Crustacea of the Atlantic coast of Canada. Can. B. Fish. Aquat. Sci., 221, 532 p.

Statistics Iceland, 2018. Catch of Icelandic vessels from all fishing areas 1945-2016. Available from:

Http://px.hagstofa.is/pxen/pxweb/en/Atvinnuvegir/Atvinnuvegir_sjavarutvegur_aflatolur_fiskveidisvaedi/SJA09005.px.

Thorsteinsson, G., 1980. Icelandic bottom trawl and Danish seine codend selection experiments on cod, haddock, redfish and plaice in 1972–1976. ICES C.M. 1980/B: 3, 14 p

Thorsteinsson, G., 1992. The use of square mesh codends in the Icelandic shrimp (*Pandalus borealis*) fishery. Fish. Res., 13, 255-266.

Tokaç, A., Herrmann, B., Aydın, C., Kaykac, H., Ünlüler, A., Gökçe, G., 2014. Predictive models and comparison of the selectivity of standard (T0) and turned mesh (T90) codends for three species in the Eastern Mediterranean. Fish. Res., 150, 76-88.

Wienbeck, H., Herrmann, B., Feekings, J.P., Stepputtis, D., Moderhak, W., 2014. A comparative analysis of legislated and modified Baltic Sea trawl codends for simultaneously improving the size selection of cod (*Gadus morhua*) and plaice (*Pleuronectes platessa*). Fish. Res., 150, 28-37.

Wileman, D.A., Ferro., R.S.T., Fonteyne, R., Millar, R.B., 1996. Manual of methods of measuring the selectivity of towed fishing gears. ICES Coop. Research Rep., No. 215, 126p.

Table 1.1. Review of redfish (*Sebastes* spp.) codend selectivity research for 1961–2016. MS represents mesh size of codend; L50 = the length of fish that has a 50% probability of being retained after entering the codend; SR = selection range which is the difference in length between the fish that has a 75% probability of retention and that with a 25% probability of retention (Adapted from Herrmann et al., 2012, with additions of more recent publications).

Species	Research area	MS (mm)	L50 (cm)	SR (cm)	Description	Source
S. norvegicus	Greenland	122	35.3	10	Knotless	Bohl, 1961
S. norvegicus	Greenland	131	33.5	14.5	T0	Bohl, 1961
S. norvegicus	Iceland	132	34.4	4.9	T0	Thorsteinsson et al., 1980
S. norvegicus	Greenland	139	37.2	13	T0	Bohl, 1961
S. norvegicus	Greenland	146	41.2	14.5	T0	Bohl, 1961
S. norvegicus	Greenland	147	38.4	15	T0	Bohl, 1961
S. mentella	NAFO 3N	88	24.5	4.4	T0	Lisovsky et al., 1995
S. mentella	NAFO 3N	118	29.4	6.6	T0	Lisovsky et al., 1995
S. mentella	NAFO 3N	132	34.6	9	T0	Lisovsky et al., 1995
S. mentella	NAFO 3Ps	91	27.2	5.9	T0	Hickey et al., 1995
S. mentella	NAFO 3Ps	86	26.9	3.3	T0 with lastridge	Hickey et al., 1995
S. mentella	NAFO 3Ps	108	26.8	6.5	T0	Hickey et al., 1995
S. mentella	NAFO 3Ps	107	32.1	3.3	T0 with lastridge	Hickey et al., 1995
S. mentella	NAFO 3Ps	115	31.5	5	T0	Hickey et al., 1995
S. mentella	NAFO 3Ps	114	32.6	3.9	T0 with lastridge	Hickey et al., 1995
S. mentella	NAFO 3M	126	36	5.6	T0	Gorchinsky el al., 1993
S. mentella	NAFO 3M	137	39.3	4.3	T0	Gorchinsky el al., 1993
S. spp	NAFO 3O	96	26.6	5.4	T0	Lisovsky et al., 2005
S. spp	NAFO 3O	100	26.1	4.1	T0	Lisovsky et al., 2005
S. spp	NAFO 3O	106	26.3	5.5	T0	Lisovsky et al., 2005
S. fasciatus	Gulf of Maine	114	22.3	3.3	T0	Pol et al., 2016
S. fasciatus	Gulf of Maine	140	29.2	4.4	T0	Pol et al., 2016
S. fasciatus	Gulf of Maine	165	33.6	5.0	T0	Pol et al., 2016

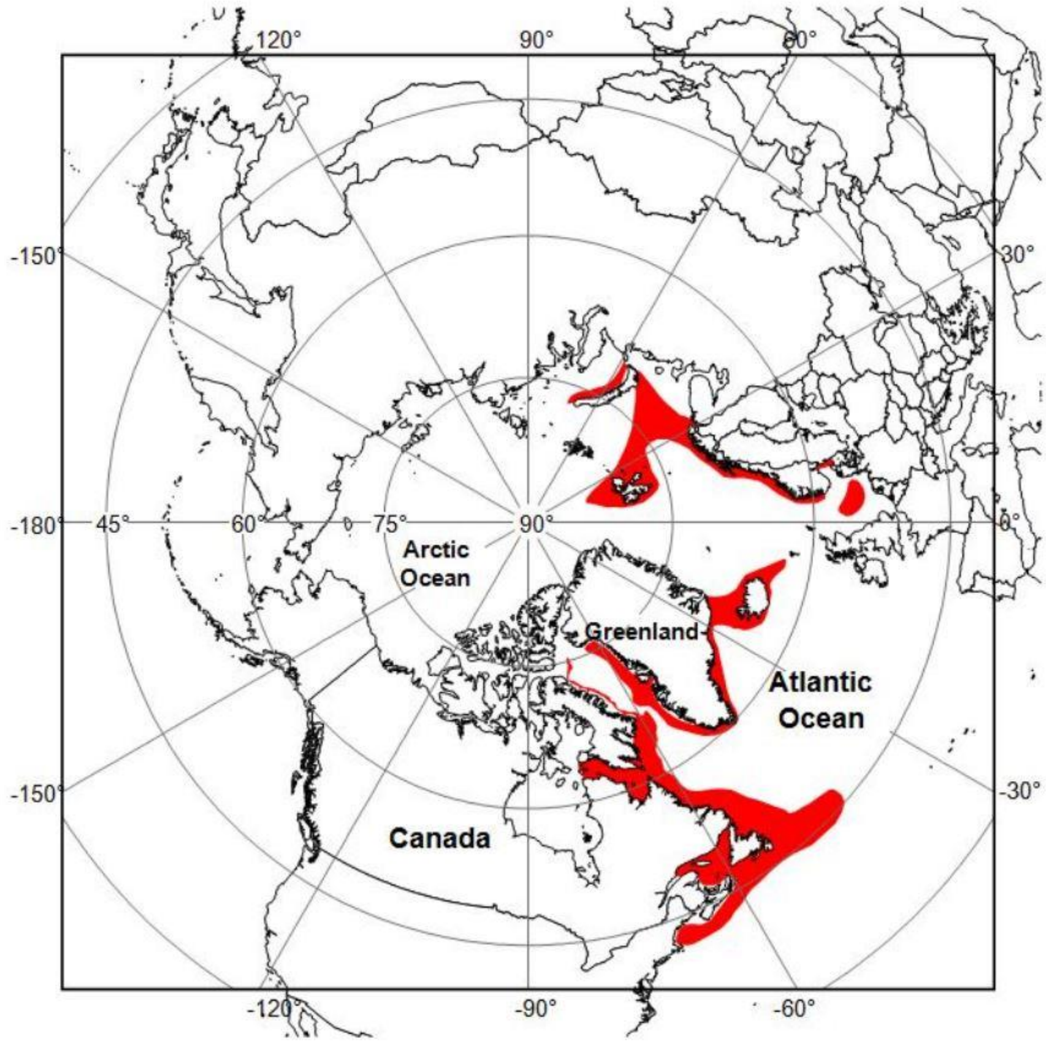

Figure 1.1. Northern shrimp distribution in the North Atlantic Ocean. The red areas indicate natural distribution (source: DFO, 2018).

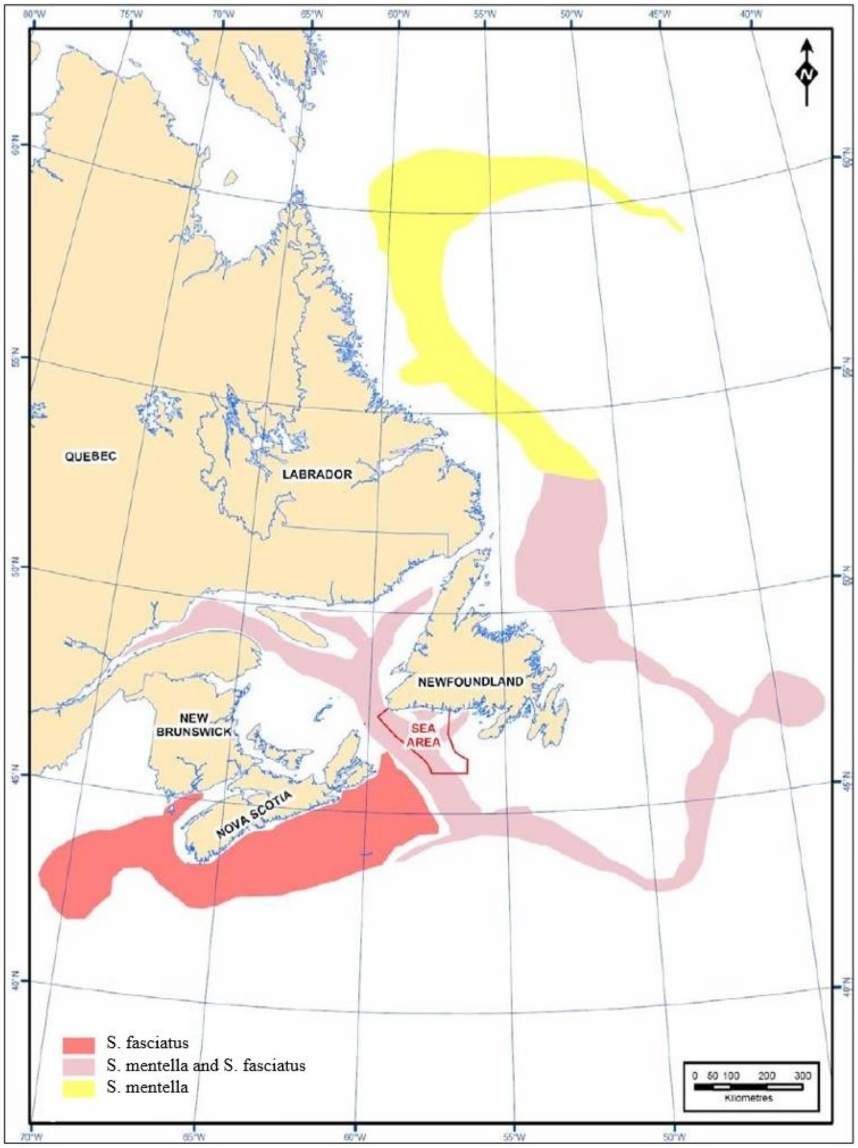

Figure 1.2. Distribution of redfish (*S. fasciatus* and *S. mentalla*) in the Northeast Atlantic of Canadian waters (source: Gascon, 2003).

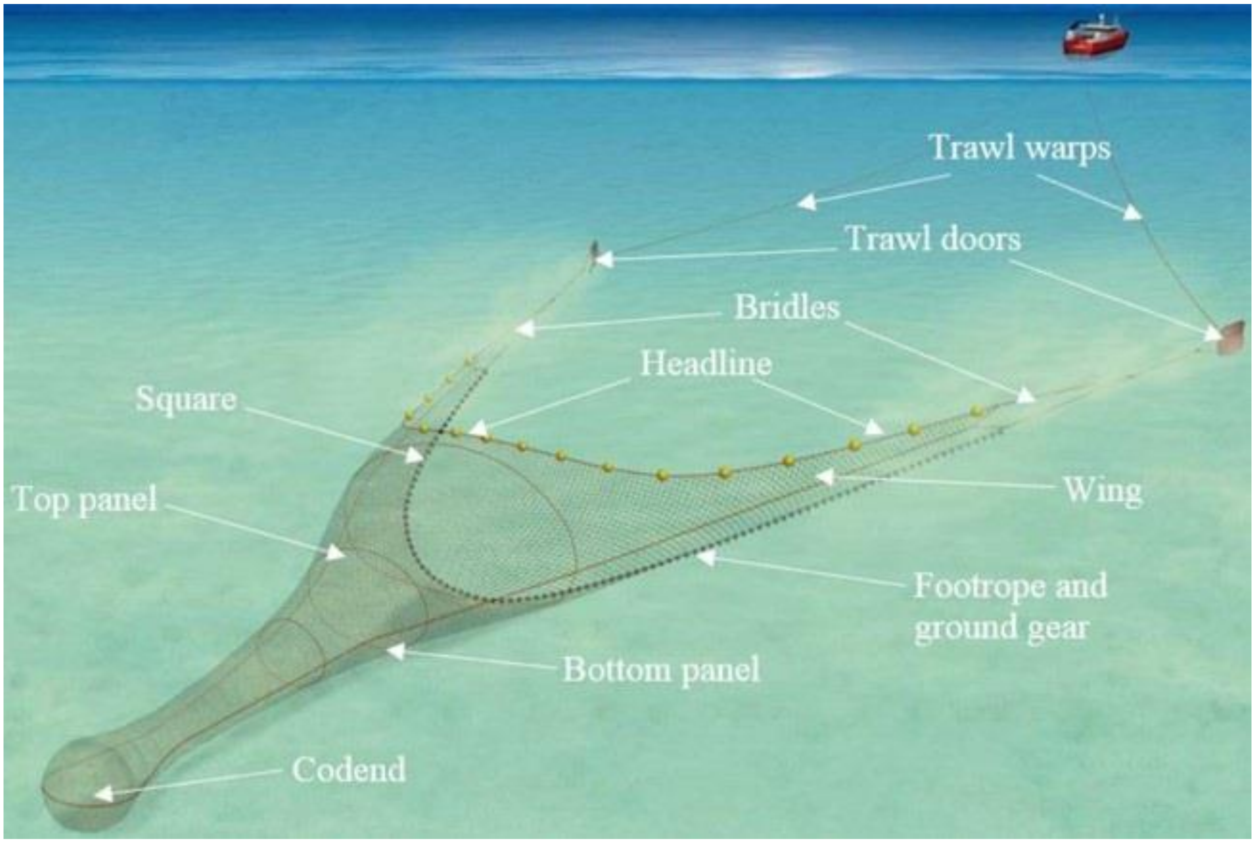

Figure 1.3. Basic components of a bottom trawl (source: Montgomerie, 2015).

CHAPTER 2. Northern Shrimp (*Pandalus borealis*) Size Selectivity in T0, T45, and T90 Mesh Codends

2.1 Abstract

The size selectivity and usability of three codends were compared in the inshore northern shrimp (*Pandalus borealis*) fishery of Iceland using the covered codend method: a two-panel diamond-mesh codend (T0), two-panel square-mesh codend (T45), and 90° turned mesh codend (T90) with four panels and shortened lastridge ropes. Results showed that the T45 and T90 codends had better size selectivity than the T0 codend in terms of releasing individuals smaller than 13 mm carapace length (Minimum References Size; MRS). The T90 codend retained significantly less northern shrimps between 9 and 19 mm than the T0 and between 15 and 19 mm than the T45. No significant difference of size selectivity between T45 and T0 was observed. All three codends presented high retention ratios of northern shrimps above MRS (> 63%) for the population encountered. However, the T0 was not effective at sorting out small northern shrimps; at least 86% of northern shrimps smaller than 13 mm were retained in the T0 codend if encountered. Catch from the T45 and T90 codends were cleaner in terms of their proportion of catch below MRS. Since discarding of undersized northern shrimps is prohibited in Iceland, using a T90 codend would enable fishers to use their quotas more efficiently.

2.2 Introduction

Discards refer to all biomass that is disposed of at sea off a fishing vessel, and bycatch is the capture of non-targeted species whether disposed of or retained (Alverson et al., 1994). Globally, shrimp trawling is associated with high amounts of both bycatch and discards due to their use of small-mesh codends to retain small-bodied target species (Howell and Langan, 1992; Alverson et al., 1994). Additionally, small-mesh codends are not selective for the relatively larger bycatch species (Bayse and He, 2017). Thus, shrimp trawling contributes significantly to ecological impacts of wild fish populations in many parts of the world (e.g., Harrington et al., 2005).

Northern shrimp (*Pandalus borealis*) is a cold-water pink shrimp that is prevalent throughout the North Atlantic Ocean (Dore and Frimodt, 1987). In Iceland, northern shrimp mainly occur off the north coast of the country, and are highly abundant in shallow inshore coastal fjords (MFRI, 2018a, b). The coastal fjord Ísafjarðardjúp had catches decrease from around 3,000 t to 1,000 t from 1990 to 2002. Thus, the fishery was subsequently closed in this area from 2003-2010 due to low biomass. Fishing started again in 2011 with landings peaking at 1,000 t, then gradually decreasing to around 400 t in 2017 (MFRI, 2018b). In Iceland, the minimum reference size (MRS) is 13 mm carapace length (CL) in the inshore fishery. The MRS functions as a reference length since discarding of small northern shrimps has been prohibited in Iceland. If more than 30% of northern shrimp catch (in number) in a designated area is below the MRS, the area is closed to fishing.

Mechanical sorting devices, such as grids, are commonly used to reduce bycatch when targeting northern shrimp (e.g. Grimaldo, 2006; He and Balzano, 2007; Larsen et al., 2018); however the use of grids is not mandatory in the coastal fjords of Iceland (Mamie et al., 2008). When grids are used in these areas, they often clog with seaweed (ICES, 2016). Clogged grids lead to substantial losses of marketable northern shrimp, and were less effective when the catch rate was high (>1 ton/10 min) which can be common in the coastal fjords (ICES, 2016; H. Einarsson, pers. comm.). Thus, in the absence of using a grid, an alternative method to reduce unwanted catch in a northern shrimp trawl is to modify the mesh of the codend.

Size selectivity can be improved by altering the codend mesh size, twine size, or mesh orientation (Herrmann et al., 2013). Codends are traditionally constructed using diamond netting oriented with its normal direction in-line with the direction of towing, otherwise known as the T0 orientation – oriented 0º in the transversal or towing direction. However, this same netting can be installed in such a way that the netting is rotated 45º (T45) or 90º (T90) in the transversal direction. T45 and T90 orientations allow the meshes to remain more open, which is in contrast to T0 meshes that tend to close under tension, decreasing size selectivity (Herrmann et al., 2007; Madsen et al., 2012). The open meshes increase the opportunity for escape, which has been particularly effective at increasing the size selectivity for several fish species, especially roundfish (e.g., Wienbeck et al., 2014; Tokaç et al., 2014; Bayse et al., 2016).

T45 mesh codends, also known as square mesh codends, have been shown to improve the selectivity of several shrimp and prawn fisheries by increasing the mean size of captured target species and decreasing bycatch (Karlsen and Larsen 1989, Broadhurst et al., 2004; Sala et al., 2008; Deval et al., 2009). For northern shrimp, T45 codends have produced mixed results. Trials in Iceland and Canada reported significant reductions of undersized northern shrimps, but also lost market-size individuals (Thorsteinsson, 1992; Hickey et al., 1993). Tests in Greenland found no differences in size selectivity between T0 and T45 codends (Lehmann et al., 1993).

In the Icelandic inshore shrimp fishery, it is mandatory to use a T45 codend if the sorting grid is not installed. However, since discarding is not allowed, a codend that could further improve the size selectivity in this fishery by reducing the capture of undersized northern shrimp should be considered. Therefore, initiated by a request from local fishers, a four-panel T90 codend with shortened lastridge ropes was designed. Previous experience in other fisheries shows that a T90 codend could potentially further improve size selectivity (Bayse et al., 2016; Deval et al., 2016; Lomeli et al., 2017). Shortened lastridge ropes allow meshes to stay open along the length of the codend, since the axial component of the drag forces acting on the accumulated catch will be transmitted through the lastridge ropes instead of the mesh bars (Isaksen and Valdemarsen, 1990). Therefore, using shortened lastridge ropes with a T90 codend could prevent stretching the meshes, which reduces mesh opening, as drag forces increase on the codend with increased catch and thereby help keep the T90 meshes more open during the capture process. Shortened lastridge ropes have been effective at improving the size selectivity of groundfish trawls with T0 codends (Isaksen and Valdemarsen, 1990; Hickey et al., 1993; Brothers and Boulos, 1994). However, shortened lastridge ropes are untested in shrimp trawls to the best or our knowledge and specifically not in a T90 mesh codend.

So far, few studies have investigated how T90 mesh codends affect shrimp size selectivity. Deval et al. (2016) reported that a T90 mesh codend significantly increased size-selectivity for four commercial shrimp species in the Eastern Mediterranean. Santos et al. (2018) compared T0, T45, and T90 codends in a predictive size-selectivity study for brown shrimp (*Crangon crangon*). They found that when mesh sizes were smaller than 25 mm, T90 codends had similar size selectivity properties with T45 codends; however, when mesh sizes were larger than 25 mm T90 codends were estimated to have better size-selectivity than T45 codends.

The purpose of this study was to compare the northern shrimp size-selectivity of three codends used in the Icelandic northern shrimp fishery: the T0 codend currently used in the Icelandic offshore northern shrimp fishery, T45 codend currently used in the inshore fishery, and the newly designed T90 codend with shortened lastridge ropes. The goal was to improve the size-selection of this fishery by reducing the capture of small northern shrimps (< 13 mm CL), and quantify and compare the usability of the three codends for the inshore fishery.

2.3 Materials and Methods

2.3.1 Sea Trials

Two sea trials were carried out on commercial fishing grounds in Ísafjarðardjúp, Iceland (Figure 2.1). The first trial was from 28 September to 9 October 2016 on the research vessel Bjarni Sæmundsson RE-30 (length 56 m; width 10.6 m; gross tonnage 822 t), and the second sea trial was carried out from 6 to 8 November 2017 on the commercial northern shrimp trawler Guðbjörg Sigurðardóttir ÍS-508 (length 26.5 m; width 7.0 m; gross tonnage 273 t). For each haul, tow duration, towing speeds, and fishing depth were recorded. Fishing was carried out 24 h a day and each trawl was hauled back when the catch weight was estimated using trawl-mounted catch sensors to be between 500 kg and 2,000 kg.

2.3.2 Gear Specifications

Forward of the codend, the trawl used for all hauls was a standard northern shrimp bottom trawl (Model 50-1010) used for northern shrimp stock assessment in shallow-water or inshore areas of Iceland (Jónsdóttir et al., 2017). The trawl had 1,010 meshes in circumference with a headline length of 24.3 m. Even though a survey trawl, it is very similar to commercial trawl designs commonly used to capture northern shrimp in Iceland inshore fishing grounds. No sorting grid was used during sea trials, which is typical for the inshore fishery in this area. The covered codend method was used to enable estimating codend size selectivity (Wileman et al., 1996). The cover was made of 10 mm knotless netting. Flexible kites were mounted on the cover net to expand the cover and avoid masking the codend (Grimaldo et al., 2009). For sea trials, the trawl and rigging of fishing gears were identical; the only change was the codend.

All codends (Figure 2.2) were constructed of similar netting (42 mm nominal mesh size, polyethylene material). The T0 and T45 mesh codends were made of single 2.5 mm diameter twine in a two-panel configuration. The T0 codend was 100 meshes in circumference, and the T45 codend was 100 bars in circumference. The stretched length of the T0 and T45 codends was 12.6 m, and the lastridge rope were 4% longer than the stretched length. The T90 mesh codend was made of single 2.5 mm diameter twine in a four-panel configuration with shortened lastridge ropes (Figure 2.2). Stretched length of the T90 codend was 14.7 m, and the lastridge rope was 12 m. Meshes were measured with the OMEGA gauge following procedures described by Fonteyne (2005) prior to sea trials. The T0 was 39.7 mm, T45 33.3 mm, and the T90 36.3 mm.

2.3.3 Catch Sampling

Total northern shrimp catch from the codend and cover were separated and weighed. Random subsampling was applied by measuring carapace length for a minimum of 500 individuals from the codend and the cover each to the nearest 0.5 mm using an electronic digital calliper (ABSOLUTE Coolant Proof Caliper Series 500, Aurora, Illinois, USA) connected to a laptop.

2.3.4 Size Selectivity Analysis

The size-selectivity analysis was carried out using the software SELNET (Herrmann et al., 2012). For the individual haul j, the proportion of northern shrimp of length l retained in the codend is modelled with function $r_j(l,\boldsymbol{v})$, where $\boldsymbol{v}$ is a vector representing two or more size selection parameters to be estimated (Herrmann et al., 2012). However, in this study, we were interested in the length-dependent values of $r_j(l,\boldsymbol{v})$ averaged over hauls ($r_{av}(l,\boldsymbol{v})$) because this would provide information about the average consequences for the size selection process of applying different codends in the fishery. Therefore, it was assumed that the size selective performance of a specific codend for all the individual hauls conducted within a trial was representative of how the codend would perform in a commercial fishery (Millar, 1993; Sistiaga et al., 2010).

Size selection was estimated by minimizing expression (2.1) with respect to parameters $\boldsymbol{v}$, which is equivalent to maximizing the likelihood for the observed data in form of the length-dependent number of northern shrimp retained in the codend versus those escaping to the cover:

$$-\sum_{j=1}^{m}\sum_{l}\left\{\frac{nR_{jl}}{qR_j}\times ln\big(r_{av}(l,\boldsymbol{v})\big)+\frac{nE_{jl}}{qE_j}\times ln\big(1.0-r_{av}(l,\boldsymbol{v})\big)\right\} \qquad (2.1)$$

where the outer summation is over the m hauls conducted with the specific codend in the specific sea trial and the inner over length classes l. nR_{jl} and nE_{jl} are the number of shrimp length measured in codend and cover in haul j belonging to length class l. qR_j and qE_j are the sampling factors for the fraction of the northern shrimp length measured in the codend and cover respectively.

Four basic selectivity models were tested to describe $r_{av}(l,\boldsymbol{v})$ for each codend: Logit, Probit, Gompertz, and Richard (Eqs. 2.2), which assume that all individuals entering the codend are subjected to the same size selection process (Wileman et al., 1996). Additional models (Eqs. 2) were also considered to estimate the codend size selection: CLogit, DLogit, TLogit and Poly4 (for details see Cheng et al., 2019).

$$r_{av}(l,\boldsymbol{v}) = \begin{cases} Logit(l,\boldsymbol{v}) \\ Probit(l,\boldsymbol{v}) \\ Gompertz(l,\boldsymbol{v}) \\ Richard(l,\boldsymbol{v}) \\ CLogit(l,\ C,\ \boldsymbol{v}) = \ 1.0\ -\ C\ +\ C\ \times\ Logit(l,\ \boldsymbol{v}) \\ DLogit(l,C_1,\boldsymbol{v}) = C_1 \times Logit(l,\boldsymbol{v}_1) + (1.0 - C_1) \times Logit(l,\boldsymbol{v}_2) \\ TLogit(l,C,\boldsymbol{v}) = C_1 \times Logit(l,\boldsymbol{v}_1) + C_2 \times Logit(l,\boldsymbol{v}_2) + (1.0 - C_1 - C_2) \times Logit(l,\boldsymbol{v}_3) \\ Poly4(l,\boldsymbol{v}) = \dfrac{exp\left(v_0 + v_1 \times \frac{l}{100} + v_2 \times \frac{l^2}{100^2} + v_3 \times \frac{l^3}{100^3} + v_4 \times \frac{l^4}{100^4}\right)}{1.0 + exp\left(v_0 + v_1 \times \frac{l}{100} + v_2 \times \frac{l^2}{100^2} + v_3 \times \frac{l^3}{100^3} + v_4 \times \frac{l^4}{100^4}\right)} \end{cases}$$

(2.2)

How well the models fit the data was inspected using the goodness-of-fit procedure described by Wileman et al. (1996). Where the p-value represented the likelihood to obtain at least as big a discrepancy between the fitted model and the observed data by coincidence should not < 0.05. If a poor statistical fit was observed (p-value < 0.05), the residuals were inspected to determine whether the poor result was due to structural problems when modelling the experimental data using the different selection curves or if it was due to overdispersion in the data (Wileman et al., 1996). The most appropriate model for each codend was selected based on Akaike information criterion (AIC) values, where the selected model had the lowest AIC (Akaike, 1974). Once a size selection model was selected for the specific codend, uncertainty in the estimated size selection curve and parameters was obtained using a double bootstrapping technique (Millar et al., 1993; Herrmann et al., 2012). This technique accounts for both within and between haul variation in size selection (Fryer, 1991). One thousand bootstrap repetitions were used. Uncertainties were provided in terms of Efron 95% percentile confidence intervals (CIs; Efron and Tibshirani, 1986).

Length-dependent selectivity between codends was compared where $\Delta r(l)$ was estimated by Eq. 2.3.

$$\Delta r(l) = r_e(l) - r_c(l) \qquad (2.3)$$

where $r_e(l)$ is the size selectivity of the experimental codend (T90 or T45), and $r_c(l)$ is the selectivity of the control (baseline) codend (T45 or T0). The 95% CIs for $\Delta r(l)$ were estimated based on the bootstrap population of results for the individual codends compared by the double bootstrap method described above. For details on this procedure consult Herrmann et al. (2018). Significant differences in size selection between codends was obtained if the 95% CIs for $\Delta r(l)$ had length classes that did not overlap 0.0.

2.3.5 Population Analysis

The population structure *nPop(l)* was generated using original datasets from this study by pooling data over all hauls (northern shrimp in the cover + northern shrimp in the codend) in the same season and same area independent of codend used. For each population, uncertainties (95% CIs) were obtained based on a double bootstrap method. This considered both the between-haul variability in the structure of the population entering the codend and within-haul variability due to limited numbers of northern shrimps entering the codend in that specific haul, as well as the effect of subsampling. Specifically, the double bootstrap procedure accounted for between-haul variability by selecting hauls *h* with replacement from the *h* number of hauls from the dataset. Within-haul uncertainty was accounted for by resampling with replacement the northern shrimp length-measured, followed by raising the numbers according to the subsampling ratios within each compartment (cover and codend). The number resampled for each compartment in this inner bootstrap loop equalled the total number of individuals length-measured in the respective compartment in the selected haul. 1,000 bootstrap repetitions were conducted and used to calculate the 95% CIs for the population *nPop(l)*.

Using the size-selection curves predicted for each codend, and applying them to *nPop*(*l*), we obtained simulated accumulated catch curves that quantifies the proportion of the catch consisting of shrimp with CL not exceeding a specific size L:

$$CDF\_nCatch(L) = \sum_{l=0}^{L}\{r_{codend}(l) \times nPop(l)\} \qquad (2.4)$$

Ideally, a good codend would catch more commercial sized than undersized individuals regardless of the population structure fished. Because *CDF_nCatch(L)* expresses the proportion of the catch up to a certain length, the rate at L = MRS denotes the proportion of undersized catch for a given population scenario fished by the specific codend.

For each *CDF_nCatch(L),* we estimated 95% CIs based on the bootstrap sets for $r_{codend}(l)$ and *nPop(l)* using the approach described by Herrmann et al. (2018). Specifically, this was obtained by the procedure described below. Because the bootstrap sets for $r_{codend}(l)$ and *nPop(l)* were obtained independently, a new bootstrap set of results for *CDF_nCatch(L)* was created using:

$$CDF\_nCatch(L)_i = \sum_{l=0}^{L}\{r_{codend}(l)_i \times nPop(l)_i\} \qquad (2.5)$$

where *i* denotes the bootstrap repetition index (Herrmann et al., 2018). In Eq. 2.5 the 1,000 bootstrap sets generated from the original datasets were multiplied to obtain the new bootstrap set for *CDF_nCatch(L)*. Based on this bootstrap set, 95% CIs for *CDF_nCatch(L)* were obtained.

2.3.6 Estimation of Usability Indicators

Using the size-selection curves predicted for each codend and applying them to the population *nPop(l)*, we obtained simulated catches, $r_{codend}(l) \times nPop(l)$. These were then summarized by calculating three different indicators (*nP−*, *nP+*, *nRatio*, and *dnRatio*), for each of the *nPop(l)* separately (Eq. 4). *nP−* and *nP+* estimate the retention efficiency of the catch below and above MRS; *nRatio* represents the landings ratio of catch below to above MRS; *dnRatio* calculates the discard ratio assuming all the individuals below and above MRS are either discarded or retained. Ideally for a target species, *nP−*, *nRatio* and *dnRatio* should be low (close to 0), while *nP+* should be high (close to 100), i.e., all individuals over MRS that enter the codend are retained. The indicators were estimated by:

$$\begin{cases} nP- = 100 \times \frac{\sum_{l<MRS}\{r_{codend}(l) \times nPop(l)\}}{\sum_{l<MRS}\{nPop(l)\}} \\ nP+ = 100 \times \frac{\sum_{l>MRS}\{r_{codend}(l) \times nPop(l)\}}{\sum_{l>MRS}\{nPop(l)\}} \\ nRatio = \frac{\sum_{l<MRS}\{r_{codend}(l) \times nPop(l)\}}{\sum_{l>MRS}\{r_{codend}(l) \times nPop(l)\}} \\ dnRatio = 100 \times \frac{\sum_{l<MRS}\{r_{codend}(l) \times nPop(l)\}}{\sum_{l}\{r_{codend}(l) \times nPop(l)\}} \end{cases} \qquad (2.6)$$

All indicators (*nP−*, *nP+*, *nRatio*, and *dnRatio*) were estimated with uncertainties for each codend and population scenario, using the bootstrap set for $r_{codend}(l)$ and $nPop(l)$. Specifically based on Herrmann et al. (2018), the bootstrap set for calculating indicator values were obtained based on each bootstrap repetition result applying $r_{codend}(l)$ and $nPop(l)$ simultaneously in Eq. 4. Finally, based on the resulting bootstrap set, 95% CIs were obtained for each of the indicators. All the analyses above were conducted with the software SELNET (Herrmann et al., 2012).

2.4 Results

2.4.1 Haul and Catch Data

A total of 38 hauls were carried out during two sea trials: 19 hauls with T0 codend, 9 hauls with T45, and 10 hauls with T90 (Table 2.1). The first trial evaluated the T0 codend at 19 stations at water depths of 47 to 120 m, and an average towing duration of 45 min (29 - 74 min) (Table 2.1). The second trial consisted of 9 hauls for the T45 and 10 hauls for the T90 codend. For hauls that fished the T45 codend, average towing duration was 19 min (ranged from 13 to 30 min), and towing depths ranged from 41 to 67 m. For T90 codend hauls, towing duration averaged 21 min (ranged 12 to 37 min), towing depths ranging from 42 to 72 m (Table 2.1). Northern shrimp was the predominantly captured species, therefore it was the only species analysed. Measurements of CL were recorded for a total of 45,549 northern shrimp.

2.4.2 Model Selection

For each codend, the eight models (Eqs. 2) were fitted to the collected data. Table 2.2 presents the AIC values for the fit of each model; the model with lowest AIC value was selected as the best one for each codend. For the T0 and T45 codends, the best model was DLogit. For the T90 codend, the best model was Poly4. Selected model fit statistics were presented in Table 2.3.

2.4.3 Size Selectivity

Size selectivity results for the T0 codend are presented in Figure 2.3. According to the selectivity curve, the T0 codend indicated high retention probability (> 85%) for all sizes of shrimp. However, for sizes below MRS confidence bands were wide due to a low number of observations at these length classes. These results indicate that the T0 codend generally had a poor size selectivity.

The selectivity curve of the T45 codend showed high retention probability for catch above MRS, > 70%, and increased to > 90% for catch above 17 mm (Figure 2.3). Catches < 17 mm suffered from low confidence; however, the model followed the experimental rates well until lengths < 12 mm. Catches below 12 mm, do not follow a clear trend and it is difficult to determine what the data indicate within the large CIs. Very few northern shrimps were captured below 10 mm in the codend and cover, which accounts for the large CIs.

The T90 codend had a much more gradual increase in retention probability as length increased when compared to the T0 and T45 codend (Figure 2.3). Few northern shrimps were observed < 10 mm, which corresponded to large CIs, however at lengths > 9 mm model estimates had high confidence. Retention probability gradually increased from 10 cm to full retention.

Codends were directly compared with Delta curves (Figure 2.3). The Delta plot comparing T0 and T45 codends contained 0.0 throughout, which shows no significant difference in size selectivity between codends. However, the model indicated that the T0 codend retained more northern shrimp below 17 mm, which gradually increased toward zero, as did the CIs. When comparing the T0 and T90 codend, significantly less individuals were retained at lengths between 9 and 19 mm (Figure 2.3). This shows that using the T90 codend significantly reduces the catch of undersized and market-sized northern shrimp. Size selectivity between the T90 and T45 codend was significantly different for market-sized northern shrimps at lengths between 14 and 22 mm. Few northern shrimp were captured below 10 mm for both of these codends, rendering results for these lengths inconclusive.

2.4.4 Population Analysis

The estimated population structure was significantly different between years (Figure 2.4). In 2016, observed lengths were shifted to the left of 2017, where 2016 had a mode at 16 mm, 2017 was bimodal with a mode of corresponding size to 2016 at 19 mm, and a relatively smaller mode at 14mm. Additionally, more smaller individuals < 11 mm entered the codend in 2016. In terms of significant differences, 2016 had higher proportions from 10-11 mm and 14-17 mm, and 2017 had higher frequencies from 17 to 21 mm).

Figures 2.5 and 2.6 illustrate the cumulative capture proportions between the different codends for 2016 and 2017, respectively. Following the population estimates from Figure 2.4, cumulative capture proportions were shifted to the left for 2016 due to smaller northern shrimp being present on fishing grounds. In 2016, the T0 codend trended higher catches at lengths of 7 to 21 mm versus both the T45 and T90 codend, however a significant difference was only observed between 12 to 21 mm for the T90 codend; no significant difference was observed between the T0 and T45 codend (Figure 2.5). The T45 codend trended higher catches from 11 to 21 mm when compared to the T90, but these differences were not significantly different. Generally, similar results were observed in 2017, the T0 codend indicated higher catches from 11 to 22 mm when compared to the T45 and T90 codends, but there were no significant differences between the T0 and T45 codends; the T0 caught significantly more northern shrimp from 11 to 22 mm (Figure 2.6). There were no significant differences between the T45 and T90 codends, however the T45 did indicate higher catches from 12 – 21 mm (Figure 2.6). For both years, cumulative capture proportions for individuals over 21 mm were around 100% for all the codends; and the results of the $\Delta r(l)$ function was approximately 0.0.

2.4.5 Usability Indicators

Table 2.4 shows the usability indicators for each codend based on the average population size structure observed in 2016 and 2017. Indicators for $nP-$ and $nP+$ were similar between codends for both years. The T0 codend had high retention of undersized and marketable catch (> 86%). The T45 also had high retention of market-sized northern shrimp (> 89%), but indicated lower catches of undersized northern shrimp (< 60%), however these differences were not significantly different from the T0 codend. The T90 codend had lower values for each indicator (< 33% and < 77%, for $nP-$ and $nP+$, respectively). Each indicator between T0 and T90 were significantly different, but none were between T45 and T90, typically due to T45 having large CIs.

The *nRatios* of northern shrimp below and above MRS were similar for the codends within each year (Table 2.4). However, *nRatio* was 6 to 7 times as high for 2016, which reflects the size distribution difference between years. For each year, the T90 codend had the lowest *nRatio*, followed by the T45, and the T0. The difference between *nRatios* was not significant for each comparison.

All the codends had low discard ratios (*dnRatio* in number) and were below the management threshold of 30% for both year-population scenarios (Table 2.4). For 2016 population, the *dnRatio* was higher across each codend when compared to 2017, and no significant difference was observed between any codend. The T0 codend had the highest *dnRatio* (19.3%), followed by the T45 (14.7%), and the T90 codend (12.3%). For the 2017 population, *dnRatios* of the codends were much smaller than those of 2016, *dnRatio* < 3.7% for each codend with no significant difference between codends.

2.5 Discussion

This research investigated the size selectivity and usability of three codends used to capture northern shrimp in Icelandic waters. Size selectivity curves of the three codends were established and compared. Compared to the T45 and T0 codends, the T90 codend presented better size selection performance to release undersized catch while its retention ratio for market-sized catch was also lower; the difference was significant for catch at certain length ranges between the T90 and T0 (9-19 mm) but not between the T45 and T0. In terms of releasing juvenile or undersized northern shrimp, the T90 codend should be considered for the sustainability of the fishery. However, using the T90 codend may be economically ambivalent for fishers in Iceland. Due to the ban on discarding of undersized catch, a T90 codend can increase catch efficiency of limited quotas, effectively increasing average catch size. However, this has to be considered in the context of losing marketable shrimp from 13-19 mm. A T90 codend is a relatively simple change to the trawl and is much easier to operate in practice than a sorting grid. Therefore, T90 codends could be a potential choice for fishery managers to maintain a healthy Iceland shrimp fishery.

CIs of each curve for individuals under 11 mm were very wide and became wider as CL decreased (Figure 2.3). This is attributed to the limited number of small individuals retained in the codend and cover, resulting in few data defining the left tail of the curve. This can also be validated from the size distribution of the population (Figure 2.3); numbers of the individuals (CL < 11 mm) retained in each gear only accounted for a small proportion of all the catch. There are two possible explanations for this situation: there were very few individuals below 11 mm in the populations at the fishing locations, or alternatively these small individuals were present but escaped through the cover net. The wide CIs affected the estimation accuracy of the selectivity making the selectivity within that length range uncertain.

When undersized northern shrimps were present in the encountered population, few could escape from the T0 codend into the cover (> 86% retention), and the T45 also displayed high undersized retention (> 60%). These results show that the T0 and T45 codends were not very effective at sorting out undersized northern shrimps, if present in the fished population. By comparison, the T90 codend was much more effective at releasing small northern shrimps (< 35% retention); however market-sized catch was significantly reduced. When considering 2016 results, the T90 codend would retain about 64 northern shrimps (in number) above MRS when there were 100 northern shrimps at this length range in the codend and cover (Table 2.4). The same indicator for the T0 and T45 codends was above 89. Thus, fishing vessels may experience an economic loss if they use T90 codend instead of T0 or T45. However, according to the Icelandic fishery regulations, discarding of undersized catch is prohibited, and the undersized catch was counted as a part of the landing quota. Therefore, with a T90 codend fishers in Iceland could potentially make the most effective use of their quota by increasing the value of their quota, while having a cleaner fishery in terms of undersized northern shrimp catch.

The above scenario is context dependent. When considering the fished population, the T90 codend produced these results for 2016 when many small northern shrimp were present in the fishery – *nRatio* and *dnRatio* was at its highest (0.24 and 19.3%, respectively for the T0 codend). However, in 2017 few relatively small northern shrimps were present, and *nRatios* and *dnRatios* dropped across all codends and had very similar, and very low values (< 0.04 and 4%, respectively). *dnRatio* of each codend (<30%) demonstrated that using the codends tested would not lead to the fishing area closure according to Iceland fishing regulations. In terms of decreasing the discard ratio, there was no significant difference for applying the T0, T45 or T90 codend in the northern shrimp fisheries, however both *nRatio* and *dnRatio* indicated less discard for the T45 codend compared to the T0 and less discard for the T90 when compared to the T45. In this scenario, the T90 codend was not the most effective codend in terms of effective quota use. The T0 or T45 codend would have been more effective, since they captured more large market-sized northern shrimp and all codends captured similar amounts of undersized northern shrimp.

Mesh orientation likely was not the only factor contributing to the observed differences in size selectivity in this study. The nominal mesh size of the three codends was the same, but measured mesh sizes were slightly different. Additionally, the T0 and T45 codends were in a two-panel configuration while the T90 codend was in a four-panel configuration and had shortened lastridge ropes. Due to these differences in design and construction, these results should be viewed as differences between codends.

An outlier (CL = 8.5 mm) for the experimental rate was observed for the T90 codend (Figure 2.3). Normally, the experimental rate is expected to increase as CL increases. However, the experimental rate at length 8.5 mm was 1.0 – full retention. This observation is vastly higher than expected, and considering that for all other length classes full retention was not achieved until 21 mm. This observation is due to a single observation at this length class. Additionally, it is due to this outlier that the selection curve starts at almost full retention, and required the best fit model to be very flexible (Poly4). Similarly, the T45 codend had extremely low catch amounts from 8 to 11 mm (n = 8 for both codend and cover over the length range), which led to the experimental rate of this length range to be larger than expected, once catch rates increased the expected trends were observed. Very small individuals may be retained in a codend that should sort them out due to not having proper contact with the codend to produce size-based selectivity. These results are due to small catch rates at these length classes combined with codend retention of extremely small individuals likely due to aggregation of catch, poor mesh opening, or meshes blocked by the catch. If more individuals were captured at these lengths, a better estimation could have been determined, however, these sizes were not observed on fishing grounds in 2017.

Thorsteinsson (1992) reported that changing from T0 to T45 codend effectively reduced the catch of undersized northern shrimp, which is not consistent with our results, nor the results of Lehmann et al. (1993) and Hickey et al. (1993). Our results indicated that the T45 codend decreased the undersized catch compared to the T0 codend, however the difference was not significant and had wide confidence intervals (Figure 2.3). Of note, the methods of each of these studies differ from ours, and each other, where we used the codend cover methodology, Thorsteinsson (1992) and Hickey et al. (1993) used the paired gear method and Lehmann et al. (1993) the trouser trawl method. Other differences include analytical methods (selectivity models with confidence intervals), materials (mesh size, twine diameter), and fishing grounds. However, when fished populations were similar between studies, similar results were observed. Our results were fished on similar population sizes when compared to Lehmann et al. (1993) and Hickey et al. (1993), which also observed no difference between codends. Interestingly, Thorsteinsson (1992) only observed large differences in length distributions at small sizes (11-13 mm), sizes where each of the other mentioned studies had low catches, and at larger sizes (> 15mm) Thorsteinsson's (1992) results were similar to the other studies – no difference between codends. Perhaps a T45 codend does reduce these sizes of northern shrimp, however we were unable to determine this from our study, and future work should address this. The measured mesh size of the T45 (33.3 mm) was smaller than the T0 (39.7 mm), which may account for the insignificant difference in selectivity between the two codends. Comparing the size selectivity between T0 and T45 codends with the same mesh size is necessary in the future.

In conclusion, this study demonstrated differences in the size selectivity and usability of three codends targeting northern shrimp in Icelandic inshore waters. The T0 and T45 codends performed poorly at releasing northern shrimp below the MRS. The T90 codend released significantly more undersized northern shrimp, but at the cost of losing some northern shrimp above MRS. Additionally, these results were very context dependent. In 2016, when many small northern shrimps were in the fishery, the T90 codend was the best choice in terms of size selectivity, efficient quota use, and conservation of resources. In 2017, it could be argued that there was no real difference between fishing any of the codends, in terms of avoiding undersized northern shrimp, since few small northern shrimps were in the fished population. Perhaps using the codend with the least selectivity would be better in terms of efficiency and conserving fuel use. As is often the case in fisheries management, there is rarely a simple solution that works in every case, and size selectivity is ultimately dependent on the fished population.

2.6 Acknowledgements

This project was funded by Marine and Freshwater Research Institute (Iceland). We would like to thank the staff from MFRI. Thanks are also extended to crew of the research vessel Bjarni Sæmundsson RE-30 and crew of the commercial shrimp trawler Guðbjörg Sigurðardóttir ÍS-508.

2.7 References

Akaike, H., 1974. A new look at the statistical model identification. IEEE Trans. Auto. Control, 19, 716-723.

Alverson, D.L., Freeberg, M.H., Murawski, S.A., Pope, J.G., 1994. A global assessment of fisheries bycatch and discards. FAO Fish. Tech. Pap., 339, 235 pp

Bayse, S.M., Herrmann, B., Lenoir, H., Depestele, J., Polet, H., Vanderperren, E. Verschueren, B., 2016. Could a T90 mesh codend improve selectivity in the Belgian beam trawl fishery? Fish. Res., 174, 201-209.

Broadhurst, M.K., Millar, R.B., Kennelly, S.J., Macbeth, W.G., Young, D.J., Gray, C.A., 2004. Selectivity of conventional diamond-and novel square-mesh codends in an Australian estuarine penaeid-trawl fishery. Fish. Res., 67, 183-194.

Brothers, G., Boulos, D.L., 1994. Experiments with lastridge rope hanging ratios. ICES C.M. 1994/B:2 pp.

Cheng, Z., Einarsson, H.A., Bayse, S., Herrmann, B. Winger, P., 2019. Comparing size selectivity of traditional and knotless diamond-mesh codends in the Iceland redfish (*Sebastes* spp.) fishery. Fish. Res., 216, 138-144.

Deval, M.C., Bök, T., Ateş, C., Ulutürk, T., Tosunoğlu, Z., 2009. Comparison of the size selectivity of diamond (PA) and square (PE) mesh codends for deepwater crustacean species in the Antalya Bay, eastern Mediterranean. J. Appl. Ichthyol., 25, 372-380.

Deval, M.C., Özgen, G., Özbilgin, H., 2016. Selectivity of 50 mm T0 and T90 codends for commercial shrimp species in the Turkish deepwater trawl fishery, Eastern Mediterranean. J. Appl. Ichthyol., 32, 1041-1057.

Dore, I.,, Frimodt, C., 1987. An illustrated guide to shrimp of the world. Osprey Books Huntington, New York, 229p.

Efron, B., Tibshirani, R., 1986. Bootstrap methods for standard errors, confidence intervals, and other measures of statistical accuracy. Stat. Sci., 1, 54-75.

Fonteyne R., 2005. Protocol for the use of an objective mesh gauge for scientific purposes, ICES Coop. Research Rep., No. 279, 8p. ISBN 87-7482-044-3.

Fryer, R.J., 1991. A model of between-haul variation in selectivity. ICES. J. Mar. Sci., 48, 281–290.

Grimaldo, E., 2006. The effects of grid angle on a modified Nordmøre-grid in the Nordic shrimp fishery. Fish. Res., 77, 53-59.

Grimaldo, E., Larsen, R.B., Sistiaga, M., Madsen, N., Breen, M., 2009. Selectivity and escape percentages during three phases of the towing process for codends fitted with different selection systems. Fish. Res., 95, 198-205.

Harrington, J.M., Myers, R.A., Rosenberg, A.A., 2005. Wasted fishery resources: discarded by-catch in the USA. Fish Fish., 6, 350-361.

He P., Balzano V., 2007. Reducing small shrimps in the Gulf of Maine pink shrimp fishery with a new size-sorting grid system. ICES. J. Mar. Sci., 64, 1551-1557.

Herrmann, B., Priour, D., Krag, L.A., 2007. Simulation-based study of the combined effect on cod-end size selection for round fish of turning mesh 90 degrees and of reducing the number of meshes in the circumference. Fish. Res., 84, 222-232.

Herrmann, B., Sistiaga, M., Nielsen, K.N., Larsen, R.B., 2012. Understanding the size selectivity of redfish (*Sebastes* spp.) in North Atlantic trawl codends. J. Northw. Atl. Fish. Sci., 44, 1-13.

Herrmann, B., Wienbeck, H., Moderhak, W., Stepputtis, D., Krag, L.A., 2013. The influence of twine thickness, twine number and netting orientation on codend selectivity. Fish. Res., 145, 22-36.

Herrmann, B., Krag, L.A., Krafft, B.A., 2018. Size selection of Antarctic krill (*Euphausia superba*) in a commercial codend and trawl body. Fish. Res., 207, 49-54.

Hickey, W.M., Brothers, G., Boulos, D.L., 1993. By-catch reduction in the northern shrimp fishery. Can. Tech. Rep. Fish. Aqua. Sci., No. 1964, 41p.

Howell, W.H., Langan, R., 1992. Discarding of commercial groundfish species in the Gulf of Maine shrimp fishery. N. Am. J. Fish. Manage., 12, 568-580.

ICES. 2016. Report of the Working Group on Fishing Technology and Fish Behaviour (WGFTFB), 25-29 April 2016, Merida, Mexico. ICES. C.M. 2016/SSGIEOM:22. 183p.

Isaksen, B., Valdemarsen, J.W. 1990. Codend with short lastridge ropes to improve size selectivity in fish trawls. ICES. C.M. 1990/B46: 8p.

Jónsdóttir I.G., Bragason G.S., Brynjólfsson S.H., Guðlaugsdóttir A.K., Skúladóttir U. 2017. Yfirlit yfir rækjurannsóknir við Ísland, 1988-2015. northern shrimp research in Icelandic waters, 1988-2015. HV2017-007: 92p.

Karlsen, L., Larsen, R., 1989. Progress in the selective shrimp trawl development in Norway. *In* Proceedings of the World Symposium on Fishing Gear and Fishing Vessel Design, St. John's, Canada. 30-38p.

Larsen, R.B., Herrmann, B., Sistiaga, M., Brinkhof, J., Santos, J., 2018. Catch and release patterns for target and bycatch species in the Northeast Atlantic deep-water shrimp fishery: Effect of using a sieve panel and a Nordmøre grid. PloS One, 13: p.e0209621.

Lehmann, K., Valdemarsen, J. W., Riget, F. 1993. Selectivity in shrimp trawl codends tested in a fishery in Greenland. ICES Mar. Sc., 196, 80–85.

Lomeli, M.J., Hamel, O.S., Wakefield, W.W., Erickson, D.L., 2017. Improving catch utilization in the US West Coast groundfish bottom trawl fishery: an evaluation of T90-mesh and diamond-mesh cod ends. Mar. Coast. Fish., 9, 149-160.

Madsen, N., Herrmann, B., Frandsen, R.P., Krag, L.A., 2012. Comparing selectivity of a standard and turned mesh T90 codend during towing and haul-back. Aquat. Living Resour., 25, 231-240.

Mamie, J.C.J., Leone, S., Valtýsson, H.Þ., Ármannsson, H., 2008. Stock assessment of shrimp *Pandalus borealis* (KRØYER 1838) in Skjálfandi Bay Northern Iceland. United Nations University, Reykjavik. Available at: http://www.unuftp.is/static/fellows/document/josephus08prf.pdf.

MFRI, 2018a. Assessment Reports 2018, Offshore northern shrimp. Technical Report. Marine and Freshwater Research Institute, Reykjavik, Iceland.

MFRI, 2018b. Assessment Reports 2018, Shrimp in Ísafjarðardjúp. Technical Report. Marine and Freshwater Research Institute, Reykjavik, Iceland.

Millar, R.B., 1993. Incorporation of between-haul variation using bootstrapping and nonparametric estimation of selection curves. Fish. Bull., 91, 564-572.

Sala, A., Lucchetti, A., Piccinetti, C., Ferretti, M., 2008. Size selection by diamond-and square-mesh codends in multi-species Mediterranean demersal trawl fisheries. Fish. Res., 93, 8-21.

Santos, J., Herrmann, B., Stepputtis, D., Günther, C., Limmer, B., Mieske, B., Schultz, S., et al., 2018. Predictive framework for codend size selection of brown shrimp (*Crangon crangon*) in the North Sea beam-trawl fishery. PloS One, 13, e0200464.

Sistiaga, M., Herrmann, B., Grimaldo, E., Larsen, R.B., 2010. Assessment of dual selection in grid based selectivity systems. Fish. Res., 105, 187-199.

Thorsteinsson, G., 1992. The use of square mesh codends in the Icelandic shrimp (*Pandalus borealis*) fishery. Fish. Res., 13, 255-266.

Tokaç, A., Herrmann, B., Aydın, C., Kaykac, H., Ünlüler, A., Gökçe, G., 2014. Predictive models and comparison of the selectivity of standard (T0) and turned mesh (T90) codends for three species in the Eastern Mediterranean. Fish. Res., 150, 76-88.

Wienbeck, H., Herrmann, B., Feekings, J.P., Stepputtis, D., Moderhak, W., 2014. A comparative analysis of legislated and modified Baltic Sea trawl codends for simultaneously improving the size selection of cod (*Gadus morhua*) and plaice (*Pleuronectes platessa*). Fish. Res., 150, 28-37.

Wileman, D.A., Ferro., R.S.T., Fonteyne, R., Millar, R.B., 1996. Manual of methods of measuring the selectivity of towed fishing gears. ICES Coop. Research Rep., No. 215, 126p.

Table 2.1. Operational conditions for all hauls during sea trials in 2016 and 2017.

Codend	Haul ID	Date	Sample number		Sampling ratio		Towing duration (min)	Maximum towing depth (m)
			Codend	Cover	Codend	Cover		
T0								
	1	28/09/2016	597	592	0.0012	0.0107	74	63
	2	02/10/2016	608	642	0.0246	0.2407	72	120
	3	03/10/2016	601	599	0.0944	0.3147	58	106
	4	03/10/2016	608	624	0.0189	0.1350	50	71
	5	04/10/2016	605	643	0.0145	0.2072	47	69
	6	04/10/2016	621	622	0.0118	0.0588	30	59
	7	04/10/2016	628	596	0.0015	0.0256	47	71
	8	04/10/2016	610	625	0.0095	0.0592	41	68
	9	05/10/2016	621	614	0.0241	0.1175	44	71
	10	05/10/2016	597	611	0.0176	0.2221	29	68
	11	05/10/2016	616	597	0.0179	0.1605	29	67
	12	06/10/2016	609	603	0.0240	0.1549	44	71
	13	06/10/2016	611	608	0.0076	0.2845	38	63
	14	07/10/2016	605	603	0.0041	0.0736	30	65
	15	07/10/2016	599	599	0.0010	0.0195	58	49
	16	08/10/2016	620	610	0.0526	0.2410	29	114
	17	08/10/2016	621	605	0.0656	0.2721	60	111
	18	09/10/2016	613	603	0.0074	0.0945	29	76
	19	09/10/2016	625	609	0.0075	0.0577	58	59
T45								
	20	06/11/2017	600	599	0.0102	0.1261	26	53
	21	06/11/2017	603	599	0.0010	0.0721	30	47
	22	06/11/2017	606	605	0.0063	0.0127	19	64
	23	06/11/2017	604	606	0.0016	0.1035	27	66
	24	07/11/2017	604	606	0.0127	0.0558	18	63
	25	07/11/2017	611	604	0.1529	0.1330	14	67
	26	07/11/2017	608	603	0.1516	0.3247	14	52
	27	07/11/2017	605	619	0.0259	0.2325	14	42
	28	07/11/2017	607	603	0.0072	0.1106	13	67
T90								
	29	07/11/2017	223	609	0.5000	0.3537	14	61
	30	07/11/2017	603	605	0.0045	0.0321	15	43
	31	07/11/2017	366	606	0.5000	0.3801	15	61
	32	08/11/2017	603	605	0.0066	0.0340	22	58
	33	08/11/2017	569	601	0.0064	0.0247	19	65
	34	08/11/2017	603	601	0.0378	0.0836	19	60
	35	08/11/2017	604	606	0.0836	0.0816	26	61
	36	08/11/2017	606	605	0.0212	0.0172	37	65
	37	08/11/2017	607	604	0.0182	0.0143	27	72
	38	08/11/2017	605	606	0.0044	0.0152	12	54

Table 2.2. Akaike's information criterion (AIC) for each model for each codend. The selected model is highlighted in bold.

Codend	Model							
	Logit	Probit	Gompertz	Richard	DLogit	TLogit	CLogit	Poly4
T0	1,632,066	1,631,556	1,632,171	1,626,596	**1,617,175**	1,618,452	1,618,446	1,618,223
T45	539,720	537,239	541,775	535,847	**535,361**	535,367	535,481	535,542
T90	715,699	715,006	719,526	713,918	713,632	713,638	713,644	**713,445**

Table 2.3. Selected model fit statistics for each codend.

Codend	T0	T45	T90
Model	DLogit	DLogit	Poly4
DOF	39	29	29
Deviance	536.4	102.5	95.6
p-value	<0.001	<0.001	<0.001

Table 2.4. Usability indicators (nP-, nP+, and dnRatio in percent) for each codend based on different year-population scenarios.

Year	2016			2017		
Codend	T0	T45	T90	T0	T45	T90
nP-	86.2(52.5-91.0)	59.5(17.3-88.0)	34.6(17.7-49.8)	87.2(65.4-91.1)	67.2(24.4-90.0)	33.0(24.6-43.9)
nP+	93.3(90.6-95.7)	89.0(68.5-96.2)	63.9(51.8-76.1)	95.6(92.9-98.4)	94.1(82.4-97.9)	77.1(65.9-83.3)
nRatio	0.24(0.02-0.64)	0.17(0.02-0.46)	0.14(0.01-0.47)	0.04(0.01-0.06)	0.03(0.01-0.06)	0.02(0.01-0.03)
dnRatio	19.3(2.3-39.1)	14.7(1.5-31.7)	12.3(1.3-32.2)	3.7(1.69-6.09)	2.9(0.94-5.35)	1.8(0.81-3.27)

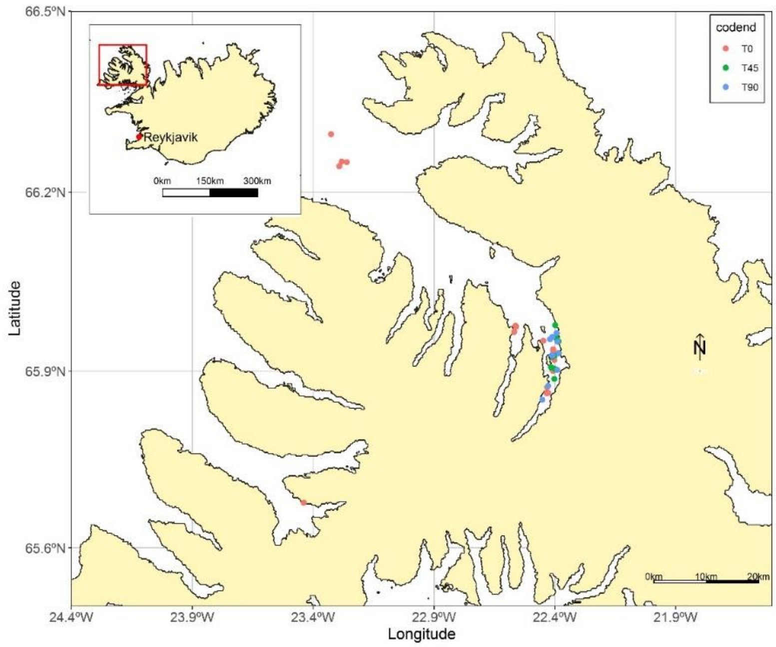

Figure 2.1. Location of the fishing trials: red points show towing start positions with T0 codend; green points with T45 codend; blue points with T90 codend.

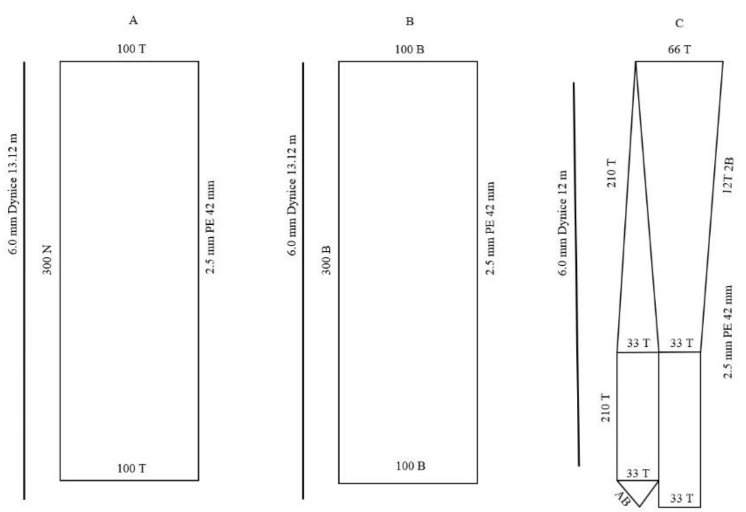

Figure 2.2. Schematic diagram of (A) T0, (B) T45 and (C) T90 codend.

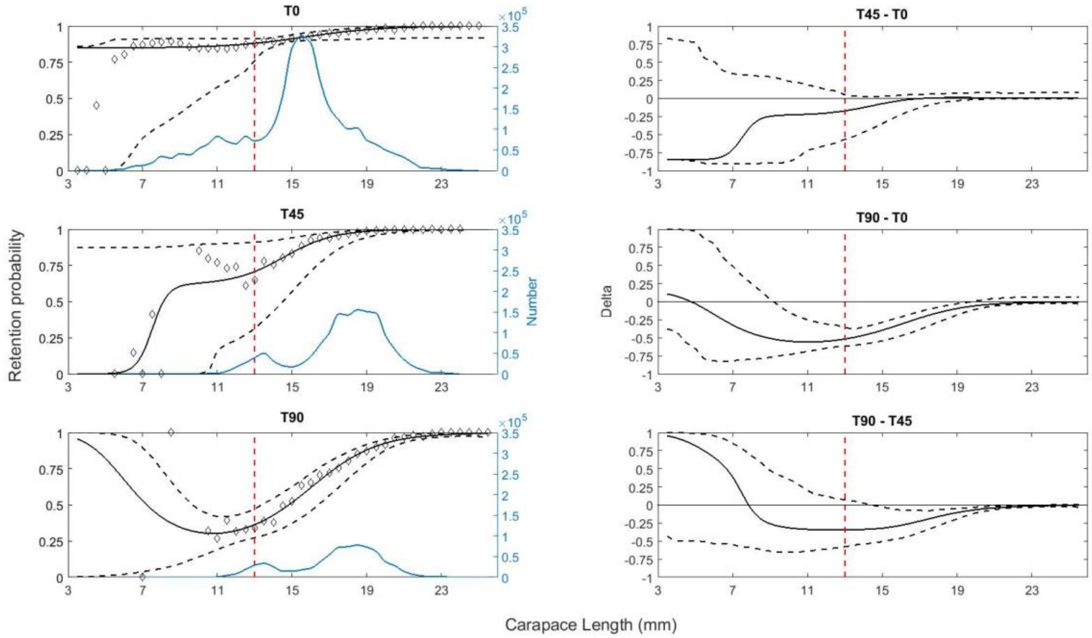

Figure 2.3. Size selection curve for each codend (first column) and corresponding Delta curves (last column): Diamond symbols represent the experiment rates of certain length class; thick black curve indicates the fitted size selection curves; stipple curves describe the 95% confidence limits for the fitted selectivity curves; blue curves shows the size distribution of the population encountered during sea trials; vertical stipple line represents the MRS for northern shrimps; Delta curves show pairwise comparison of each codend selectivity.

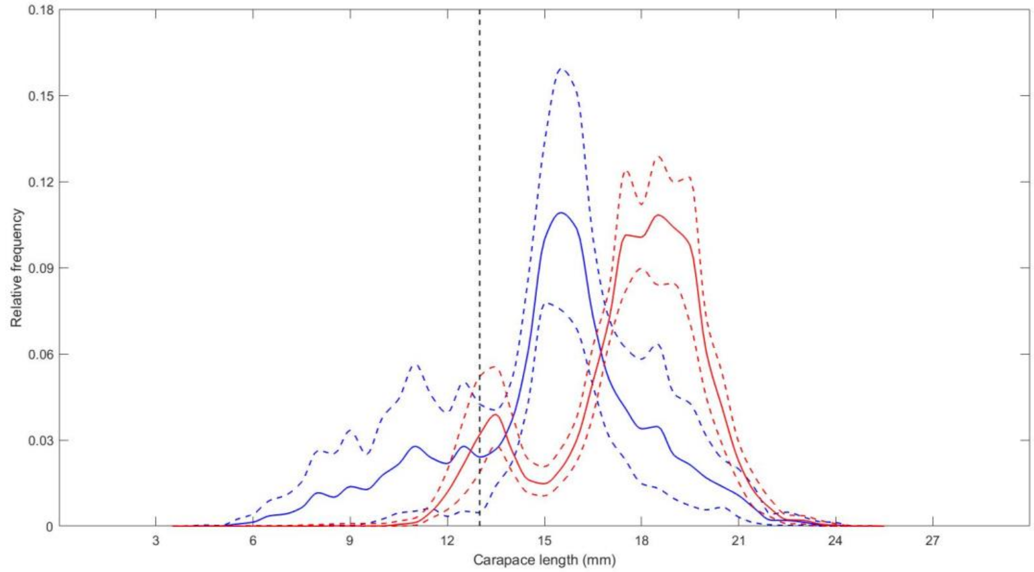

Figure 2.4. Estimated average population from all hauls at the same fishing area and season. Blue line represents data from sea trials conducted in year 2016. Red line shows data from sea trials done in year 2017. Red and blue stipple lines show 95% Efron CIs.

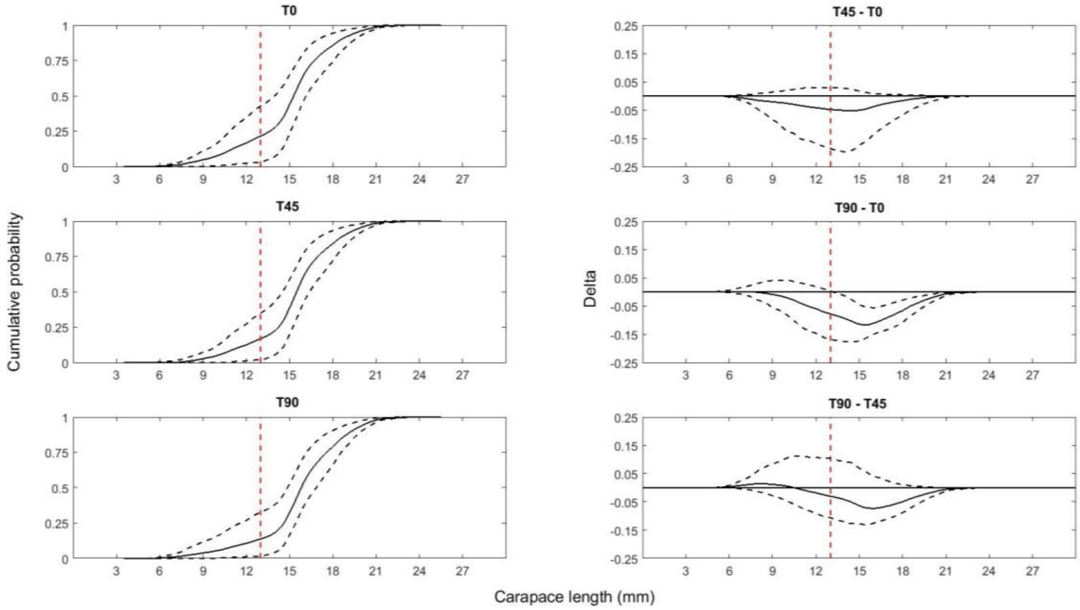

Figure 2.5. Cumulative capture population based on estimated average population in year 2016. (first column) and corresponding Delta curves (last column): thick black curve indicates the cumulative proportion of catch retained in each codend; stipple curves describe the 95% Efron CIs; vertical stipple line represents the MRS; Delta curves show pairwise comparison of cumulative capture populations.

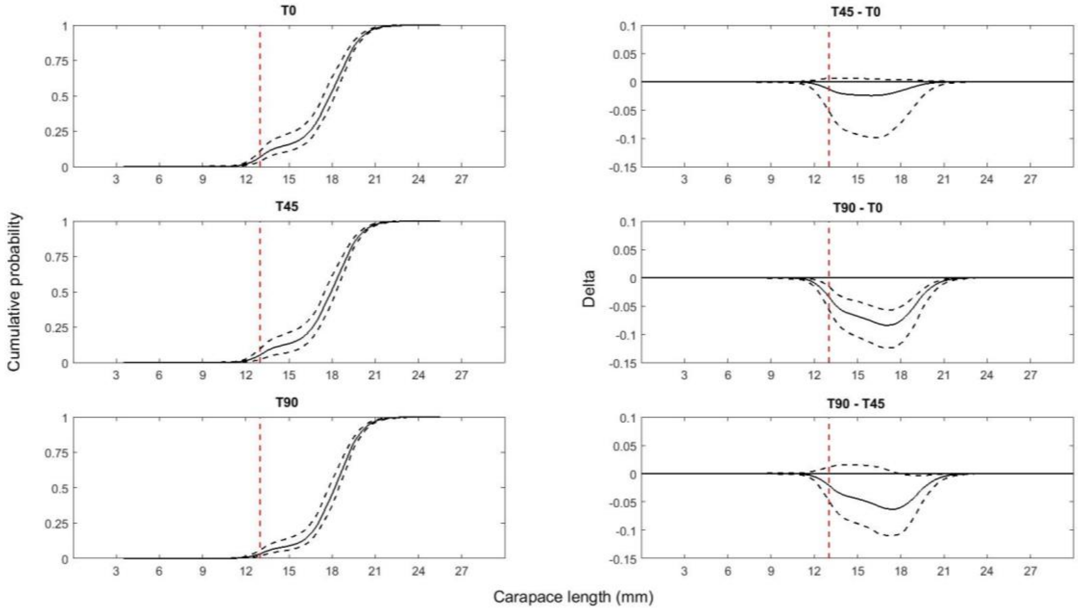

Figure 2.6. Cumulative capture population based on estimated average population in year 2017. (first column) and corresponding Delta curves (last column): thick black curve indicates the cumulative proportion of catch retained in each codend; stipple curves describe the 95% Efron CIs; vertical stipple line represents the MRS; Delta curves show pairwise comparison of cumulative capture populations.

CHAPTER 3. Comparing Size Selectivity of Traditional and Knotless Diamond-mesh Codends in the Iceland Redfish (*Sebastes* spp.) Fishery

3.1 Abstract

The size selectivity and usability of two diamond mesh codends, a traditional two-panel codend versus a four-panel ultra-cross knotless mesh codend, were compared using the covered codend method in the Iceland redfish (*Sebastes norvegicus and S. viviparous*) fishery. Results showed that there was no significant difference in size selectivity between the codends at lengths greater than 29 cm for *S. norvegicus* and 19 cm for *S. viviparous*. At smaller lengths, size selectivity was undetermined due to small catches at those sizes. For *S. norvegicus*, both codends demonstrated a high retention ratio (93.4 and 92.9%, respectively) above the minimum reference length (MRL; 33 cm), but also had a high retention below MRL (90.9 and 83.4%, respectively). However, the actual proportion of catch below MRL was low due to few small fish on fishing grounds. Since these fish are difficult to tell apart and have similar morphologies, we investigated the size selectivity of the two codends for both species combined, resulting in similar results of no difference in size selectivity, but a large increase in actual catches below MRL, which were primarily *S. viviparous*. This study concludes that the experimental codend does not improve the size selectivity or usability in the Iceland redfish fishery and both codends will retain large proportions of undersized fish if present on fishing grounds; however, few undersized fish were present in the study area.

3.2 Introduction

One of the key industries in Iceland is fishing (Sigfusson et al., 2013), and the redfish (*Sebastes* spp.) trawl fishery is one of its largest fisheries in terms of capture volume and value (FAO, 2010). Three redfish species are present in Icelandic waters: golden redfish (*Sebastes norvegicus*), Norway redfish (*S. viviparous*) and deepwater redfish (*S. mentella*). Currently, golden and deepwater redfish are targeted commercial species, while Norway redfish is unwanted due to its small size (MFRI, 2018a). All three species grow slowly and mature late, and they are difficult to differentiate due to similarities in meristic and morphological characteristics (Pampoulie and Daníelsdóttir, 2008; Christensen et al., 2018).

The Icelandic redfish fishery requires a minimum diamond-shaped codend mesh size of 135 mm (Ciccia Romito et al., 2015), and discarding is prohibited (ICNAF, 1975). Additional regulations for golden redfish include a minimum reference length (MRL) of 33 cm; if more than 20% in number in the catch is below the MRL, a closure will incur on fishing grounds (MFRI, 2018a). The unwanted capture of small redfish can be problematic for fishers that cannot discard small fish, and redfish population abundance due to the slow growing and late maturing nature of the species group. Additionally, when the relatively smaller Norway redfish (rarely > 30 cm; MFRI, 2018a) is mixed with the larger, targeted species, it can lead to further unwanted catch. Improvements in the size selectivity of Icelandic trawls is necessary to prevent the capture of small redfish.

Redfish size selectivity has been previously investigated, and several modifications have been attempted to improve the size selectivity of redfish trawls. Icelandic and Greenland redfish fisheries have had mesh selectivity studies dating as far back as the 1960s and 1970s (Bohl, 1961; Thorsteinsson, 1980). More recently, Lisovsky (2001) and Lisovsky et al. (2005) found that mesh size can affect redfish size selectivity. Other codend size selectivity studies investigated the effects of lastridge ropes (Hickey et al., 1995), and the size selectivity of three different diamond-shaped mesh sizes in the Gulf of Maine redfish fishery (Pol et al., 2016).

Compared with conventional diamond-mesh codends, knotless codends may have better size selectivity for roundfish. The shape and opening of the traditional knotted codend may be affected by the knot, making it more difficult for juvenile or undersized fish to escape through the mesh. Without the knot, knotless netting has a larger opened area, which could potentially increase the ability for undersized fish to escape. Additionally, knotless codends may reduce abrasion and damage caused by contact with the knot, increasing selectivity and market value. The aim of this study was to compare the size selectivity and usability of a traditional diamond-shaped mesh codend versus a diamond-shaped mesh knotless codend in the Icelandic redfish fishery. An improvement in selectivity could increase this fishery's capture efficiency for redfish above MRL and reduce the capture of unwanted, small redfish below MRL (both *Sebastes norvegicus* and *S. viviparous*).

3.3 Materials and Methods

3.3.1 Sea Trials

Sea trials were conducted on the commercial stern trawler *Helga María AK-16* (length 54.4 m; gross tonnage 1469.7 t; engine power 2991 hp) from 6 to 10 May 2016 on commercial fishing grounds off southwest Iceland (Figure 3.1). Fishing locations were determined based on the captain's experience and were typical for the fishery. All hauls were carried out following routine commercial fishing procedures. For each haul, fishing time, towing speeds, and fishing depth were recorded following the protocols of Wileman et al. (1996). A GPS-logger tracked the vessel's movement over the entire fishing process for each haul. A catch sensor was mounted on the codend to estimate catch size in weight, and the trawl was hauled back when the catch weight reached about 2 t.

3.3.2 Gear Specifications

The traditional codend was made of double 6.2 mm diameter mesh in a two-panel configuration and the measured mesh size (stretched inside mesh opening between opposite knots) was 131 mm. The knotless codend was made of 9.4 mm diameter ultra-cross knotless mesh in a four-panel configuration, and the measured mesh size (stretched inside mesh opening between opposite knots) was 127 mm (Figure 3.2). The mesh size of the two codends was measured with an ICES OMEGA gauge prior to the sea trials (Fonteyne, 2005). Both codends were made by a local fishing company, Hampiðjan Iceland, and were in use in the local redfish (*S.* spp.) fisheries before the sea trials of this research were carried out.

The covered codend method was used for estimating the codend selectivity (Wileman et al., 1996). The dimensions of the cover were kept in line with the recommendations of Wileman et al. (1996). The cover attached to the codend had 50mm mesh sizes. To avoid the masking effect of the cover, flexible kites made of PVC-coated canvas (e.g., He, 2007; Grimaldo et al., 2009) were attached to the front, middle front and back parts of the cover, 16 kites in total (4×4). The trawl system used in the sea trials was similar with commercial trawls fishing in the area. The codends were the only difference between traditional and experimental gear, and differed in presence of knots, material, and number of panels (Fig. 3.2).

3.3.3 Catch Sampling

Catches from the codend and the cover of each haul were processed separately on board the vessel. After hauling up, catches from the cover were emptied first; then codend catches were deposited on separated areas of the deck. All the catches were sorted by species, and the total number of each species were recorded for the codend and the cover separately. Total length of full or subsamples of the species was measured to the nearest cm below. The whole catches were measured if the number of individuals were below or around 200 in the codend or cover; otherwise random sub-sampling was applied.

3.3.4 Analysis of Size Selection Data

The applied experimental design enabled analysis of the collected catch data as binomial data, where individuals either are retained by the codend cover or by the codend itself, and are used to estimate the size selection in the codend (i.e., length-dependent retention probability). The probability of finding a fish of length l in a codend in haul j is expressed by the function $rj(l)$. The purpose of the analysis is to estimate the values of this function for all relevant sizes and species individually. Thus, the analysis was conducted separately for each species and codend following the description below.

Between hauls with the same codend, the value of $rj(l)$ is expected to vary (Fryer, 1991). In this study, we were interested in the length-dependent values of $r(l)$ averaged over hauls with the same codend, since this would provide information about the average consequences for the size selection process when applying the codend in the fishery. Thus, it was assumed that the size selective performance of the codend, for the hauls conducted, was representative of how the codend would perform in a commercial fishery (Millar, 1993; Sistiaga et al., 2010).

Estimation of the average size selection over hauls $r_{av}(l)$ involved pooling data from the different hauls (Herrmann et al., 2012). Since we tested different parametric models for $r_{av}(l)$, we write $r_{av}(l,\boldsymbol{v})$, where $\boldsymbol{v}$ is a vector consisting of the parameters of the model. The purpose of the analysis is to estimate the values of the parameter v that make experimental data (averaged over hauls) most likely to be observed, assuming that the model is able to describe the data sufficiently well. Therefore, expression (3.1) was minimized with respect to parameters $\boldsymbol{v}$, which is equivalent to maximizing the likelihood for the observed data in form of the length-dependent number of fish retained in the codend (nR_{jl}) versus those escaping to the cover (nE_{jl}):

$$-\sum_{j=1}^{m}\sum_{l}\left\{\frac{nR_{jl}}{qR_j}\times ln\big(r_{av}(l,\boldsymbol{v})\big)+\frac{nE_{jl}}{qE_j}\times ln\big(1.0-r_{av}(l,\boldsymbol{v})\big)+\right\} \qquad (3.1)$$

Where the outer summation is over the m hauls conducted and the inner over length classes l. qR_j and qE_j are the sampling factors for the fraction of the fish length measured in the codend and cover respectively.

Four basic selectivity models were tested to describe $r_{av}(l,\boldsymbol{v})$ for each codend and species individually: Logit, Probit, Gompertz and Richard (Eqs. 3.2), which assume that all individual fish entering the codend are subjected to the same size selection process. More information about the four selection models can be found in Wileman et al., (1996).

$$
r_{av}(l,\boldsymbol{v}) = \begin{cases} Logit(l,\boldsymbol{v}) \\ Probit(l,\boldsymbol{v}) \\ Gompertz(l,\boldsymbol{v}) \\ Richard(l,\boldsymbol{v}) \\ CLogit(l,\ C,\ \boldsymbol{v}) = \ 1.0\ -\ C\ +\ C\ \times\ Logit(l,\ \boldsymbol{v}) \\ DLogit(l,C_1,\boldsymbol{v}) = C_1 \times Logit(l,\boldsymbol{v}_1) + (1.0 - C_1) \times Logit(l,\boldsymbol{v}_2) \\ TLogit(l,C,\boldsymbol{v}) = C_1 \times Logit(l,\boldsymbol{v}_1) + C_2 \times Logit(l,\boldsymbol{v}_2) + (1.0 - C_1 - C_2) \times Logit(l,\boldsymbol{v}_3) \\ Poly4(l,\boldsymbol{v}) = \dfrac{exp\left(v_0 + v_1 \times \frac{l}{100} + v_2 \times \frac{l^2}{100^2} + v_3 \times \frac{l^3}{100^3} + v_4 \times \frac{l^4}{100^4}\right)}{1.0 + exp\left(v_0 + v_1 \times \frac{l}{100} + v_2 \times \frac{l^2}{100^2} + v_3 \times \frac{l^3}{100^3} + v_4 \times \frac{l^4}{100^4}\right)} \end{cases}
$$

(3.2)

Additional models tested include the CLogit model (Eqs. 3.2), where *C* represents the assumed length-independent contact probability with the codend meshes that provides fish with a length-dependent chance of escape (Bayse et al., 2016). *C* is a value from 0.0-1.0, and if *C* = 1.0, all fish were able to have sufficient contact with the codend meshes. For the double logistic model (DLogit), C_1 represents the fraction of fish entering the codend will be subjected to one logistic size selection process with parameters $\boldsymbol{v_1}$ while the remaining fraction (1.0 – C_1) will be subjected to an additional logistic size selection process with parameters $\boldsymbol{v_2}$ (Lipovetsky, 2010). Compared with DLogit, the triple logistic model (TLogit) introduces an additional size selection process, totaling three different processes C_1, C_2 and (1.0-C_1-C_2) probabilities of being the process that determine the codend size selection of the individual fish entering the codend (Frandsen et al., 2010). Finally, a quartic polynomial model (Poly4) was considered to estimate the codend size selection (Krag et al., 2015). For the Poly4 model, leaving out one or more of the parameters *v0…v4* in Eqs. 3.2 provided 31 additional models that were also considered as potential models to describe $r_{av}(l,v)$.

The capacity of a model to describe the data was inspected following the procedure of inspecting goodness-of-fit as described by Wileman et al. (1996). Therefore, the *p*-value representing the likelihood to obtain at least as big a discrepancy between the fitted model and the observed data by coincidence should not be below 0.05. In case of a poor statistical fit (p-value < 0.05), the residuals were inspected to determine whether the poor result was due to structural problems when modelling the experimental data using the different selection curves or if it was due to overdispersion in the data (Wileman et al., 1996). The most appropriate model for each species and codend was selected based on comparing Akaike information criterion (AIC) values, where the selected model had the lowest AIC (Akaike, 1974).

Once the specific size selection model was identified for a particular species and codend, bootstrapping was applied to estimate the confidence limits for the average size selection. We applied the software tool SELNET (Herrmann et al., 2012) for the size selection analysis and utilized the double bootstrap method implemented in this tool to obtain the confidence limits for the size selection curve and the corresponding parameters. This bootstrapping approach is identical to the one described in Millar (1993) and takes both within-haul and between-haul variation into consideration. The hauls for each codend were used to define a group of hauls. To account for between-haul variation, an outer bootstrap resample with replacement from the group of hauls was included in the procedure. Within each resampled haul, the data for each length class was bootstrapped in an inner bootstrap with replacement to account for within-haul variation. Each bootstrap resulted in a “pooled” set of data, which was then analysed using the identified selection model. Thus, each bootstrap run resulted in an average selection curve. For each species analysed, 1000 bootstrap repetitions were conducted to estimate the Efron percentile 95% confidence limits (Herrmann et al., 2012).

To compare the difference in length-dependent selectivity of the codends, $\Delta r(l)$ was estimated:

$$\Delta r(l) = r_{Kt}(l) - r_{Td}(l) \qquad (3.4)$$

where $r_{Kt}(l)$ is the size selectivity of the knotless codend, and $r_{Td}(l)$ is the selectivity of traditional codend. The 95% confidence intervals (CI) for $r_{Kt}(l)$ were estimated based on the bootstrap population results by the method described in Herrmann et al. (2018). The inspection of length class with a lack of overlap between 95% CI and 0.0 was conducted to determine whether there were any significant differences between codends.

3.3.5 Estimation of Usability Indicators

To evaluate how the tested codends would affect the specific fishery, three codend usability indicators, *nP-*, *nP+* and *nRatio* (Eqs 3.5-3.7) were calculated for species or species groups with a MRL. Contrary to the size selection properties, which provide information that is independent of the size structure of the population encountered by the gear, the indicators directly depend on the size structure of the population encountered during the sea trials providing additional information for the evaluation of the catch performance of each codend.

$$nP- = 100 \times \frac{\sum_j \{\sum_{l<MRL} nCd_{jl}\}}{\sum_j \{\sum_{l<MRL} (nCd_{jl} + nCv_{jl})\}} \quad (3.5)$$

$$nP+ = 100 \times \frac{\sum_j \{\sum_{l>MRL} nCd_{jl}\}}{\sum_j \{\sum_{l>MRL} (nCd_{jl} + nCv_{jl})\}} \quad (3.6)$$

$$nRatio = \frac{\sum_j \{\sum_{l<MRL} nCd_{jl}\}}{\sum_j \{\sum_{l>MRL} nCd_{jl}\}} \qquad (3.7)$$

where the summation of j is over hauls with a specific codend, and l over length classes. nCd_{jl} and nCv_{jl} represents the number of individuals of length l in haul j which found in respectively the codend and in the cover. $nP-$ and $nP+$ estimate the retention efficiency of the catch below and above MRL. *nRatio* represents the landings ratio between captured fish below and above MRL of the fished populations size structure.

These indicators evaluate the effects each codend has on the specific fishery. Ideally for a target species, $nP-$ and *nRatio* should be low (close to zero), while $nP+$ should be high (close to 100), i.e., all individuals over MRL that enter the codend are retained. The double bootstrapping method was used to estimate the Efron percentile 95% CI for the indicator values considering the effect of between-haul variation and that of the uncertainty related to within-haul variation (Herrmann et al., 2012).

3.4 Results

A total of twenty-one hauls were carried out during the sea trials, eleven with the traditional codend and ten with the experimental codend. The water depth of the towed area ranged from 290 to 396 m, the towing speed varied between 3.3 and 3.8 knots (average 3.6 knots), and the average towing duration was 54 min (26 - 115 min). Golden redfish and Norway redfish were the predominantly captured species for all hauls, with few other captured species, therefore they were the only species analysed (Table 3.1).

3.4.1 Golden Redfish

For golden redfish, the best model describing the size selection properties of the traditional codend was the TLogit, and the Poly4 model was the most appropriate model for the knotless codend (Table 3.2). Confidence intervals for the selection curves were very wide for lengths less than 29 cm (Figure 3.3). This was related to the relatively low number of small individuals captured by the codend and cover during sea trials. The selectivity performance of both codends could not be determined for these lengths. However, for lengths above 29 cm, CIs were narrow and Delta plots contained 0.0 within the CI, which means there was no significant difference in selectivity between codends (Figure 3.3).

3.4.2 Norway Redfish

For Norway redfish, size selectivity for the traditional and experimental codends was best described by the TLogit model (Table 3.2). Similar to golden redfish, high CIs were observed for small length classes (< 19 cm). Therefore, size selectivity of these length classes could not be determined. For lengths greater than 19 cm, CIs were relatively smaller, and the Delta plot contained 0.0, showing that there was no significant difference between codends (Figure 3.3).

3.4.3 Two Species Combined

Since these two species have similar morphological features, and are difficult to tell apart, especially when mixed together on the same fishing grounds, we combined both species to understand the size selectivity observed under commercial fishing operations, where species identification is not a priority. The best fit model for the traditional codend was the TLogit, the DLogit for the experimental codend (Table 3.2). The population structure contained two modes

(Figure 3.3), and this represents the difference in size between the two species with little overlap in the fished population. Confidence intervals were quite large throughout most of the length classes (< 49 cm), and the Delta plot contained 0.0 showing no significance in size selectivity between codends.

3.4.4 Usability Indicators

For golden redfish, the traditional codend retained 93.4% of individuals above MRL whereas the experimental codend retained 92.9% (*nP+;* Table 3.3). Both codends showed a high retention ratio for fish below MRL (*nP-*; 83.4 and 90.9%, respectively). The ratio of catches under MRL to catches over MRL was near 0.0 for each codend (*nRatio*; 0.01 and 0.02, respectively). No significant differences between usability indicators were observed for golden redfish. Codend usability could not be determined for Norway redfish since they do not have a MRL.

Codend usability was investigated for both species when combined. An MRL of 33 cm was used and assumed no difference in species (i.e., if a fish was below 33 cm it was considered only an undersized redfish, and which species was not considered). The retention of fish above MRL (*nP+*) for the traditional codend was 87.3% versus 74.0% for the experimental, but not significantly different. For fish below MRL (*nP-*), the traditional retained 83.8% and the experimental 53.8%, a difference of 30% but not significant due to CIs overlapping (Table 3.3). *nRatio* for the traditional was 0.70 and 0.54 for the experimental, also not significantly different.

3.5 Discussion

Size selectivity and usability of the traditional and experimental codends were compared for golden and Norway redfish separately, and combined in Iceland waters. According to the selection curves and delta plots, no difference in size selectivity was observed between the codends. For golden redfish, both codends presented a high retention ratio of catch above MRL (*np+*; above 80%) and low discard-to-landings ratios (*nRatio;* less than 0.03), both the aim of a commercial fishery. This scenario can be explained by two factors. First, both codends caught mostly golden redfish above MRL, retaining more than 85%. Second, juvenile and undersized golden redfish were rarely encountered in the fished population, which led to the low *nRatios*.

The measured codend meshes had similar openings (131 vs.127 mm), but differed in material and the presence of knots. Differences in twine diameter can affect selectivity (Herrmann and O'Neill, 2006). While twine diameter was arranged differently between codends, double vs single twine, the practical size of each twine's diameter was very similar. The experimental twine diameter was 9.4 mm, and the traditional twine diameter was 6.2 mm of double twine. According to O'Neill et al. (2005), to estimate double twine diameter requires applying the formula $1+2/\pi$ to the single twine diameter, which in this case equals 10.1 mm, a difference of only 0.7 mm, which likely had a negligible effect on size selectivity. These results should be interpreted as the difference between two codends, not simply the difference between the presence or absence of knots. However, each codend had similar mesh openings and twine diameters, therefore were made practically similar in these regards.

Due to current limitations of fishing gears and technology, golden and Norway redfish cannot be targeted separately, and are often mixed on fishing grounds. Therefore, fishers regard the two species as one for practical purposes. Additionally, fishers are not concerned with identifying redfish to the species level – interest is only on size. Thus, combining and analysing the two species together is of practical significance. Based on the selection curves and delta plots of the combined species, the size selectivity of the traditional codend trended higher for all size classes < 44 cm, but the difference was not significant due to the confidence intervals containing 0.0. The lack of significance could be due to the small overlap between the length classes for each species on the fishing grounds. From 28 to 32 cm, few redfish of either species were captured. These lengths represent the maximum length of Norway redfish, which are rarely captured, and combined with few captured golden redfish less than 33 cm leads to more complicated selectivity models that allow curves, or bends, due to changes in selectivity and likely lead to lower confidence estimations when combined with the multimodal distribution.

Codend usability indicators, *nP-* and *nP+*, for the combined species analysis decreased when compared with analysis for just the golden redfish. Although the addition of Norway redfish did not lead to significant changes in codend usability between codends, each value did drop when compared to the golden redfish analysis, with the experimental codend having the largest decrease, 29% less *nP-* and 19% less *nP+* than for the golden redfish alone. This comparison presents a clearer indication of the bycatch that is incurred in this fishery, since the Norway redfish and small golden redfish are unwanted catch.

Another indicator, *nRatio*, greatly increased when comparing both species versus golden redfish alone. These increases can be considered almost entirely from the addition of Norway redfish capture due to golden redfish having *nRatio* values less than 0.02 for each codend, and values greater than 0.54 for each codend when including Norway redfish. This increase proved that both codends retained high catch amounts of small fish, and if a similar selection (morphology) between both species of equal size was considered (which has been suggested by Herrmann et al. 2012 for several redfish species), small golden redfish would have been captured if they were encountered in the fishery.

The research to date on trawl selectivity for redfish (*Sebastes* spp.) using knotless netting was limited. One study compared a 122 mm knotless mesh codend made of “Perlon” for redfish versus several other knotted codends of varying size and material in the Denmark Strait (Bohl, 1961). While results were positive for this codend compared to braided Perlon codends and manila codends of larger mesh sizes, these results suffer from low sample sizes (5 hauls) and are difficult to compare with our work using modern material and analytical techniques.

The experimental codend did not improve the selectivity in the Icelandic redfish fishery, nor did it capture significantly less commercial-sized redfish. Thus, these codends should be considered equal in terms of selectivity of redfish and the transition to knotless mesh should only be considered for positive gains in fuel efficiency or to reduce damage to fish from contact with the knot, neither of which were investigated in this study. Further, future research should be concentrated on avoiding the capture of Norway redfish and small golden redfish due to the lack of selectivity observed in this study for small-sized redfish.

Although this study did not show any changes in size selectivity between the tested codends, reporting these results is valuable from both the management and fishing industry perspective; it enhances our understanding of fishing gear selectivity and particularly for this fishery; it provides guidance on what fishing strategies can be used to limit the capture of small redfish.

3.6 Acknowledgements

We would like to thank the staff from Hampiðjan Iceland and Hampiðjan Canada. Thanks are also extended to crew of the commercial trawler *Helga Maria AK-16* and HB-Grandi for providing the trawler and codends. This study was supported by Marine and Freshwater Research Institute (Iceland) and was partially funded by Ocean Frontier Institute (Sustainable Fisheries Theme, Module H) and Research & Development Corporation of Newfoundland and Labrador.

3.7 References

Akaike, H., 1974. A new look at the statistical model identification. IEEE Trans. Auto. Control, 19, 716-723.

Bayse, S.M., Herrmann, B., Lenoir, H., Depestele, J., Polet, H., Vanderperren, E., Verschueren, B., 2016. Could a T90 mesh codend improve selectivity in the Belgian beam trawl fishery? Fish. Res., 174, 201-209.

Bohl, H. 1961. German mesh selection experiments on redfish. Coun. Meet. ICES, Comp. Fish. Comm., Doc. Nr., 88, 1991.

Broadhurst, M.K., Millar, R.B., Kennelly, S.J., Macbeth, W.G., Young, D.J., Gray, C.A., 2004.

Selectivity of conventional diamond-and novel square-mesh codends in an Australian estuarine penaeid-trawl fishery. Fish. Res., 67, 183–194.

Christensen, H.T., Rigét, F., Backe, M.B., Saha, A., Johansen, T., Hedeholm, R.B., 2018. Comparison of three methods for identification of redfish (*Sebastes mentella* and *S. norvegicus*) from the Greenland east coast. Fish. Res., 201, 11-17.

Ciccia Romito, V., Assessor Dankert Skagen, L., Geraldine Criquet, A., 2015. FAO-Based Icelandic Responsible Fisheries Management Redfish Surveillance Report.

Fishery and Aquaculture Country Profiles. Iceland, 2010. Country Profile Fact Sheets. In: FAO Fisheries and Aquaculture Department. Rome.

Fonteyne, R., 2005. Protocol for the use of an objective mesh gauge for scientific purposes. ICES Cooperative Research Report No. 279, 8p. ISBN 87-7482-044-3.

Frandsen, R.P., Herrmann, B., Madsen, N., 2010. A simulation-based attempt to quantify the morphological component of size selection of *Nephrops norvegicus* in trawl codends. Fish. Res., 101, 156-167.

Fryer, R.J., 1991. A model of between-haul variation in selectivity. ICES J. Mar. Sci., 48, 281-290.

Grimaldo, E., Larsen, R.B., Sistiaga, M., Madsen, N., Breen, M., 2009. Selectivity and escape percentages during three phases of the towing process for codends fitted with different selection systems. Fish. Res., 95, 198-205.

He, P., 2007. Selectivity of large mesh trawl codends in the Gulf of Maine I: Comparison of square and diamond mesh. Fish. Res., 83, 44-59.

Herrmann, B., Sistiaga, M., Nielsen, K.N., Larsen, R.B., 2012. Understanding the size selectivity of redfish (*Sebastes* spp.) in North Atlantic trawl codends. J. Northwest Atl. Fish. Sci., 44, 1–13.

Herrmann, B., Krag, L.A., Krafft, B.A., 2018. Size selection of Antarctic krill (*Euphausia superba*) in a commercial codend and trawl body. Fish. Res., 207, 49-54.

Herrmann, B., O'Neill, F.G., 2006. Theoretical study of the influence of twine thickness on haddock selectivity in diamond mesh cod-ends. Fish. Res., 80, 221-229.

Hickey, W.M., Boulos, D.L., Brothers, G., 1995. A Study of the Influence of Lastridge Ropes on Redfish Selectivity in a Bottom Trawler. Can. Tech. Rep. Fish. Aquat. Sci., No. 2076, 25p.

ICNAF, 1975. Minimum Fish and Mesh Size Regulation in Iceland. International Commission for the Northwest Atlantic Fisheries Comm. Doc. 75/19, Serial No. 3582.

Krag, L.A., Herrmann, B., Karlsen, J.D., Mieske, B., 2015. Species selectivity in different sized topless trawl designs: Does size matter? Fish. Res., 172, 243-249.

Lisovsky, S., 2001. On optimal mesh size when fishing redfish in the Atlantic. NAFO SCR Doc., 01/21, Serial No. N4389, 16p.

Lipovetsky, S., 2010. Double logistic curve in regression modeling. J. Appl. Stat. 37, 1785-1793.

Lisovsky, S.F., Pavlenko, A.A. Vaskov, M.S., 2005. On the minimal trawl codend mesh size in the fishery of redfish species in Division 3O of the NAFO Regulation Area. NAFO SCR Doc., 05/18, Serial No. N5099, 17 p.

MFRI, 2018a. MFRI Assessment Reports 2018 on Golden redfish, Technical Report. Marine and Freshwater Research Institute, Reykjavik, Iceland.

MFRI, 2018b. MFRI Assessment Reports 2018 on Demersal beaked redfish, Technical Report. Marine and Freshwater Research Institute, Reykjavik, Iceland.

MFRI, 2018c. MFRI Assessment Reports 2018 on Norway redfish, Technical Report. Marine and Freshwater Research Institute, Reykjavik, Iceland.

Millar, R.B., 1993. Incorporation of between-haul variation using bootstrapping and nonparametric estimation of selection curves. Fish. Bull., 91, 564-572.

ICNAF, 1975. Minimum fish and mesh size regulation in Iceland. International Commission for the Northwest Atlantic Fisheries Comm. Doc. 75/19, Serial No. 3582.

O'Neill, F.G., Knudsen, L.H., Wileman, D.A., McKay, S.J., 2005. Cod-end drag as a function of catch size and towing speed. Fish. Res., 72, 163-171.

Pampoulie, C., Daníelsdóttir, A.K., 2008. Resolving species identification problems in the genus *Sebastes* using nuclear genetic markers. Fish. Sci., 93, 54-63.

Pol, M.V., Herrmann, B., Rillahan, C., He, P., 2016. Impact of codend mesh sizes on selectivity and retention of Acadian redfish *Sebastes fasciatus* in the Gulf of Maine trawl fishery. Fish. Res., 184, 54-63.

Sigfusson, T., Arnason, R., Morrissey, K., 2013. The economic importance of the Icelandic fisheries cluster-Understanding the role of fisheries in a small economy. Mar. Pol., 39, 154-161.

Sistiaga, M., Herrmann, B., Grimaldo, E., Larsen, R.B., 2010. Assessment of dual selection in grid based selectivity systems. Fish. Res., 105, 187-199.

Thorsteinsson, G., 1980. Icelandic bottom trawl and Danish seine cod-end selection experiments on cod, haddock, redfish and plaice in 1972-1976. ICES Fish Capture Comm. 14. ICES. C.M. 1980/B3.

Wileman, D.A., Ferro., R.S.T., Fonteyne, R., Millar, R.B., 1996. Manual of methods of measuring the selectivity of towed fishing gears. ICES Coop. Research Rep., No. 215, 126p.

Table 3.1. Overview of the 21 hauls with towing duration and depth, and number of length measurements obtained for each species. *indicates that data were not available. *nCd* is the number of individuals in the codend; *nCv* is the number of individuals in the cover; *sRd* is the sampling ratio of the codend; *sRv* represents the sampling ratio of the cover.

Haul ID	Codend	Depth (m)	Towing duration (min)	Golden redfish				Norway redfish			
				nCd	sRd	nCv	sRv	nCd	sRd	nCv	sRv
1	Traditional	337	44	250	0.403	34	1.000	201	0.282	203	0.510
2	Traditional	290	115	200	0.104	182	1.000	43	0.112	107	0.294
3	Traditional	310	34	220	0.014	203	0.501	166	0.719	101	0.564
4	Traditional	311	44	200	0.027	200	0.188	4	0.085	101	0.168
5	Traditional	297	57	219	0.030	200	0.284	79	0.026	100	0.029
6	Traditional	304	48	209	0.030	206	0.530	4	0.029	159	0.513
7	Traditional	312	49	203	0.024	199	0.505	136	0.070	120	0.093
8	Traditional	310	68	203	0.377	212	0.555	99	0.066	107	0.053
9	Traditional	317	51	180	0.052	206	0.904	133	0.049	164	0.406
10	Traditional	318	51	186	0.048	200	0.475	55	0.044	164	0.139
11	Traditional	342	92	185	0.310	182	1.000	67	0.072	110	0.137
12	Experimental	338	61	190	0.107	29	1.000	110	0.060	110	0.224
13	Experimental	336	26	200	0.028	145	1.000	138	0.052	161	0.095
14	Experimental	303	43	222	0.733	62	1.000	92	0.526	196	0.269
15	Experimental	*	31	156	0.223	29	0.058	10	0.222	131	0.102
16	Experimental	329	51	186	0.032	187	0.588	72	0.032	174	0.072
17	Experimental	329	68	170	0.034	204	0.586	90	0.034	185	0.066
18	Experimental	396	76	159	0.017	196	0.359	57	0.017	122	0.042
19	Experimental	318	29	133	0.009	130	0.115	59	0.009	100	0.009
20	Experimental	310	52	171	0.083	152	1.000	33	0.180	117	0.047
21	Experimental	*	52	188	0.049	199	0.337	83	0.146	143	0.080

Table 3.2. Akaike's information criterion (AIC) for each model for each species or species group. Selected model in bold.

Species	Codend	Logit	Probit	Gompertz	Richard	DLogit	TLogit	CLogit	Poly4
S. norvegicus	Traditional	31,976	31,975	31,976	31,977	31,902	**31,887**	31,977	31,962
	Experimental	26,839	26,823	26,843	26,818	26,792	26,799	26,812	**26,788**
S. viviparus	Traditional	31,845	31,844	31,834	31,837	31,756	**31,730**	31,847	31,783
	Experimental	63,407	63,408	63,409	63,406	63,250	**63,203**	63,371	63,372
Both species	Traditional	23,832	23,893	23,769	23,618	23,206	**23,094**	23,420	22,972
	Experimental	11,094	11,089	11,097	11,062	**10,943**	10,949	11,066	10,929

Table 3.3. Codend usability indicators with fit statistics for each species. "Na" means data are not available since there is no MRL for *S. viviparus.* Numbers in () represent the 95% CI for the estimated data.

	S. norvegicus		*S. viviparus*		Both species	
Codend	Traditional	Experimental	Traditional	Experimental	Traditional	Experimental
Model	TLogit	Poly4	TLogit	TLogit	Poly4	Poly4
nP+	93.4(88.6-96.3)	92.9(89.9-96.0)	Na	Na	87.3(55.5-93.7)	74.0(50.4-86.7)
nP-	90.9(82.2-96.3)	83.4(65.0-95.6)	Na	Na	83.8(41.6-93.8)	53.8(29.1-67.6)
nRatio	0.02(0.01-0.03)	0.01(0.00-0.01)	Na	Na	0.70(0.32-0.81)	0.54(0.36-0.59)
DOF	22	22	11	9	41	34
Deviance	13.7	58.1	22.1	41.5	190.8	133.0
p-value	0.911	<0.001	0.023	<0.001	<0.001	<0.001

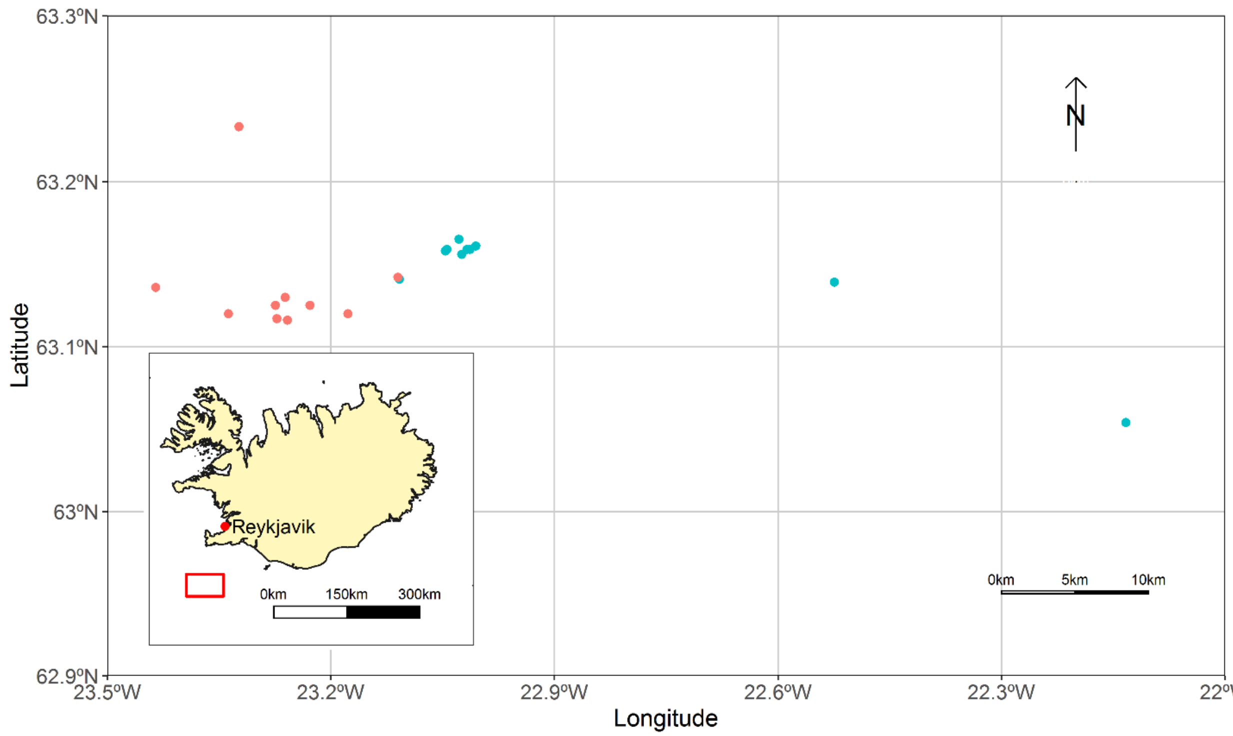

Figure 3.1. Location of fishing trials: green and orange spots indicate tow start locations; green spots = traditional codend; orange spots = experimental codend.

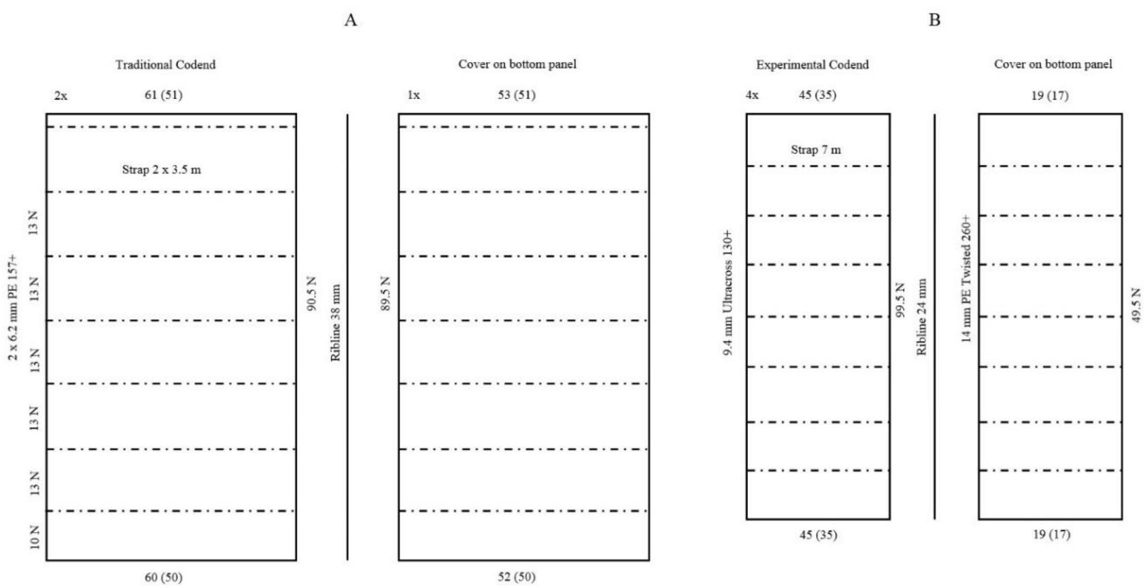

Figure 3.2. Schematic diagram of (A) traditional codend and (B) knotless codend (Right panel of each codend is the top panel for the cover; both codends were constructed by Hampidjan Iceland.

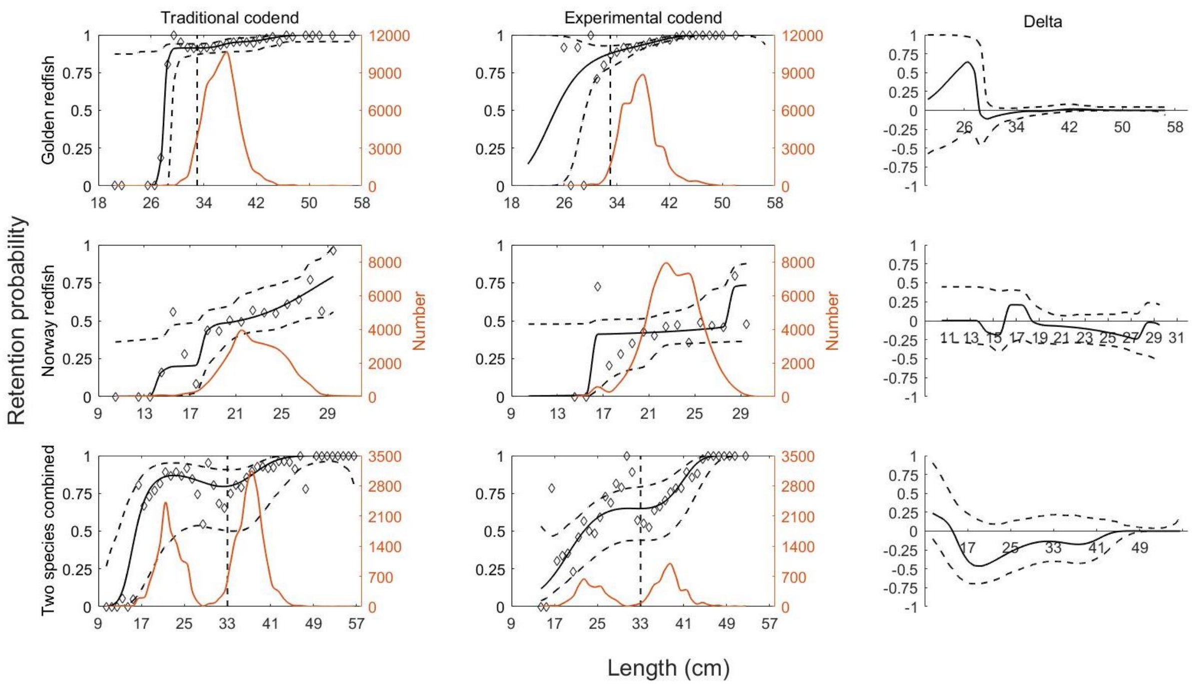

Figure 3.3. Size selection of *S. norvegicus* and *S. viviparus* in the traditional and experiment codends: Diamond symbols represent the experimental data; thick black curve indicates the fitted size selection curves; stipple curves describe the 95% confidence limits for the fitted size selection curves; vertical stipple line represents the MRL for *S. norvegicus*; brown curves shows the size distribution of the population encountered during sea trials.

CHAPTER 4. Out with the Old and In with the New: T90 Codends Improve Size Selectivity in the Canadian Redfish (*Sebastes mentella*) Trawl Fishery

4.1 Abstract

The size selectivity of four codends were compared in the Gulf of St. Lawrence, Canada redfish fishery, including the traditional diamond mesh codend with a mesh opening of 90 mm and three experimental codends of different nominal mesh sizes (90, 100, 110 mm) in which the netting is turned 90° to the direction of tow (T90). Results showed that the traditional codend had poor size selectivity, catching greater than 97% of redfish over all of the length classes observed. Considering the fished population, the smallest T90 codend would catch 30% fewer redfish under the minimum landing size (MLS) of 22 cm than the T0 codend, but would also lose 16% of catch above 22 cm. The size selectivity of the T90 codend with 100-mm mesh size did not significantly differ from that of the smallest T90 codend. The 110-mm T90 codend would catch 50% less redfish below MLS but lose 40% of redfish above. Overall, results show that T90 codends improve size selectivity in which large proportions of undersized fish are successfully released, reducing unintended fishing mortality of juvenile redfish.

4.2 Introduction

Three redfish species (*Sebastes* spp.) inhabit the Northwest Atlantic Ocean off the east coast of Canada: deepwater redfish (*S. mentella*), Acadian redfish (*S. fasciatus*) and golden redfish (*S. norvegicus*) (DFO, 1999). Historically, deepwater and Acadian redfish dominated the commercial redfish trawl fishery in the Gulf of St. Lawrence until a moratorium was imposed in 1995 due to low stock abundance and poor recruitment (DFO, 2018). However, recent large recruitment events in the 2010s (DFO, 2018), particularly for deepwater redfish, have led to large populations and an incipient commercial fishery.

Redfish are slow growing and long-lived, which makes them particularly susceptible to over-exploitation (DFO, 2011). Generally, redfish take 6 to 8 years to reach a length of 22 cm (regulated minimum landing size (MLS)), 7 to 10 years to reach maturity, and can live up to 50 years of age with a maximum length of 45-50 cm (Mayo et al., 1983; Gascon, 2003). Deepwater and Acadian redfish have biological, recruitment, and reproductive differences (COSEWIC, 2010), but due to an overlap in distribution and difficulties in distinguishing them with biological and morphological characteristics (Ni and Sandeman, 1984; DFO, 2011), they are managed as a single biological stock, known as Unit 1 redfish for the stock in Gulf of St. Lawrence (Brassard et al., 2017) and presently targeted commercially in index and experimental fisheries primarily using bottom trawls.

In the Gulf of St. Lawrence, the redfish trawl fishery started in the early 1950s (Brassard et al., 2017). The highest annual total landing of 136,000 t was recorded in 1973, and from 1977 to 1994 the average annual landings decreased to 37,000 t, leading to a fishery closure in 1995 of Unit 1 (DFO, 2018). After the fishery was closed, an index fishery began in 1998 with a total allowable catch (TAC) of 2,000 t/year. An experimental fishery was also recently established with an additional TAC of 2,500 t for 2018-2019 and 3,950 t for 2019-2020. Both fisheries have resulted in annual landings of less than 1,000 t/year to date (DFO, 2020). The modal size is currently 23 cm and if anticipated growth continues, 62% of the biomass should be larger than

25 cm by 2020 (DFO, 2020). Prospects for the deepwater redfish fishery are positive, although catches of Acadian redfish are expected to remain at cautious levels (DFO, 2020).

Several conservation measures are currently implemented in the Unit 1 redfish fishery, including seasonal spawning closures, a small fish protocol, 100% dockside monitoring, 10% on-board observer coverage, bycatch protocols, and a minimum inside stretched diamond mesh size of 90 mm (DFO, 2016). However, recent size-selectivity studies suggest that the 50% length retention (L50) with a 90 mm mesh size is well below 22 cm for Acadian redfish in Gulf of Maine (Pol et al., 2016). Considering that the fishery was previously closed due to a large decline in biomass and catch (Duplisea et al., 2016), and the proportion of small fish landed may have been underestimated (Duplisea, 2018), reopening the Gulf of St. Lawrence redfish fishery to commercial size catch limits with a different codend mesh size or shape should be considered.

Most of the size selectivity of trawls takes place in the codend (Glass, 2000) and several studies have investigated the codend size selectivity of redfish (see review by Herrmann et al., 2012). Beyond size of the meshes, several characteristics of codends can affect size selection. Bohl (1961) investigated knotless and knotted diamond mesh codends on the East Greenland redfish fishery and found that knotless codends had a smaller selection range than knotted codends. However, Cheng et al. (2019) showed no difference in size selectivity of redfish with knotted versus knotless diamond codends in the Icelandic fishery. Hickey et al. (1995) compared the selectivity of diamond codends with and without shortened lastridge ropes in the Newfoundland redfish fishery and found that 90-mm mesh codend with shortened lastridge ropes performed the best with 1.1% of redfish below 23 cm (versus 13.3% without the shortened ropes) being retained. Larger mesh sizes with the shortened-lastridge ropes lost more commercial size fish when compared to 90-mm diamond mesh codends (Hickey et al., 1995). Recently, Pol et al. (2016) compared the size selectivity of three diamond-mesh codends with different mesh sizes for the Acadian redfish in the Gulf of Maine, and predicted the L50 of Acadian redfish over a large range of mesh sizes. Given the history of Canada's east coast fishery in Unit 1 and the L50 trend reported by Pol et al. (2016), we hypothesized that the size selectivity of the Gulf of St. Lawrence redfish fishery could be improved (i.e., catch fewer redfish under MLS) by using a different mesh configuration than the regulated 90 mm in the T0 orientation.

The previous research tested codend with the traditional orientation, or diamond shaped mesh, known as T0. Recent experiments have shown that rotating the diamond netting 90 degrees to the direction of tow (T90) has the potential to improve size selectivity for roundfish (i.e., reduce capture of small roundfish) compared to traditional T0 codends constructed of the same netting (e.g., Moderhak, 1997; Herrmann et al., 2007; Madsen et al., 2012; Tokaç et al., 2014). The T90 mesh orientation keeps meshes open under tension, allowing for more escape of small roundfish, while T0 meshes tend to close under tension, reducing L50 and increasing the selection range (Herrmann et al., 2007). Several studies have documented the effectiveness of T90 codends at improving the size selectivity of roundfish versus T0 codends (Tokaç et al., 2014; Wienbeck et al., 2014; Bayse et al., 2016). To our knowledge, the size selectivity of redfish, which is a roundfish, has not been tested in a scientific setting with a T90 codend.

The purpose of this study was to improve the size selectivity (i.e., reduce the capture of undersized redfish, <22cm) of the Unit 1 redfish fishery in the Gulf of St. Lawrence on the east coast of Canada. Thus, we conducted an at-sea experimental trial comparing the size selectivity of a traditional T0 codend used by industry against three experimental T90 codends of different mesh sizes. We discuss the results in relation to sustainable fishing practices and conservation-oriented fisheries management.

4.3 Materials and Methods

4.3.1 Sea Trials and Gear Specifications

Sea trials were conducted on commercial fishing grounds in the northeast corner of the Gulf of St. Lawrence, Canada (Fig. 4.1) onboard the commercial trawler *F/V Lisa M* (length 19.8 m; gross tonnage 122.5 t; engine power 700 hp). Fishing was carried out from 16 to 31 July 2019. Towing speeds, duration, fishing depth, warp length, and door spread were recorded for each haul. After each haul, the fishing gear was visually inspected and twisted or damaged hauls were deemed invalid and removed from further analysis. On average, haul duration was shorter than commercial fishing practices due to high catch volumes and limited experimental quotas. All hauls were conducted during daytime hours to reduce the effect diel vertical migration of redfish can have on demersal trawl catch rates (Aglen et al., 1999). Mesh sizes in the codends were measured prior to each fishing trip using an ICES OMEGA mesh gauge following procedures described by Fonteyne (2005).

Four codends were evaluated in this experiment, including one traditional (control) T0 codend used by industry and three experimental T90 codends of different mesh sizes (Fig. 4.2). All codends were in a four-panel configuration, and attached to its own extension section with the same nominal mesh size 110 mm. The extension section of the control codend was made of T0 netting while extensions of the experimental codends were made of T90. All codends and their extension nets were constructed of double-braided polyethylene (PE) twine with 4.6 mm Ø (diameter) and were made by the same manufacturer (Hampidjan Canada Ltd., Spaniard's Bay, NL, CA). The control codend was the traditional T0 codend typically used in Canadian east-coast redfish trawl fisheries. The nominal inside mesh size of the T0 codend was 90 mm (T0-90). The three experimental codends were made of T90 netting with different nominal mesh sizes: 90, 100 and 110 mm (termed as T90-90, T90-100 and T90-110, respectively). These experimental codends had the same number of meshes in circumference, but varied in the number of meshes deep (N-direction) to keep all codends appropriately the same length (Fig. 4.2). The lastridge ropes were 5% shorter in length than the selvedge of each net; the lastridge ropes of the T0 were made of 3-strand polypropylene rope (30 mm Ø) while all the lastridge ropes of T90 nets were made of DynIce Quicklines™ (Dyneema, 30 mm Ø) designed by Hampidjan Iceland (Reykjavík, Iceland).

Each codend was attached to the vessel’s commercial groundfish bottom trawl (Hi-Lift Balloon Trawl) for evaluation at-sea. The trawl had a headline length of 40.2 m and a fishingline length of 44.5 m. It was constructed with 170 mm diamond PE netting (3.5 to 4.0 mm twine Ø) throughout the forward panels and bellies of the trawl. Floatation was provided by 132 floats (20.3 cm Ø) mounted on the headline. A rockhopper footgear was attached to the fishing line of the trawl, consisting of rubber discs of varying Ø (36-41 mm), spacers, and chain. The trawl was towed using a pair of low-aspect Injector trawl doors (4 m^2, Injector Door Limited; Søvik, Norway). Distance between the doors was recorded for each haul using acoustic sensors mounted on the doors (Notus Electronics Ltd., St. John's, NL, CA).

The covered codend method was applied in order to enable the estimation of codend size selectivity (see Wileman et al., 1996). This method employs a small-mesh cover over the codend being evaluated as a means to collect all of the fish escaping from the codend. The cover in this study was a 2-seam design made of single 2.5 mm Ø PE twine with a nominal mesh size of 50 mm. A total of 29 flexible kites were mounted around the circumference of the cover net to expand the cover and avoid masking of the codend meshes (e.g., He, 2007; Grimaldo et al., 2009). The cover net was attached to the extension part of the codend and was 1.5 times the length of the longest codend.

4.3.2 Catch Sampling

Catch from the codend and the cover were processed separately. The cover and the codend were loaded aboard the vessel together but the catch from the cover was emptied first. For the catch from the cover, redfish were separated from bycatch species and total weights were taken for the entire catch by species. Random subsamples of redfish were taken from each net compartment, and the number of individuals of the subsample and each subsample weight were recorded. The fork length of the subsampled fish was measured to the nearest cm. Redfish species identification was conducted by an at-sea fisheries observer using anal fin ray counts (Rubec et al., 1991).

4.3.3 Selectivity Data Analysis

The size selectivity data were analyzed using the software SELNET (Herrmann et al., 2012). We assumed that the probability of each redfish being retained after entering the codend was independent, and that the number of individuals of a specific length class remained in the codend or the cover has a binomial distribution, i.e., length-dependent retention probability. For the individual haul j, the proportion of redfish of length l retained in the codend is modelled with function $r_j(l,\boldsymbol{v})$, where $\boldsymbol{v}$ is a vector representing two or more size selection parameters to be estimated (Herrmann et al. 2012). However, in this study, we were interested in the length-dependent values of $r_j(l,\boldsymbol{v})$ averaged over hauls ($r_{av}(l,\boldsymbol{v})$) because this would provide information about the average consequences for the size selection process of applying different codends in the fishery. Therefore, it was assumed that the size-selective performance of a specific codend for all the individual hauls conducted within a trial was representative of how the codend would perform in a commercial fishery (Millar, 1993; Sistiaga et al., 2010).

Size selection was estimated by minimizing expression (4.1) with respect to parameters $\boldsymbol{v}$, which is equivalent to maximizing the likelihood for the observed data in form of the length-dependent number of redfish retained in the codend versus those escaping to the cover:

$$-\sum_{j=1}^{m}\sum_{l}\left\{\frac{nR_{jl}}{qR_j}\times ln\big(r_{av}(l,\boldsymbol{v})\big)+\frac{nE_{jl}}{qE_j}\times ln\big(1.0-r_{av}(l,\boldsymbol{v})\big)\right\} \qquad (4.1)$$

where the outer summation is over the m hauls conducted with the specific codend and the inner over length classes l. nR_{jl} and nE_{jl} are the number of redfish lengths measured in the codend and cover in haul j belonging to length class l. qR_j and qE_j are the sampling factors for the fraction of the redfish length measured in the codend and cover respectively.

Four basic selectivity models were tested to describe $r_{av}(l,\boldsymbol{v})$ for each codend: Logit, Probit, Gompertz, and Richard, which all assume that each individual entering the codend is subjected to the same size selection process (Wileman et al., 1996). How well the models fit the data was inspected using the goodness-of-fit procedure described by Wileman et al. (1996), where the *p*-value represented the likelihood to obtain at least as big a discrepancy between the fitted model and the observed data by coincidence should not be < 0.05. If a poor statistical fit was observed (*p*-value < 0.05), the residuals were inspected to determine whether the poor result was due to structural problems when modelling the experimental data using the different selection curves or if it was due to overdispersion in the data (Wileman et al., 1996). The most appropriate model for each codend was selected based on Akaike information criterion (AIC) values, where the selected model had the lowest AIC (Akaike, 1974). Once a size selection model was selected for the specific codend, uncertainty in the estimated size selection curve and parameters were obtained using a double bootstrapping technique (Millar, 1993; Herrmann et al., 2012). This technique accounts for both within and between haul variation in size selection (Fryer, 1991). One thousand bootstrap repetitions were used. Uncertainties were provided in terms of Efron 95% percentile confidence intervals (CIs; Efron and Tibshirani, 1986).

Length-dependent selectivity between codends was compared with Delta curves where $\Delta r(l)$ was estimated by Eq. 4.2.

$$\Delta r(l) = r_e(l) - r_c(l) \qquad (4.2)$$

where $r_e(l)$ and $r_c(l)$ are the size selectivity of two tested codends. The 95% CIs for $\Delta r(l)$ were estimated based on the bootstrap population of results for the individual codends compared by the double bootstrap method described above. For details on this procedure consult Herrmann et al. (2018). Significant differences in size selection between codends was determined if the 95% CIs for $\Delta r(l)$ had length classes that did not overlap 0.0.

4.3.4 Usability Indicators

Size selectivity curves estimate fish retention independent of the fished population. To infer how the tested codends would directly affect the fished population, three different indicators, *nP−*, *nP+*, *nRatio*, and *dnRatio* (Eqs. 3; Wienbeck et al., 2014) were calculated and are directly related to the fished population's size structure (*nPop(l)*). *nP−* and *nP+* estimate the retention efficiency of the catch below and above the MLS. Ideally, for any species the *nP−* should be low (close to 0, no undersized fish capture), and for target species the *nP+* should be high (close to 100, or full retention). *nRatio* represents the landings ratio (in numbers) of catch below and above MLS, and *nRatio* should be low (near 0) to show accordance between the MLS and fished gear. *dnRatio* calculates the discard ratio assuming all individuals are below or above MLS, and an appropriate codend should have a low *dnRatio*.

The indicators were estimated by,

$$\begin{cases} nP- = 100 \times \frac{\sum_{l<MRS}\{r_{codend}(l) \times nPop(l)\}}{\sum_{l<MRS}\{nPop(l)\}} \\ nP+ = 100 \times \frac{\sum_{l>MRS}\{r_{codend}(l) \times nPop(l)\}}{\sum_{l>MRS}\{nPop(l)\}} \\ nRatio = \frac{\sum_{l<MRS}\{r_{codend}(l) \times nPop(l)\}}{\sum_{l>MRS}\{r_{codend}(l) \times nPop(l)\}} \\ dnRatio = 100 \times \frac{\sum_{l<MRS}\{r_{codend}(l) \times nPop(l)\}}{\sum_{l}\{r_{codend}(l) \times nPop(l)\}} \end{cases} \quad (4.3)$$

where each indicator was estimated with uncertainties using a double bootstrap set to estimate 95% CIs. Significant differences between codends is determined when CIs do not overlap between indicator values. Indicator analyses were conducted with the software SELNET (Herrmann et al., 2012).

4.3.5 Meshed Fish

Every individual redfish that remained meshed in codend mesh was counted at the end of each haul. These data were considered count data and were analyzed with generalized linear mixed models (GLMMs) with R statistical software (R Development Core Team 2009) using the lme4 package (Bates et al., 2013). The dependent variable was the number of meshed fish, independent variable was codend, and the random effect was haul on the intercept. Data were initially fit with a Poisson distributed model with the glmer function and dispersion was estimated with the DHARMa package (Hartig, 2017), which approximates dispersion via simulations. If equidispersion (dispersion ~ 1.0) was determined, then the analysis continued with the Poisson distributed model. If overdispersion was observed (dispersion > 1.0), then the model was fit with a negative binomial model with the glmer function. Differences between codends was determined by a type II Wald χ^2-test (via the ANOVA function from the car package) at an α of 0.05. If a difference between codends was observed, a multiple comparison post hoc test was performed using the glht function in the multicomp package (Hothorn et al. 2008). Confidence intervals were estimated with bootstrapping via the bootmer function using 1,000 simulations deriving 95% CIs using the predict function.

4.4 Results

Forty-five hauls were successfully completed of which three were invalid due to a twisted net. Eleven hauls each were conducted with the T90-90 mm and T90-110 mm codends, and 10 hauls each for the T0-90 mm and T90-100 mm codends. The mean haul duration was 7.3 min (range: 4-18 min) at a mean velocity (speed over ground) of 2.4 knots (2.2-2.7 knots). The length of warp deployed ranged from 373 to 413 m (mean = 391 m) depending on the fishing depth, which ranged from 256 to 331 m and had a mean of 314 m. Door spread ranged from 114 to 130 m (mean = 121 m) (Table 4.1). The measured inside stretched mesh size before fishing was 95.0

mm (SD = 2.4) for T0-90, 93.6 mm (SD = 2.5) for T90-90, 104.6 mm (SD =2.9) for T90-100, and 110.7 mm (SD = 2.1) for T90-110.

Species identification by anal fin ray count showed that all redfish captured were deepwater redfish (C. Senay 2019: pers. comm.). Redfish was the predominant species captured for all hauls with very little bycatch observed (Table 4.2). Total weight of captured redfish was 27,798.2 kg, versus only 58.7 kg for all bycatch combined, less than 0.2% of the total catch. Bycatch consisted of 14 species, and white hake (*Urophycis tenuis*) had the highest total weight (Table 4.2). The total number of redfish measured was 23,976 with a size range of 16 to 40 cm. Reported catch-at-length were extrapolated based on sampling ratios for each codend (Fig. 4.3). Bycatch species were not captured in enough numbers to perform length analyses and thus their effect on selectivity is considered negligible.

4.4.1 Size Selectivity

Size selectivity results for each codend are presented in Figure 4.3. The T0-90 codend's best-fit model was the Gompertz (Table 4.3), and showed very high retention probability across all observed sizes of redfish, beginning at 88% (based on the lower CI) at 17 cm and increasing to 99% at MLS of 22 cm. The modal length of the population fished with T0-90 codend was 23 cm, and lengths ranged from 17 to 39 cm.

For the T90 codend with the smallest mesh size, T90-90, the best-fit model was the Richard (Table 4.3), and retention probability for redfish at 17 cm was close to 50% and rose to 77% at the MLS (Fig. 4.3). As redfish length increased to 30 cm, retention probability approached 1.

Most of fish in the sampled population for these hauls were at length 23 cm with a minimum length of 17 cm and a maximum of 37 cm.

For the T90-100 codend, the best-fit model was the Gompertz (Table 4.3), and the retention probability for redfish at 16 cm was 23%, increasing to 78% at the MLS. The T90-100 codend retained all redfish above 32 cm. The lengths of all individuals caught with this codend ranged from 16 to 35 cm with a mode of 23 cm.

The best-fit model for the T90-110 codend selectivity curve was the Probit (Table 4.3). This codend showed the lowest retention probability (56%) for redfish at the MLS compared to the other codends. Predicated retention probability for small redfish was similar to the T90-100, 23% at 17 cm. Retention probability approached 1 at a larger length (35 cm), than for the other codends. The length range of catch was from 17 to 40 cm with a mode of 22 cm.

The effect of changing codend mesh orientation from T0 to T90 on the size selectivity of redfish is shown in the Delta plot (Fig. 4.4). When comparing T0-90 and T90-90 codends, for lengths < 29 cm, the T90-90 codend retained significantly less redfish than the T0-90; no significant difference was detected for redfish > 29 cm between the two codends (Fig. 4.4). Compared with the T90-100 codend, T0-90 retained significantly more redfish at lengths < 32 cm, and there was no significant difference for fish > 32 cm. When comparing the T90-110 codend with the T0-90, redfish < 35 cm decreased significantly, with no difference between codends > 35 cm (Fig. 4.4).

Comparisons of the size selectivity between T90 codends suggested the effect of mesh-size change on the selection performance (Fig. 4.4). No significant difference in size selectivity between T90 codends was detected when the mesh size was increased from 90 to 100 mm. The T90-110 codend retained significant less redfish at lengths between 18 and 33 cm when compared to the T90-90, and significant less redfish at lengths between 19 and 29 cm than T90-100.

4.4.2 Usability Indicators

The usability indicators for each codend based on the fished population is listed in Table 4.4. The T0-90 codend had a high retention of undersized redfish (*nP-* > 97%), which was consist with its selectivity curve. When the mesh orientation was changed (from T0-90 to T90-90), *nP-* decreased about 30% while catch of redfish above the MLS (*nP+*) decreased about 16%. Increasing the T90 mesh size from 90 to 100 mm did not change the retention of undersized redfish, however the T90-110 had the lowest *nP-* (47%) among the tested codends, and the lowest *nP+* (60%). The difference between usability indicators *nP-* and *nP+* was significant among the codends except between the T90-90 and T90-100.

Changing the codend from T0-90 to T90-90 did not significantly affect the ratio of catches under MLS to catches over MLS (*nRatio*; 0.2 and 0.2, respectively). The *nRatio* increased significantly as the mesh size of T90 codends increased from 90 to 110 mm. The T90-110 codend had the highest *nRatio* (0.5) followed by T90-100 (0.3).

The discard ratio in number (*dnRatio*) was low for both the T0-90 and T90-90 codends, and did not differ between codends. The *dnRatio* increased by 8% when changing the mesh size of T90s from 90 to 100 mm, which was significant. Additionally, the T90-110 codend had relatively high *dnRatio* compared with the 90 mm codends (almost double). The difference of *dnRatios* between T90-100 and T90-110 was not significant.

4.4.3 Meshed Fish

Meshed redfish were observed in nearly all hauls (86%) and for each codend. The data were first fit with a Poisson model and were shown to be overdispersed (dispersion = 5.148, $p < 0.001$). Consequently, a negative binomial model was fit to the data and indicated that the T0-90 codend had the fewest number of meshed fish (predicted mean of 1.4). The T90-90 codend had the most meshed fish (predicted mean of 22.6), and the number of meshed fish gradually reduced for the larger T90 codends, predicted means of 16.2 and 8.9 for the T90-100 and T90-110, respectively (Table 4.5, Fig. 4.5). The post hoc test showed that the T0 codend had significantly fewer meshed redfish than all other codends (Table 4.5, Fig. 4.5). The number of meshed fish for the T90-90 codend did not significantly differ from the T90-100 codend, and the T90-110 codend had the significantly fewer meshed fish than each of the other codends except the T90-100 codend (Table 4.5, Fig. 4.5).

4.5 Discussion

This research documents the first known study that evaluates the size selectivity of a T90 codend in Canada's east coast redfish fishery. Our results demonstrate that the traditional T0 codend used by industry has a poor size selectivity for redfish, retaining more than 97% of undersized individuals. Changing the mesh orientation from T0-90 to T90-90 significantly reduced the catch of undersized redfish, which was accompanied by a 16% reduction in catch of commercial-sized fish. While increasing the T90 codend mesh size from 90 to 100 mm had no effect on the size selectivity of redfish, likely due to not a large enough change in mesh size to have an effect, increasing the T90 codend mesh size by 20 mm decreased the undersized catch by 20%, and reduced commercial catch by 22%. This research showed that the T90 codend could be a potential replacement to the T0 codend by improving the size selectivity of redfish and maintaining commercial catch rates.

With a large population of deepwater redfish currently in the Gulf of St. Lawrence, an incipient commercial redfish fishery is looking for measures to develop sustainable fishing practices. The application of a T90 codend is a clear improvement in terms of avoiding capture of small redfish. Additionally, while not the goal of this study, 100% of redfish captured were considered deepwater redfish. Given that Acadian redfish remain in the cautious zone of their precautionary approach (DFO, 2020), a fishery that can solely target deepwater redfish is currently preferable. It is noteworthy that both research surveys and our fishing trials have shown that the current size structure of the redfish population is dominated by a smaller length range than the Icelandic golden redfish fishery, which has larger sizes on average and larger maximum sizes (50+ cm) (Cheng et al., 2019). It may be beneficial to wait for the average size of redfish to increase before they are commercially exploited to fully avail of economic benefits and biological sustainability. DFO (2020) predicts that 62% of the biomass will be above 25 cm by 2020.

The narrow size range of redfish that is currently found in the Gulf of St. Lawrence elucidated some of the effects of changing codends in the redfish fishery, while others remain unclear. The lack of any fish below 16 cm compromised discard ratios (i.e., *nRatio and dnRatio*), where expected differences based upon clear changes in size-selectivity were not shown (see *nRatio and dnRatio* for T0-90 versus T90-90). Additionally, the lack of larger fish in the population could have a similar, but opposing effect on discard ratios. Clear differences were shown on how codend changes influence the capture of fish above and below MLS (i.e., *nP-* and *nP+*), but the magnitude of these differences could be quite different as this current population of redfish grows, and the addition of any future recruitment classes.

Meshed redfish has been reported as a serious problem in trawl fisheries (Isaksen and Valdemarsen, 1986; ICES, 2012), as well as other fisheries (Brčić et al., 2019). Meshed fish can affect size selectivity (Brčić et al., 2019) and generate negative impacts including increased processing time, damaged and unsalable fish, increased bycatch, and economic loss (Isaksen and Valdemarsen, 1986; Pol et al., 2016). Square-mesh codends have been avoided in the redfish fishery due to concerns of meshing, or called sticking (Pol et al., 2016). Since square mesh, similar to T90 mesh, remains more open than T0, the effect of sticking needed to be evaluated. The only other study to quantify meshed fish in terms of how it affects size selectivity used a three-compartment scenario for the probability of retention (captured, meshed, or escape) and predicted the mesh-sticking probability as a bell-shaped curve (Brčić et al., 2019). However, due to a relatively low number of meshed fish (< 30 per haul) and limited size range of observed fish that were meshed, we resorted to a count-based model to determine differences in meshed redfish between codends. Likely, as observed for other species by Brčić et al. (2019), redfish meshed probability follows a bell-shaped curve also, and these results should be considered for the fished population, which mostly consisted of fish from 20 to 26 cm. If smaller redfish were in the population, an increase in meshed fish would be expected for the T0-90 codend, and a corresponding change in meshed fish would be expected for the T90 codends.

The results of minimal bycatch and all redfish captured determined as deepwater redfish are positive outcomes for the fishery, and are results that are not likely driven by the experimental treatment (codend mesh orientation and size change). The study design, however, may have affected some of these results. Relatively deep areas were fished, which may have avoided Acadian redfish, and the choice of fishing bottom trawls only during the day may have reduced the capture of non-target species. According to Duplisea (2018), a midwater trawl with a T0 codend was commonly used in the redfish fishery during the 1980s and potentially doubled the catch rate of a bottom trawl; catch rates for bottom trawls targeting redfish at night can be comparatively low due to redfish migrating up the water column at night. Additionally, these midwater trawls may have had a higher catch rate of undersized redfish since small redfish are more concentrated higher in the water column (Duplisea, 2018). In addition, bottom trawls fished at night targeting redfish can have a larger catch rate of redfish (Duplisea, 2018). From these reports, there is insight into ways to improve the redfish fishery, and reducing the capture of undersized redfish and bycatch is not only accomplished by changing the codend mesh.

Decreasing the capture of undersized redfish by changing the codend mesh orientation may not be constrained to deepwater redfish targeted by a bottom trawl. Future research should test T90 codends in other redfish fishing grounds and for different redfish species, such as Acadian redfish in the United States or golden redfish in Iceland. These results could be contrasted against studies that used T0 codends, such as Pol et al. (2016) and Cheng et al. (2019). Additionally, using a T90 codend in a midwater trawl could reduce the capture of undersized redfish reported by Duplisea (2018) when using a midwater trawl versus a bottom trawl.

In conclusion, this study revealed that the regulated 90 mm T0 mesh codend (T0-90) currently used in Unit 1 redfish fisheries in the Gulf of St. Lawrence is not effective at releasing undersize redfish below the MLS of 22 cm. Improving the size selection performance of the codend is necessary for the sustainable development of this redfish fishery. Our results show that replacing the T0 codend with a T90 codend will significantly improve the size selectivity of redfish by reducing undersized catch. A change to a T90 codend will result some loss of commercial-sized catch, 16% for the 90 mm T90 codend with the current fished population. However, when compared to a poor-selective T0 codend, it is a great improvement for developing a sustainable redfish fishery.

4.6 Acknowledgements

We thank the captain and crew of the *F/V Lisa M* for their professional service. We are grateful to the many staff and graduate students who assisted with the study, including Vang Nguyen, Mark Santos, George Legge, Meghan Donovan, and Kelley Moret. We appreciate the assistance from Jason Spingle of Fish Food & Allied Workers Union (FFAW) and the at-sea observer Paul Stuckless. Special thanks to Caroline Senay, DFO/ IML in Quebec for access to redfish survey data. We also owe a special gratitude to Bent Herrmann for use of the SELNET software. Financial support for this project was provided by the Canada First Research Excellence Fund

(CFREF) through the Ocean Frontier Institute (Module H), as well as the Research and Development Corporation (RDC) of Newfoundland and Labrador (Ocean Industries Student Research Awards).

4.7 References

Aglen, A., Engås, A., Huse, I., Michalsen, K., Stensholt, B.K. 1999. How vertical fish distribution may affect survey results. ICES J. Mar. Sci., 56, 345–360.

Akaike, H. 1974. A New Look at the Statistical Model Identification. IEEE Trans. Auto. Control., 19, 716–722.

Bates D., Maechler M., Bolker B., Walker S. 2013. lme4: Linear mixed-effects models using Eigen and S4 [online]. R Foundation for Statistical Computing, Vienna, Austria. Available from https://cran.r-project.org/web/packages/lme4/index.html (accessed 26 November 2019).

Bayse, S.M., Herrmann, B., Lenoir, H., Depestele, J., Polet, H., Vanderperren, E., Verschueren, B. 2016. Could a T90 mesh codend improve selectivity in the Belgian beam trawl fishery? Fish. Res., 174, 201–209.

Bohl, H. 1961. German mesh selection experiments on redfish. Coun. Meet. ICES, Comp. Fish. Comm., Doc. Nr. 88, 1991.

Brassard, C., Bourdages, H., Duplisea, D., Gauthier, J., Valentin, A. 2017. The status of the redfish stocks (*Sebastes fasciatus* and *S. mentella*) in Unit 1 (Gulf of St. Lawrence) in 2015. DFO Can. Sci. Advis. Sec. Res. Doc. 2017/023. 53 p.

Brčić, J., Herrmann, B., Masanovic, M., Krstulovic Sifner, S., Baranovic, M., Škeljo, F. 2019. Mesh sticking probability in fishing gear selectivity: Methodology and case study on

Norway lobster (*Nephrops norvegicus*) and mantis shrimp (*Squilla mantis*) in the Mediterranean Sea creel fishery. Mediterr. Mar. Sci., 20, 487–495.

Cheng, Z., Einarsson, H.A., Bayse, S.M., Herrmann, B., Winger, P.D. 2019. Comparing size selectivity of traditional and knotless diamond-mesh codends in the Iceland redfish (*Sebastes* spp.) fishery. Fish. Res., 216, 138–144.

COSEWIC. 2010. COSEWIC assessment and status report on the Deepwater Redfish/Acadian Redfish complex *Sebastes mentella* and *Sebastes fasciatus,* in Canada. Committee on the Status of Endangered Wildlife in Canada, Ottawa. 80p.

DFO. 1999. Status of Redfish Stocks in the Northwest Atlantic: Redfish in Units 1, 2, and 3, and in Division 3O. DFO Can. Sci. Advis. Sec., Sci. Advis. Rep. 1999/A1-01.

DFO. 2011. Recovery potential assessment of redfish (*Sebastes fasciatus* and *S. mentella*) in the northwest Atlantic. DFO Can. Sci. Advis. Sec., Sci. Advis. Rep. 2011/044.

DFO. 2016. Assessment of redfish stocks (*Sebastes fasciatus* and *S. mentella*) in Units 1 and 2 in 2015. DFO Can. Sci. Advis. Sec. Sci. Advis. Rep. 2016/047.

DFO. 2018. Assessment of Redfish Stocks (*Sebastes mentella and S. fasciatus*) in Units 1 and 2 in 2017. DFO Can. Sci. Advis. Sec. Sci. Advis. Rep. 2018/032.

DFO. 2020. Redfish (*Sebastes mentella* and *S. fasciatus*) stocks assessment in Unit 1 in 2019. DFO Can. Sci. Advis. Sec. Sci. Advis. Rep. 2020/000.

Duplisea, D.E., Bourdages, H., Brassard, C., Gauthier, J., Lambert, Y., Nitschke, P.C., Valentin, A. 2016. Fitting a statistical catch at length model (NFT-SCALE) to Unit 1+2 redfish (*Sebastes mentella* and *Sebastes fasciatus*). DFO Can. Sci. Advis. Sec. Res. Doc. 2016/095.

Duplisea, D.E. 2018. Fishermen's historical knowledge leads to a re-evaluation of redfish catch. Mar. Coast. Fish., 10, 3–11.

Efron, B., Tibshirani, R. 1986. Bootstrap methods for standard errors, confidence intervals, and other measures of statistical accuracy. Stat. Sci., 1, 54-75.

Fonteyne, R. 2005. Protocol for the use of an objective mesh gauge for scientific purposes. ICES Cooperative Research Report, No. 279, 8p. ISBN 87-7482-044-3.

Fryer, R.J. 1991. A model of between-haul variation in selectivity. ICES J. Mar. Sci. 48, 281–290.

Gascon, D. 2003. Redfish multidisciplinary research zonal program (1995-1998): Final Report. Can. Tech. Rep. Fish. Aquat. Sci. 2462: xiii + 139 p.

Glass, C.W., 2000. Conservation of fish stocks through bycatch reduction: a review. Northeast. Nat., 7, 395–411.

Grimaldo, E., Larsen, R.B., Sistiaga, M., Madsen, N., Breen, M. 2009. Selectivity and escape percentages during three phases of the towing process for codends fitted with different selection systems. Fish. Res., 95, 198–205.

Hartig, F. 2017. DHARMa: residual diagnostics for hierarchical (multi-level/mixed) regression models[online]. R Foundation for Statistical Computing, Vienna, Austria. Available from https://cran.r-project.org/web/packages/DHARMa/vignettes/DHARMa.html (accessed 26 November 2019).

He, P., 2007. Selectivity of large mesh trawl codends in the Gulf of Maine I: Comparison of square and diamond mesh. Fish. Res., 83, 44-59.

Herrmann, B., Krag, L.A., Krafft, B.A. 2018. Size selection of Antarctic krill (*Euphausia superba*) in a commercial codend and trawl body. Fish. Res., 207, 49–54.

Herrmann, B., Priour, D., Krag, L.A. 2007. Simulation-based study of the combined effect on cod-end size selection of turning meshes by 90 and reducing the number of meshes in the circumference for round fish. Fish. Res., 84, 222–232.

Herrmann, B., Sistiaga, M., Nielsen, K.N., Larsen, R.B. 2012. Understanding the size selectivity of redfish (*Sebastes* spp.) in North Atlantic trawl codends. J. Northwest Atl. Fish. Sci., 44, 1–13.

Hickey, W.M., Boulos, D.L., Brothers, G. 1995. A study of the influence of lastridge ropes on redfish selectivity in a bottom trawler. Can. Tech. Rep. Fish. Aquat. Sci., No. 2076, 25p.

Hothorn, T., Bretz, F., Westfall, P. 2008. Simultaneous inference in general parametric models. Biom. J., 50, 346–363.

ICES, 2012. Report of the ICES-FAO Working Group on Fishing Technology and Fish Behaviour (WGFTFB). ICES C. M. SSGESST:07, 214p.

Isaksen, B., Valdemarsen, J.W. 1986. Selectivity experiments with square mesh codends in bottom trawl. ICES C. M. 1986/B:28.

Madsen, N., Herrmann, B., Frandsen, R.P., Krag, L.A., 2012. Comparing selectivity of a standard and turned mesh T90 codend during towing and haul-back. Aquat. Living Resour., 25, 231-240.

Mayo, R.K., Dozier, U.B., Clark, S.H. 1983. An assessment of the redfish, *Sebastes fasciatus*, stock in the Gulf of Maine-Georges Bank region. NMFS, Woods Hole Lab. Ref Doc, 83-22.

Millar, R.B., 1993. Incorporation of between-haul variation using bootstrapping and nonparametric estimation of selection curves. Fish. Bull., 91, 564–572.

Moderhak, W., 1997. Determination of selectivity of cod codends made of netting turned through 90. Bull. Sea Fish. Inst., 140, 1-14.

Ni, I.H., Sandeman, E.J., 1984. Size at maturity for Northwest Atlantic redfishes (*Sebastes*). Can. J. Fish. Aquat. Sci., 41, 1753–1762.

Pol, M.V., Herrmann, B., Rillahan, C., He, P., 2016. Impact of codend mesh sizes on selectivity and retention of Acadian redfish *Sebastes fasciatus* in the Gulf of Maine trawl fishery. Fish. Res., 184, 54–63.

R Development Core Team, 2009. R: A Language and Environment for Statistical Computing [online]. R Foundation for Statistical Computing, Vienna, Austria, http://www.R-project.org [accessed 26 November 2019].

Rubec, P.J., McGlade, J.M., Trottier, B.L., Ferron, A. 1991. Evaluation of methods for separation of Gulf of St. Lawrence beaked redfishes, *Sebastes fasciatus* and *S. mentella*: malate dehydrogenase mobility patterns compared with extrinsic gasbladder muscle passages and anal fin ray counts. Can. J. Fish. Aquat. Sci., 48, 640–660.

Sistiaga, M., Herrmann, B., Grimaldo, E., Larsen, R.B., 2010. Assessment of dual selection in grid based selectivity systems. Fish. Res., 105, 187–199.

Tokaç, A., Herrmann, B., Aydın, C., Kaykac, H., Ünlüler, A., Gökçe, G., 2014. Predictive models and comparison of the selectivity of standard (T0) and turned mesh (T90) codends for three species in the Eastern Mediterranean. Fish. Res., 150, 76–88.

Wienbeck, H., Herrmann, B., Feekings, J.P., Stepputtis, D., Moderhak, W., 2014. Acomparative analysis of legislated and modified Baltic Sea trawl codends forsimultaneously improving the size selection of cod (*Gadus morhua*) and plaice (*Pleuronectes platessa*). Fish. Res., 150, 28–37.

Wileman, D.A., Ferro., R.S.T., Fonteyne, R., Millar, R.B., 1996. Manual of methods of measuring the selectivity of towed fishing gears. ICES Coop. Research Rep., No 215, 126p.

Table 4.1. Operational conditions and fishing gear performance for all hauls conducted in this study.

Codend	Haul ID	Hauling speed (knot)	Towing duration (min)	Warp length (m)	Door spread (m)	Depth (m)	Catch numbers		Sampling ratios (%)	
							Codend	Cover	Codend	Cover
T0-90	1	2.4	7	732	122	329	306	46	21	100
	2	2.3	8	732	122	331	353	57	4.4	100
	3	2.4	5	732	122	318	329	42	8.7	100
	4	2.5	5	732	122	318	322	17	9.5	100
	5	2.4	7	732	122	324	311	84	5.4	100
	6	2.4	7	732	122	318	330	144	5.4	100
	7	2.4	5	732	122	326	332	136	5.4	100
	8	2.3	4	732	122	324	309	23	10.7	100
	9	2.4	6	732	122	329	338	14	9.9	100
	10	2.4	7	732	122	316	331	18	12.1	100
T90-90	1	2.4	5	732	122	327	287	81	64.3	100
	2	2.3	9	777	130	331	133	156	20.4	100
	3	2.6	10	777	130	326	349	319	9.6	37.4
	4	2.5	9	777	130	324	358	358	5.7	15.3
	5	2.5	7	732	122	326	234	337	8.7	100
	6	2.5	7	732	122	322	138	65	21	100
	7	2.4	10	732	122	315	384	384	11.1	65.4
	8	2.4	8	732	122	315	362	407	9.8	48.2
	9	2.5	6	732	122	326	334	339	8.4	21.1
	10	2.6	5	732	122	324	364	328	7.1	33.8
	11	2.4	4	732	122	315	335	305	5.6	18.6
T90-100	1	2.3	6	732	122	320	343	319	8.5	26.4
	2	2.4	5	732	122	326	352	290	27	87
	3	2.3	8	732	122	324	366	317	8.4	19.7
	4	2.4	7	732	122	326	321	265	34.3	64.5
	5	2.5	8	732	122	320	351	323	15.3	57
	6	2.4	8	732	122	324	329	338	19.7	77.9
	7	2.7	7	777	130	327	377	267	10	25
	8	2.2	7	732	122	327	375	337	7.7	37.9
	9	2.4	7	732	122	322	354	345	6.6	24
	10	2.4	7	732	122	324	314	149	36.5	100

T90-110	1	2.5	7	686	114	256	309	329	38.1	45.7
	2	2.4	8	686	114	267	396	369	7.4	8.9
	3	2.5	5	686	114	276	393	340	9.2	13.9
	4	2.6	4	686	114	285	335	317	30.9	59
	5	2.5	6	686	114	294	350	307	23.7	38
	6	2.3	8	686	114	302	311	343	17.2	49.5
	7	2.4	18	732	122	318	284	361	52.1	100
	8	2.5	12	732	122	324	327	296	48.2	75
	9	2.6	10	732	122	296	319	300	17.1	27.6
	10	2.6	10	732	122	278	382	336	9.3	5.2
	11	2.6	8	686	114	265	316	326	38.5	45.6

Table 4.2. Catch weight (in kg) and species caught with each codend (hauls combined).

Species		Codend				Total weight (kg)
		T0-90	T90-90	T90-100	T90-110	
Redfish	*Sebastes mentella*	7438.0	7464.9	6524.1	6371.2	27798.2
White hake	*Urophycis tenuis*	1.1	1.7	9.7	4.6	17.1
Greenland halibut	*Reinhardtius hippoglossoides*	3.8	2.2	5.5	0.0	11.5
Atlantic argentine	*Argentina silus*	0.0	0.0	0.0	11.1	11.1
Shortfin squid	*Illex illecebrosus*	0.5	2.6	1.8	4.8	9.7
Atlantic cod	*Gadus morhua*	0.0	0.9	0.4	1.5	2.8
Black dogfish	*Centroscyllium fabricii*	0.3	2.0	0.5	0.0	2.8
Witch Flounder	*Glyptocephalus cynoglossus*	0.0	0.2	0.3	0.4	0.9
Lumpfish	*Cyclopterus lumpus*	0.9	0.0	0.0	0.0	0.9
Monkfish	*Lophius americanus*	0.0	0.7	0.0	0.0	0.7
Thorny Skate	*Amblyraja radiata*	0.0	0.0	0.0	0.5	0.5
American plaice	*Hippoglossoides platessoides*	0.1	0.2	0.0	0.0	0.3
Lanternfish	*Benthosema glaciale*	0.0	0.0	0.0	0.2	0.2
Roughead grenadier	*Macrourus berglax*	0.0	0.0	0.1	0.0	0.1
Arctic cod	*Boreogadus saida*	0.0	0.1	0.0	0.0	0.1

Table 4.3. Akaike's information criterion (AIC) for each model for each codend. Selected model in bold.

Codend	Model			
	Logit	Probit	Gompertz	Richard
T0-90	6,109.9	6,110.0	**6,109.9**	6,111.9
T90-90	45,281.9	45,269.9	45,302.5	**45,260.1**
T90-100	38,013.4	38,014.8	**38,012.8**	38,014.7
T90-110	55,257.0	**55,253.8**	55,263.1	55,258.5

Table 4.4. Codend usability indicators with fit statistics. Numbers in () represent the 95% CI for the estimated data.

Parameter	T0-90	T90-90	T90-100	T90-110
Model	Gompertz	Richard	Gompertz	Probit
nP-	98.0(97.0-98.8)	67.2(61.3-73.1)	70.0(63.5-74.9)	47.3(39.3-58.1)
nP+	98.8(98.3-99.3)	82.6(79.4-86.7)	81.8(79.6-84.2)	60.2(52.9-68.0)
nRatio	0.20(0.17-0.26)	0.21(0.17-0.24)	0.34(0.27-0.41)	0.46(0.41-0.51)
dnRatio	16.9(14.3-20.4)	17.1(14.4-19.7)	25.2(21.1-29.3)	31.5(29.17-33.8)
DOF	11	16	15	22
Deviance	4.99	13.42	14.93	32.07
p-value	0.930	0.640	0.460	0.076

Table 4.5. Summaries of meshed redfish in number and pairwise comparison of meshed individuals from the codends. SE, standard error. p values < 0.05 are considered significant.

Codends	Estimate	SE	z-value	p-value
T0-90	1.4	1.405	0.989	0.322
T90-90	22.6	1.492	6.961	< 0.001
T90-100	16.2	1.503	6.01	< 0.001
T90-110	8.9	1.503	4.542	< 0.001
Comparisons				
T90-90 - T0-90	22.6	1.492	6.961	<0.001
T90-100 - T0-90	16.2	1.503	6.010	<0.001
T90-110 - T0-90	8.9	1.503	4.542	<0.001
T90-100 - T90-90	-6.4	1.360	-1.088	0.694
T90-110 - T90-90	-7.3	1.360	-3.032	0.013
T90-110 - T90-100	-13.7	1.374	-1.884	0.232

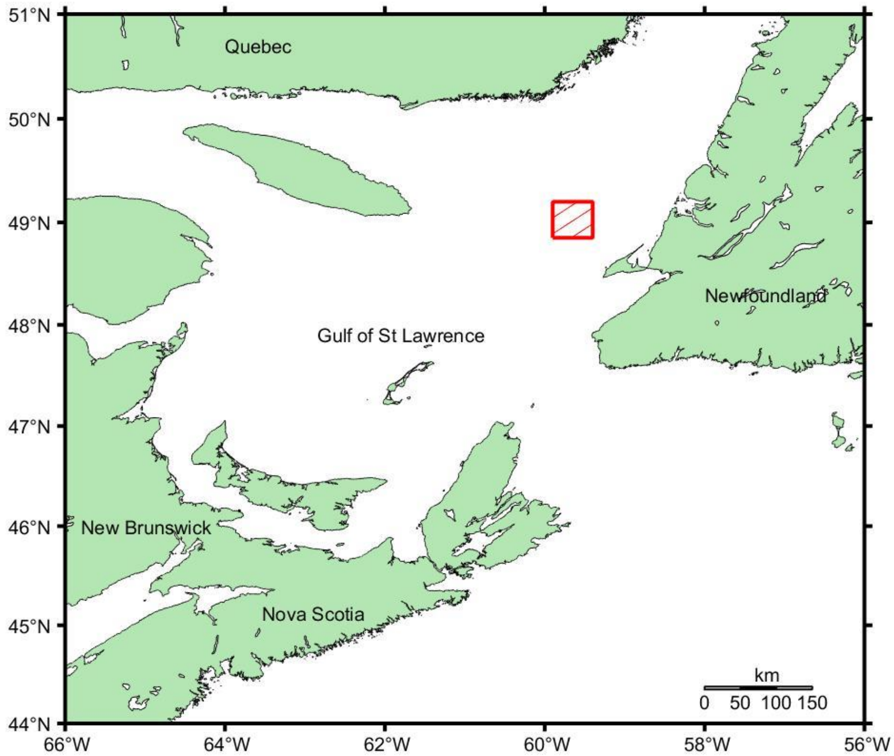

Figure 4.1. Location of fishing trials (red square) in the Gulf of St. Lawrence, Canada.

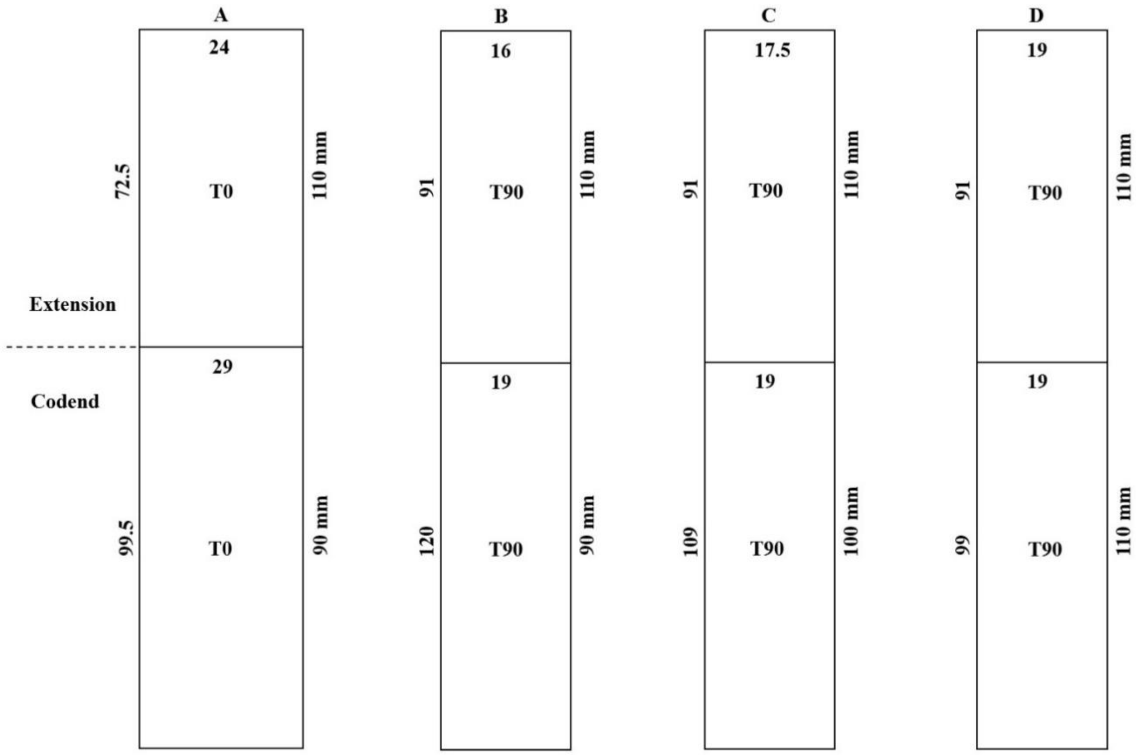

Figure 4.2. Schematic diagram of (A) T0-90, (B) T90-90, (C) T90-100, and (D) T90-110 codends. Non-denoted numbers are the number of meshes at corresponding sections, and numbers denoted with mm are the mesh size of the netting section.

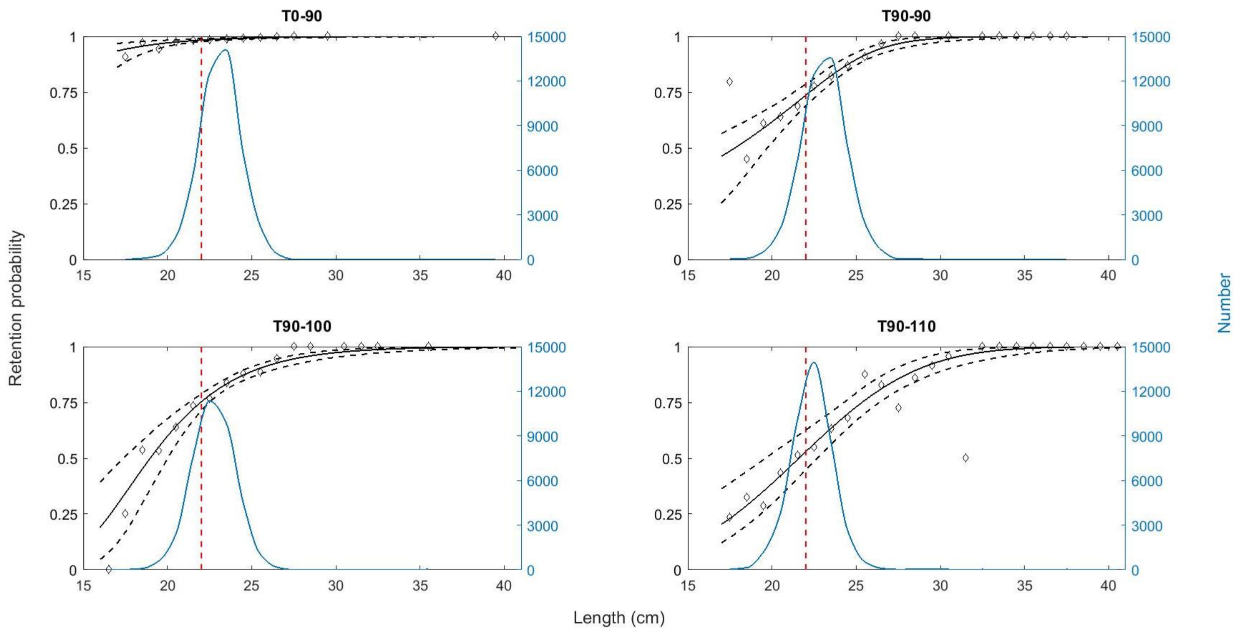

Figure 4.3. Size selection of deepwater redfish (*Sebastes mentella*) in T0 and T90 codends: Diamond symbols represent the experimental data; thick black curve indicates the fitted size selection curves; stipple curves describe the 95% confidence limits for the fitted curves; red stipple line represents the MLS for redfish; blue curves shows the size distribution of the population encountered during sea trials.

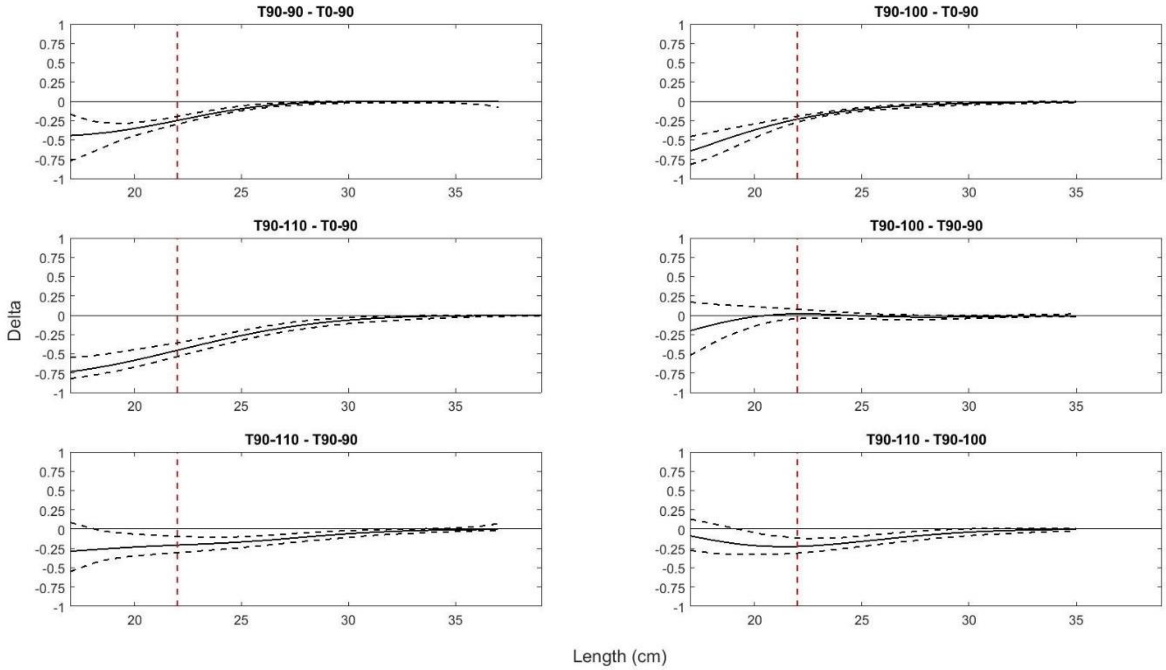

Figure 4.4. Delta curves for each pair of codends: thick black curve indicates the fitted Delta curves; stipple curves describe the 95% confidence limits for the curves; red stipple line represents the MLS for redfish (*Sebastes mentella*).

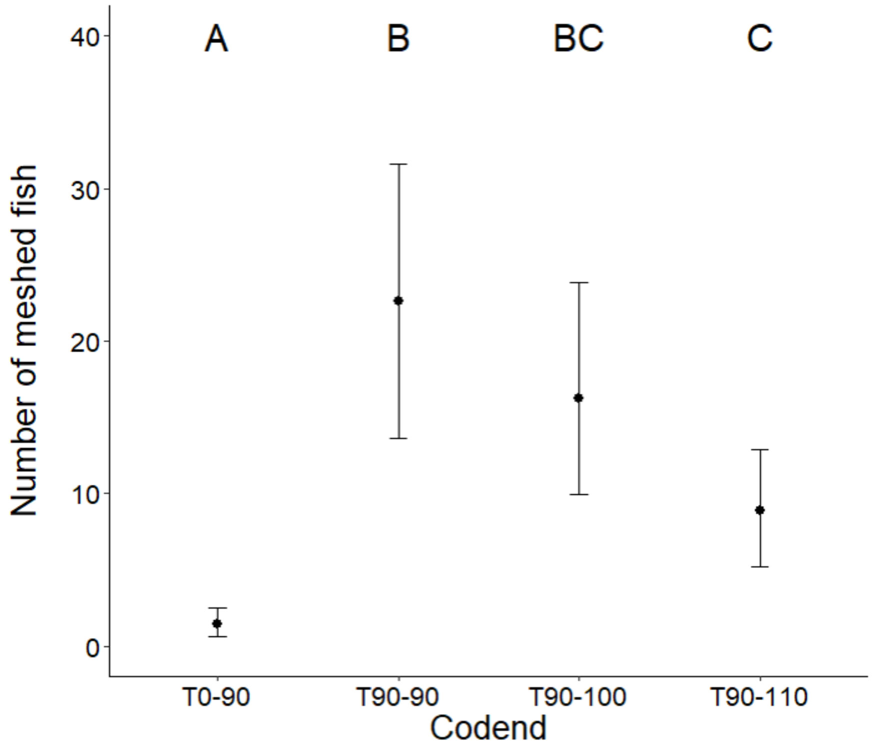

Figure 4.5. Number of meshed redfish (*Sebastes mentella*) from each codend. Different letters indicate significant difference per codend at an α of 0.05.

CHAPTER 5. Comparing the Hydrodynamic Performance of T0 and T90 Codends With and Without a Codend Cover

5.1 Abstract

The hydrodynamic performance of four, full-scale T0 (n = 1) and T90 (n =3) codends was investigated and compared through flume tank testing, with and without a codend cover. We evaluated how flow velocity, mesh circularity, and drag changed in each codend at five different towing speeds (1.0-1.8 knots). We also investigated flow velocity inside codends and between codends and a cover net. The results demonstrated that flow velocity decreased along the length of a codend, and this effect was pronounced in the T0 codend. Increasing the mesh size of T90 codends from 90 to 110 mm did not significantly affect flow velocity inside the codend. A new parameter, termed *mesh circularity*, is developed and introduced to describe mesh opening. Mesh circularity in the T0 codend decreased along the length of the codend, which contrasts with the T90 codends which exhibited a slight increase. These results show that the T90 codends maintained relatively open meshes (circularity ranged from ~0.8 to 1.0 along the length of the codend) compared to the T0 (circularity ranged from ~0.6 to 0.4). With the same simulated catch, each T90 codend indicated a significantly ($p < 0.05$) higher drag than the T0 codend. For the covered codend comparisons, the flow velocity in the area between a codend and its cover did not change for the T0 codend ($p > 0.05$), but was significantly different for the T90 codend (90 mm, $p < 0.05$). The results of this research provide fundamental

knowledge useful for understanding and improving selectivity of trawls in marine fisheries.

5.2 Introduction

The codend is the terminal section of a trawl where the catch accumulates and is retained. It is considered the most important trawl component in terms of the selection process, where the sorting of captured animals occurs by species and size (Wileman et al., 1996). However, during this process, the incidental capture of juvenile, undersized, or non-marketable species also occurs (called bycatch or discards) and are problematic for fisheries management and population conservation (He, 2010).

Many studies have been undertaken to improve the size selectivity of trawls, generally focusing on modifications to the codend (e.g., He, 2007; Pol et al., 2016; Bayse et al., 2016; Cheng et al., 2019). The hydrodynamic performance of a codend including its mesh shape, mesh opening, and water flow has significant effects on selectivity (Ferro and O'Neill, 1994; Wileman et al., 1996). The effects of different mesh orientation (T0 and T90) on size selectivity has been simulated and predicated to affect size selectivity (Herrmann et al., 2007; ICES, 2011). O'Neill (1997) estimated the mesh opening along T0 codends using mathematical equations, which provided a basis of predictive modeling of codend selectivity. Herrmann et al. (2009) simulated the codend selection process with FISHSELECT, which incorporates the relationship between fish cross-sectional geometry and mesh shape.

Nonetheless, to characterize the hydrodynamic performance of a codend, one of the most reliable methods is to test the codend full-scale through sea trials and observe its performance using underwater cameras, divers, or vehicles (e.g., Main and Sangster, 1983). However, it is difficult to measure the flow velocity, mesh opening, and drag during sea trials. The ocean current, wind, sea state, etc. cannot be controlled. Another option to test full-scale codends is using a flume tank, where variable environmental conditions can be avoided, and experimental conditions can be carefully manipulated (Winger et al., 2006).

Rotating diamond netting 90° to the direction of tow (called T90) was proposed in the 1980s (Moderhak, 1993). The T90 codend was reported to have better size selectivity for many round-body fish species than a T0 codend made of the exact same netting (Herrmann et al., 2007; Wienbeck et al., 2011). This is due to T0 codend meshes closing when tension acts on the tow direction of the trawl, whereas T90 meshes remain open. While several studies have observed T0 and T90 codends in a flume tank (e.g., Madsen et al., 2001; Hansen, 2004; Pichot et al., 2009), to our knowledge there is currently no published literature on the relative performance of T0 and T90 codends with regard to empirical data on flow velocity in and outside of the codend, mesh shape, and drag.

The purpose of this study was to compare the hydrodynamic performance of full-scale T0 and T90 codends, with and without a cover, using a flume tank. Important parameters that affect the performance of codends were quantified and compared between T0 and T90 codends, including: flow velocity, mesh circularity, drag. We also investigate the flow velocity between codend and codend cover, for both T0 and T90 codends. The results are discussed in relation to codend selectivity and previous engineering studies.

5.3 Materials and Methods

5.3.1 Gear Specifications

All four codends were designed and constructed by Hampidjan Canada Ltd. All codends were constructed with four panels using double-braided polyethylene netting (nominal 4.6 mm Ø), typical for Northwest Atlantic groundfish trawls (see descriptions in Table 5.1). The T0 codend (T0) design was typical for fisheries in eastern Canada with a nominal stretched inside mesh size of 90 mm. Each codend was attached to an extension made of the same netting (Table 5.1). Three meshes constituted the selvedge. The lastridge rope was made of three-strand polypropylene rope (30 mm Ø) and was 5% shorter in length than the selvedge.

The T90 codend with the smallest mesh size (T90-90; nominal 90 mm stretched inside mesh opening) was designed to be a direct comparison to the T0 codend and only differed by mesh orientation and lastridge ropes (see below). The other two T90 codends were exactly the same except mesh size: 100 mm (T90-100) and 110 mm (T90-110), respectively. The selvedge of two meshes was laced to the lastridge ropes, which were DynIce Quicklines^{TM} designed by Hampidjan Iceland and was 5% shorter than the selvedge. Each T90 codend was attached to an extension of the same netting material (see

Table 5.1). Stretched inside mesh size was measured using an ICES OMEGA gauge following procedures described by Fonteyne (2005).

5.3.2 Flume Tank

Each codend was tested in the flume tank located at the Centre for Sustainable Aquatic Resources (CSAR), Fisheries and Marine Institute of Memorial University, St. John's, NL, Canada. The test section of the tank is 22.3 m long, 8.0 m wide and 4 m deep with a side observation window of 20 m x 3 m. The maximum water speed (towing speed) was 1.8 knot (Winger et al., 2006).

The codends were mounted on a steel ring (140 cm Ø) which was attached by four bridles (2 m) to a towing mast in the flume tank (Figure 5.1). Codend catch was simulated with trawl floats (n = 80; 20 cm Ø; Pescaflot N-90, Castro, Donostia, Gipuzkoa, Spain). Each float had six 2.6 cm diameter holes drilled to balance weight and water buoyancy. Total float weight in water was measured at 0.0 kg (neutrally buoyant) and estimated to simulate a small catch weight of approximately 350 kg (estimated according to the total volume of the floats).

5.3.3 Trawl Geometry and Flow Velocity Measurement

An underwater camera system (Sony FCB-ER8300, Minato, Tokyo, Japan) was used to determine each measurement point along each codend (described below, Figure 5.1) and the horizontal opening of each codend. A side-view camera (Panasonic MDV12885, Kadoma, Osaka, JP) perpendicular to the flume tank window was used to measure the vertical opening of the codends. Flow velocity was measured with a two-axis electromagnetic current meter (Valeport Model 802, Valeport, St Peter's Quay, Totnes, UK) with a sampling rate of 96 Hz at the center point of each codend. The measurement accuracy was ±5 mm/s plus 1% of averaged data.

Towing speeds ranged from 1.0 to 1.8 knots at increments of 0.2 knot. At each towing speed, the mean flow velocity through the centre of each codend was measured at different measurement points along the length of the codend and its extension. The number of points were determined by the total length of the codend with successive measurement position of 1.5 m along the lastridge ropes (Figure 5.1). Measurement points were calculated and marked on each codend and its extension before the testing. The first measurement point was set as a reference; no data was collected at this point. Measurement points from 2 to 6 were along the extension piece, and 7 to 10 along the codend.

The electromagnetic current meter recorded the flow velocity at each measurement point. Measurements were collected over a period of one minute (96 Hz) and were then averaged to get the velocity. At some locations the vertical opening was too small and flow data were not measured at these points, especially at the end of the codend.

5.3.4 Mesh Opening

The meshes used for mesh opening analysis were at the middle point of the top panel. The downward-looking underwater camera system recorded the mesh image at the marked points. At least five meshes around the mark were recorded for image analysis. The mesh shape was fitted with an ellipse shape; circularity (Circ, Eq. 5.1) of the fitted ellipse was applied to describe the mesh opening (Figure 5.2). The mesh opening at different positions of the codend were analysed using ImageJ software. Mesh shape fitting and Circ calculation were carried out from recorded images. The image analysis was conducted following procedures described by Ferreira and Rasband (2012).

$$Circ = \frac{2 \times a \times b}{a^2 + b^2} \qquad (5.1)$$

where a is the length of major axis of the fitted ellipse and b is the minor axis. The value of Circ cannot be smaller than 0.0 with a maximum value of 1.0. When Circ equals 0.0, this indicates a totally closed mesh. Circ equaling 1.0 suggests a perfect circle shape fitting the mesh.

5.3.5 Drag

A load cell (Honeywell Sensotec Model 31, Honeywell International Inc., Charlotte, North Carolina, USA) connecting the bridles and towing mast was used to measure the total drag (kgf, kilogram force) of the codend system. The drag at each towing speed was recorded for all codends with the same simulated catch amount. Measurements were collected over a period of one minute (50 Hz) and were then averaged to get the drag.

5.3.6 Codend cover

The flow velocity within/around the T0 and T90-90 codends were measured with a codend cover attached as in typical of size selectivity studies (Wileman et al., 1996). The two-panel codend cover was made of single 2.5 mm Ø PE twine with a nominal mesh size of 50 mm. A total of 29 flexible kites were mounted around the circumference of the cover codend to expand the cover and avoid masking of the codend meshes (e.g., Madsen et al., 2001; He, 2007; Grimaldo et al., 2009). The cover codend was 1.5 times the length of the T0 codend, the longest codend. To fit into the flume tank, the extension of each codend was removed (Figure 5.3). The codend and the cover were mounted on two steel rings (100 cm Ø). The ring with the codend was attached by four bridles (2 m in length) to the towing mast of the flume tank. The ring with the cover was linked to the one with the codend by four bridles (each 2 m in length). Flow velocities were measured by the current meter at that measurement point that corresponds to point 8 of the codend, inside the codend and at the same longitudinal position between the cover and the codend. At point 8, the effects of the kites and simulated catch to the flow could be ignored. The inside measurement point was at the centreline of the codend while the other point was at the middle between the cover and the codend. The two measurement points were determined by averaging the vertical distance between the top and bottom panels of the codend and by averaging the vertical distance between the cover and the codend. Towing speeds ranged from 1.4 to 1.8 knot with 0.2 knot intervals. Measurements were collected over a period of one minute (96 Hz) and were then averaged to get the velocity.

5.3.7 Statistical Analysis

The flow velocity was fit with a multiple regression including codends, towing speeds and measurement points as independent variables. Regressions were performed using the GLM function in MATLAB including all the variables (Eq. 5.2).

$$Mv = \alpha + \beta_1 Cd + \beta_2 Ts + \beta_3 Mp + \beta_4 Mp^2 + \varepsilon \qquad (5.2)$$

where α is the intercept, β terms are regression coefficients, and ε is the error term. *Mv* represents the measurement flow velocity. *Cd* is the codend type. *Ts* is the towing speed. *Mp* represents measurement point along the codend. *Cd* is a categorical variable; the others are the continuous variables.

A Pearson's correlation was run to determine the relationship between the circularity values and the measurement points. Circ of each codend was fit using a regression and the GLM function in MATLAB (Eq. 5.3).

$$Circ = \alpha + \beta_1 Cd + \beta_2 Ts + \beta_3 Mp + \varepsilon \qquad (5.3)$$

where α is the intercept, β terms are regression coefficients and ε is the error term. *Cd* is the codend type. *Ts* is the towing speed. *Mp* represents measurement point along the codend. A *p*-value of <0.05 was considered to be statistically significant. When terms were found to be nonsignificant, the highest *p*-value term was removed, and the model was refitted until all terms were significant.

Analyses of variance (ANOVA) was used to examine differences between the flow velocity through the centre of the codends and the towing speed. A level of significance

($p < 0.05$) was used to evaluate the null hypothesis in the ANOVA analyses. To compare the flow velocity among the different codends, flow data recorded at points 7 to 10 were utilized.

A regression using the GLM function in MATLAB was used to analyze the difference in the drag of the codends (Eq. 5.4).

$$Dr = \alpha + \beta_1 Ts + \beta_2 Cd + \varepsilon \quad (5.4)$$

where α is the intercept, β terms are regression coefficients, and ε is the error term. *Dr* represents the drag of codend. *Cd* is the codend type. *Ts* is the towing speed.

For the codend cover experiment, the measured flow velocity was fit with a regression with towing speeds and measurement areas (inside the codend and between the cover and the codend) as independent variables. Regressions were performed using the GLM function in MATLAB including all the variables (Eq. 5.5).

$$Mv = \alpha + \beta_1 Ts + \beta_2 Ma + \varepsilon \quad (5.5)$$

where α is the intercept, β terms are regression coefficients, and ε is the error term. *Ts* represents the towing speed. *Ma* represents measurement area including inside the codend and between the cover and the codend. *Ts* is a continuous variable and *Ma* is a categorical variable.

5.4 Results

5.4.1 Gear Specifications

Design parameters of each codend are listed in Table 5.1. The measured mesh size for the T0 codend was 95.0 mm (SD = 2.4), 93.6 mm (SD = 2.5) for T90-90, 104.6 mm (SD =2.9) for T90-100, and 110.7 mm (SD = 2.1) for T90-110.

5.4.2 Flow Velocity

The flow velocity observed at the measurement points is shown in Figure 5.4. All codends exhibited an early reduction in flow velocity (at location point 2) compared to the test speed of the flume tank. Flow velocity generally decreased as the water travelled down the length of the extension and codend, with the greatest reductions observed near the terminal part of the codend (point 10). The shape of the fitted regressions is noticeably different between the T0 and T90 codends (Figure 5.4). The T0 codend showed the greatest reductions in flow velocity. At a towing speed of 1.8 knots, the flow velocity of the T0 codend dropped more than 34% between points 2 and 10. By comparison, the T90 codends exhibited less reduction in flow velocity along their length. The decrease in flow velocity at the last measurement point was less than 14% with respect to the beginning position.

The results of the regression describing flow velocity in the codends indicated that the model explained 93.1% of the variability in the response variable (R^2). The most important factor affecting the flow velocity inside a codend was towing speed (t=43.46, *p*<0.001). Holding the other variables constant, a one-unit increase (by 1 knot) in towing speed would significantly increase the inside flow velocity by 0.51 m/s.

Differences in flow velocity between the T0 and T90 codends was interpreted with the coefficient of category variable (*Cd*). Holding the other variables constant, the flow velocity in the T90-90 codend was 0.11 m/s higher than the T0-90 codend, and this difference was statistically significant ($p<0.001$). The other T90 codends also had significantly higher mean flow (>0.1 m/s) than the T0 codend under same experimental conditions (Table 5.2).

5.4.3 Mesh Circularity

Figure 5.5 shows the change of mesh opening observed along the extension and codend at different towing speeds. The circularity of the T0 codend was 0.53 at point 2, decreasing to 0.39 at the last point. According to this figure, the circularity of the T0 codend showed a decreasing trend from the front to the rear of the codend for all towing speeds. The coefficient was statistically significant ($r = -0.73$, $p < 0.001$), indicating a strong negative correlation between the two variables (Evans, 1996). The results for the T0 codend indicated that mesh circularity decreased as towing speed increased, however this difference was not significant ($r = -0.25$, $p=0.09$).

In comparison, mesh circularity in the T90 codends exhibited a slight increasing tendency along the length of the extension and codends (point 2 to 10). At the leading edge (point 2), the mean circularity value was 0.80 (SD=0.026), 0.83 (SD=0.042), and 0.74

(SD=0.054) for T90-90, T90-100 and T90-110, respectively. These increased to 0.92 (SD=0.017), 0.91 (SD=0.033) and 0.85 (SD=0.040) at the end of the codend (point 10).

Results of the Pearson correlation coefficient indicated that there was a strong positive association between the mesh circularity and measurement points for the T90-90 codend ($r = 0.75$, $p < 0.001$), as well as the T90-100 codend ($r = 0.66$, $p < 0.001$) and T90-110 codend ($r = 0.61$, $p < 0.001$). The correlation between mesh circularity and towing speed was negative, indicating that increasing the towing speed lead to greater mesh closure.

The results of the regression indicated the three predictors (*Cd*, *Ts*, and *Mp*) explained 91.7% of the variance observed ($F_{(5, 188)} = 413$, $p < 0.001$). The coefficient for towing speed was negative, indicating that mesh circularity decreases with increasing towing. More specifically, for every additional one knot in towing speed, mesh circularity decreases by 6.3%. The circularity also changed along the length of the extension and codend, as indicated by the statistically significant coefficient for *Mp* ($p < 0.001$). Moving the measurement point by one unit generated a 0.7% increase in mesh opening (Table 5.3).

Comparing the T0-90 and T90-90 codends, which have the same mesh size, the results reveal the T90-90 codend had higher overall circularity (mean = 0.4) compared with the T0. Changing the mesh orientation from T0 to T90 significantly increased the mesh opening ($p < 0.001$). T90-100 and T90-110 also had significantly higher mesh opening than did the T0 ($p < 0.001$) (Table 5.3; Figure 5.5).

5.4.4 Drag

The total drag of each codend (with the simulated catch) at different towing speeds is shown in Figure 5.6. The drag of each codend increased with increasing towing speed, as expected. At a towing speed of 1.0 knot, the difference in drag between the T0 and T90 codends was approximately 25.3 kgf. This difference increased up to 75.0 kgf when the towing speed increased to 1.8 knots. The curve for the T0 codend is noticeably lower than the T90 codends (Figure 5.6). The regression analysis indicated that the drag of T90 codends were significantly higher than the T0 codend (p < 0.001; Table 5.4).

5.4.5 Covered Codend

Flow velocities measured at point 8, inside the codend and between the cover and the codend, are shown in Figure 5.7. Observed values for each codend were fitted with a linear function. Flow velocity showed an increasing trend as *Ts* increased from 1.4 to 1.8 knots. The coefficient for *Ts* was positive and statistically significant for both codends (Table 5.5). For the T0 codend, measurements of flow were not statistically different inside the codend versus between the cover and the codend (t=-0.501; p>0.05; Table 5.5). Conversely, flow velocity between the cover and T90-90 codend was noticeably and statistically lower than the flow velocity recorded inside the codend (p<0.001; Table 5.5).

5.5 Discussion

This study investigated the hydrodynamic performance of full-scale T0 and T90 codends with and without a codend cover using a large flume tank in Newfoundland and Labrador, Canada. These results further the work on codend dynamic performance conducted in flume tanks located in Australia (Wakeford, 2004), England (O'Neill et al., 2005), Denmark (Madsen et al., 2001; Hansen, 2004), and France (Pichot et al., 2009).

Our results demonstrated that flow velocity decreased along the length of the extension and codend. This finding is consistent with Hansen (2004) and Wakeford (2004). Whether they were model or full-scale codends, all three studies documented that filtration efficiency was hindered due to blockage from the netting. Depending on the design of the codend, water will always be entrained and carried along while the codend is towed forward. We found that all three T90 codends, regardless of their mesh size, exhibited a relatively high flow velocity along their lengths. Hansen (2004) obtained a similar conclusion for one of his T90 codend designs, but for not another. Thus, the extent of entrainment and resulting flow reduction can vary depending on a trawl designer's choice of netting, codend design, and towing speed. In many cases, this may not be known at the design stage, justifying the need for controlled flume experiments prior to sea trials (Winger et al., 2006).

To our knowledge, this is the first study to compare the relative performance of T0 and T90 codends of similar design under controlled flume tank conditions. Our results demonstrate that T90 codends are fundamentally different from T0 codends in their flow profile, mesh circularity, and drag. These results are helpful in explaining selectivity differences between T0 and T90 codends, and provide insights into mechanisms that affect selectivity. T90 codends have been shown to improve size selectivity for many round-body fish species compared to T0 codends made of the exact same netting (Herrmann et al., 2007; Wienbeck et al., 2011). This is due to T0 codend meshes closing when tension acts on the tow direction of the trawl, whereas T90 meshes remain open.

To investigate mesh opening, many studies have used the parameter known as *opening angle* (e.g., Sistiaga et al., 2011; Herrmann et al., 2012; Krag et al., 2014). In this study, we elected to develop and use a novel parameter, which we call *mesh circularity*. This is because the bar of T90 mesh is distorted and shows a curvilinear shape (Figure 5.2). Thus, the two sides of the triangle defining the opening angle are not straight, making the estimation of an opening angle difficult. Given that measurements of opening angle at sea are generally based on image analysis (e.g., Krag et al., 2014), measurement error can result in the event the underwater camera and netting are not perpendicular. Describing mesh opening with circularity can avoid this error. The circularity value is a ratio without units; measurement errors from the numerator and denominator of the function are canceled out (Eq. 5.1). Comparison of mesh opening using circularity is therefore reliable and more accurate than using opening angle.

Mesh circularity also corresponds well with general fish morphology, especially the cross-sectional body shape and body height to width ratio (Tosunoğlu et al., 2003; Herrmann et al., 2009). Previous studies have shown that associating fish morphology with mesh opening can be helpful for understanding the selectivity of netting (Stergiou and Karpouzi, 2003; Broadhurst et al., 2006). When circularity equals one, a mesh has reached its maximum opening, which promotes the escapement of round fish (e.g., body height to width ratio was one). As circularity approaches zero, the mesh shape may be good for undersized flatfish to escape. Therefore, the circularity combined with species morphology data could be applied to design selective fishing gears.

This study reports new data on the hydrodynamics of attaching a cover over a codend. While our data is limited to a single location (point 8) for only a few towing speeds, to our knowledge, no other scientific literature exists on flow velocities between a codend and its cover. We speculate that the lower flow velocities observed in the T90 codend may be attributed to greater frontal area. O'Neill et al. (2005) found that the maximum frontal area of codend was a good predictor of its total drag in a flume tank. Given that the T90-90 codend had greater drag than the T0-90 codend, we speculate that this may have been related to differences in frontal area (projection area) between the codends. Unfortunately frontal area was not quantified in this study. We recommend additional experiments be conducted to fully elucidate this phenomenon, perhaps using a combination of numerical simulations with a computer and physical modelling in a flume tank.

The four codends used in this study were also evaluated at sea for their size selectivity in an experimental redfish (*Sebastes* spp.) fishery in the Gulf of St. Lawrence (Chapter 4). The results showed that the T90 codends had better size selectivity than the T0 at releasing undersized individuals (< 25 cm). Changing the mesh orientation alone (T0-90 to T90-90) significantly affected the selection properties of the codend. This research can thus help to explain why the change was effective by analyzing and comparing the hydrodynamic performance of the codends.

Although full-scale codends were tested in this study, the experimental conditions of a flume tank are different from sea trials. The simulated catch size and towing speeds we used are significantly lower than those expected at sea. During sea trials, towing speeds are typically closer to 2.5 knots and catch sizes can be several thousand kilograms. The drag of the codend would increase with increasing towing speed and catch weight, and the flow velocity inside the codend and mesh opening may be affected accordingly. Nevertheless, our research methods can be used to investigate and compare the hydrodynamic performance of different codends under controlled experimental conditions, and may prove helpful in interpreting codend selectivity. Coupling the knowledge on the engineering performance of codends with underwater observations of fish behaviour in response to trawl netting (Winger et al., 2010) is key to fully understand the mechanisms of codend selectivity.

5.6 Acknowledgements

Financial support for this study was provided by the Canada First Research Excellence Fund through the Ocean Frontier Institute (Module H), as well as the Research and Development Corporation (RDC) of Newfoundland and Labrador (Ocean Industries Student Research Awards), and the Graduate Research Accelerator for Fisheries Science (Fisheries and Oceans Canada). We would like to thank many staff and graduate students from CSAR who assisted with the project, including Harold DeLouche, Craig Hollett, George Legge, Jessica Wood, Meghan Donovan, Vang Nguyen, Mark Santos, and Kelly Moret. We are also grateful to Haraldur Arnar Einarsson, Steve Walsh, and Michael Pol for invaluable assistance during all stages of this study.

5.7 References

Bayse, S.M., Herrmann, B., Lenoir, H., Depestele, J., Polet, H., Vanderperren, E., Verschueren, B., 2016. Could a T90 mesh codend improve selectivity in the Belgian beam trawl fishery? Fish. Res., 174, 201-209.

Broadhurst, M.K., Dijkstra, K.K., Reid, D.D., Gray, C.A., 2006. Utility of morphological data for key fish species in southeastern Australian beach-seine and otter-trawl fisheries: Predicting mesh size and configuration. N.Z. J. Mar. Freshwater Res., 40, 259-272.

Cheng, Z., Einarsson, H.A., Bayse, S., Herrmann, B., Winger, P., 2019. Comparing size selectivity of traditional and knotless diamond-mesh codends in the Iceland redfish (*Sebastes* spp.) fishery. Fish. Res., 216, 138-144.

Evans, J. D., 1996. Straightforward statistics for the behavioral science, Pacific Grove, CA: Brooks/Cole Publishing

Ferro, R.S.T., O’Neill, F.G., 1994. An overview of the characteristics of twines and netting that may change codend selectivity. ICES C.M. 1994/B: 35.

Ferreira, T., Rasband, W., 2012. ImageJ User Guide. IJ1.46r. Natl. Inst. Health, Bethesda, MD. http://rsb.info.nih.gov/ij/docs/guide/user-guide.pdf

Fonteyne, R. ed., 2005. Protocol for the use of an objective mesh gauge for scientific purposes. ICES Coop. Res. Rep., No. 279, 10p.

Grimaldo, E., Larsen, R.B., Sistiaga, M., Madsen, N., Breen, M., 2009. Selectivity and escape percentages during three phases of the towing process for codends fitted with different selection systems. Fish. Res., 95, 198–205.

Hansen, U.J., 2004. Performance of a trawl codend made from 90° turned netting (T90) compared with that of traditional codends. ICES-FAO Working Group on Fishing Technology and Fish Behaviour (WGFTFB), Gdynia, Poland. April 20–23, 2004. Conference Paper, 17p.

He, P., 2007. Selectivity of large mesh trawl codends in the Gulf of Maine I: Comparison of square and diamond mesh. Fish. Res., 83, 44-59.

He, P., 2010. Behavior of marine fishes: capture processes and conservation challenges. Wiley-Blackwell, Ames, USA. 375p.

Herrmann, B., Krag, L.A., Frandsen, R.P., Madsen, N., Lundgren, B., Stæhr, K.J., 2009. Prediction of selectivity from morphological conditions: methodology and a case study on cod (*Gadus morhua*). Fish. Res., 97, 59-71.

Herrmann, B., Priour, D. and Krag, L.A., 2007. Simulation-based study of the combined effect on cod-end size selection of turning meshes by 90 and reducing the number of meshes in the circumference for round fish. Fish. Res., 84, 222-232.

Herrmann, B., Sistiaga, M., Nielsen, K.N., Larsen, R.B., 2012. Understanding the size selectivity of redfish (*Sebastes spp.*) in North Atlantic trawl codends. J. Northwest Atl. Fish. Sci., 44, 1–13.

ICES, 2011, Report of the study group on turned 90º codend selectivity, focusing on Baltic cod selectivity (SGTCOD). ICES CM 2011/SSGESST:08.

Krag, L.A., Herrmann, B., Iversen, S.A., Engås, A., Nordrum, S., Krafft, B.A., 2014. Size selection of Antarctic krill (*Euphausia superba*) in trawls. PloS One, 9, p.e102168.

Madsen, N., Hansen, K.E., Moth-Poulsen, T., 2001. The kite-cover: a new concept for covered codend selectivity studies. Fish Res., 49, 219-226.

Main, J., Sangster, G.I., 1983. TUV II: a towed wet submersible for use in fishing gear research. Scott. Fish. Res. Rep., No. 29, 19p.

Moderhak, W., 1993. Some problems of water flow through trawl codend. ICES CM 19931B:11.

O'Neill, F.G., 1997. Differential equations governing the geometry of a diamond mesh cod-end of a trawl net. J. Appl. Mech. Mar., 64, 7-14

O'Neill, F.G., Knudsen, L.H., Wileman, D.A., McKay, S.J., 2005. Cod-end drag as a function of catch size and towing speed. Fish. Res., 72, 163-171.

Pichot, G., Germain, G., Priour, D., 2009. On the experimental study of the flow around a fishing net. Eur. J. of Mech-B/Fluid, 28, 103-116.

Pol, M.V., Herrmann, B., Rillahan, C., He, P., 2016. Impact of codend mesh sizes on selectivity and retention of Acadian redfish *Sebastes fasciatus* in the Gulf of Maine trawl fishery. Fish. Res., 184, 54-63.

Sistiaga, M., Herrmann, B., Nielsen, K.N., Larsen, R., 2011. Understanding limits to cod and haddock separation using size selectivity in a multispecies trawl fishery: an application of FISHSELECT. Can. J. Fish. Aquat. Sci., 68, 927-940.

Stergiou, K.I., Karpouzi, V.S., 2003. Length-girth relationships for several marine fishes. Fish. Res., 60, 161-168.

Tosunoğlu, Z., Özbilgin, Y.D., Özbilgin, H., 2003. Body shape and trawl cod end selectivity for nine commercial fish species. J. Mar. Biol. Assoc. UK, 83, 1309-1313.

Wakeford, J., 2004. An investigation into the influence of the Super-shooted TED and several types of bycatch reduction devices on water flow through a prawn trawl codend. *In*: Assessment and improvement of TEDs and BRDs in the NPF: a co-operative approach be fishers, scientists, fisheries technologists, economists and conservationists. Brewer, D. T., Heales, D. S., Eayrs, S. J., Taylor, B. R., Day, G., Sen, S., et al. (eds). Final Report on FRDC Project 2000/173. CSIRO Cleveland. 412p.

Wienbeck, H., Herrmann, B., Moderhak, W., Stepputtis, D., 2011. Effect of netting direction and number of meshes around on size selection in the codend for Baltic cod (*Gadus morhua*). Fish. Res., 109, 80-88.

Wileman, D.A., Ferro., R.S.T., Fonteyne, R., Millar, R.B., 1996. Manual of methods of measuring the selectivity of towed fishing gears. ICES Coop. Research Rep., No. 215, 126p.

Winger, P.D., DeLouche, H., Legge, G., 2006. Designing and testing new fishing gears: the value of a flume tank. Mar. Technol. Soc. J., 40, 44-49.

Winger, P.D., Eayrs, S., Glass, C.W., 2010. Fish behaviour near bottom trawls. *In:* Behavior of Marine Fishes: Capture Processes and Conservation Challenges. Edited by P. He. Blackwell Publishing. pp. 67-103.

Table 5.1. Design parameters of the four experimental codends and their extensions. Numbers in brackets represent standard deviation.

Net		Nominal mesh size (mm)	Twine	Length (meshes)	Circumference (meshes)	Measured mesh size (mm)
Codend						
	T0-90	90	Magnet Yellow 2x4.6 mm	99.5	116	95.0 (2.4)
	T90-90	90	Magnet Yellow 2x4.6 mm	120	76	93.6 (2.5)
	T90-100	100	Magnet Yellow 2x4.6 mm	109	76	104.6 (2.9)
	T90-110	110	Magnet Yellow 2x4.6 mm	99	76	110.7 (2.1)
Extension						
	T0-90	110	Magnet Yellow 2x4.6 mm	72.5	96	112.3 (3.5)
	T90-90	110	Magnet Yellow 2x4.6 mm	91	79.5	110.0 (3.2)
	T90-100	110	Magnet Yellow 2x4.6 mm	91	85	114.2 (2.1)
	T90-110	110	Magnet Yellow 2x4.6 mm	91	87.9	112.0 (1.9)

Table 5.2. The results of the GLM model explaining the variability in flow velocity. Ts indicates towing speed, Mp for measurement point, Cd for codend type.

GLM

Variable	Coefficient	SE	t-Statistic	p-Value
Intercept	-0.19	0.026	-7.49	<0.001
Ts	0.51	0.012	43.46	<0.001
Mp	0.043	0.007	6.2	<0.001
Cd_T90-90	0.11	0.0094	12.2	<0.001
Cd_T90-100	0.12	0.0094	12.62	<0.001
Cd_T90-110	0.10	0.0094	11.11	<0.001
Mp^2	-0.0049	0.00057	-8.61	<0.001

Number of observations: 180

Error degrees of freedom: 173

Root Mean Squared Error: 0.045

R-squared: 0.931, Adjusted R-Squared: 0.928

F-statistic vs. constant model: 388, p-value <0.001

Table 5.3. The results of the GLM model explaining the variability in mesh circularity. Ts indicates towing speed, Mp for measurement point, Cd for codend type.

GLM

Variable	Coefficient	SE	t-Statistic	p-Value
Intercept	0.499	0.022	22.45	<0.001
Ts	-0.063	0.014	-4.65	<0.001
Mp	0.007	0.001	5.23	<0.001
Cd_T90-90	0.417	0.011	37.85	<0.001
Cd_T90-100	0.426	0.011	38.82	<0.001
Cd_T90-110	0.383	0.011	34.93	<0.001

Number of observations: 194

Error degrees of freedom: 188

Root Mean Squared Error: 0.0533

R-squared: 0.917, Adjusted R-Squared 0.914

F-statistic vs. constant model: 413, p-value = <0.001

Table 5.4. The results of the GLM model explaining the variability in drag. Ts indicates towing speed, Cd for codend type.

GLM

Variable	Coefficient	SE	t-Statistic	p-Value
Intercept	-123.67	11.5	-10.75	<0.001
Ts	131.38	7.62	17.25	<0.001
Cd_T90-90	46.6	6.09	7.65	<0.001
Cd_T90-100	54.82	6.09	9.00	<0.001
Cd_T90-110	48.83	6.09	8.01	<0.001

Number of observations: 20

Error degrees of freedom: 15

Root Mean Squared Error: 9.63

R-squared: 0.964, Adjusted R-Squared: 0.954

F-statistic vs. constant model: 100, p-value <0.001

Table 5.5. The results of the GLM model for explaining the variability in flow velocity around each codend with cover net. Ts indicates towing speed, Ma_B for measurement area between the cover and the codend.

GLM -T0-90

Variable	Coefficient	SE	t-Statistic	p-Value
Intercept	-0.213	0.246	-0.865	0.451
Ts	0.496	0.152	3.264	0.047
Ma_B	-0.025	0.050	-0.501	0.651

Number of observations: 6
Error degrees of freedom: 3
Root Mean Squared Error: 0.0608
R-squared: 0.784, Adjusted R-Squared: 0.64
F-statistic vs. constant model: 5.45, p-value = 0.1

GLM-T90-90

Variable	Coefficient	SE	t-Statistic	p-Value
Intercept	0.095	0.073	1.303	0.284
Ts	0.367	0.045	8.159	0.004
Ma_B	-0.245	0.015	-16.679	<0.001

Number of observations: 6
Error degrees of freedom: 3
Root Mean Squared Error: 0.018
R-squared: 0.991, Adjusted R-Squared: 0.986
F-statistic vs. constant model: 172, p-value <0.001

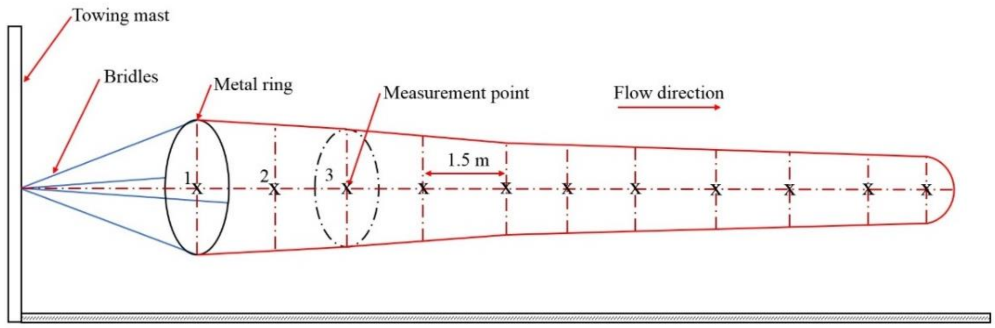

Figure 5.1. Experimental setup of the flume tank test. Solid orange line represents the net profile (not to scale); black cross indicates the meansurement point through the centre of the net; numbers above green cross represent the measurement point from the front to the end of the net.

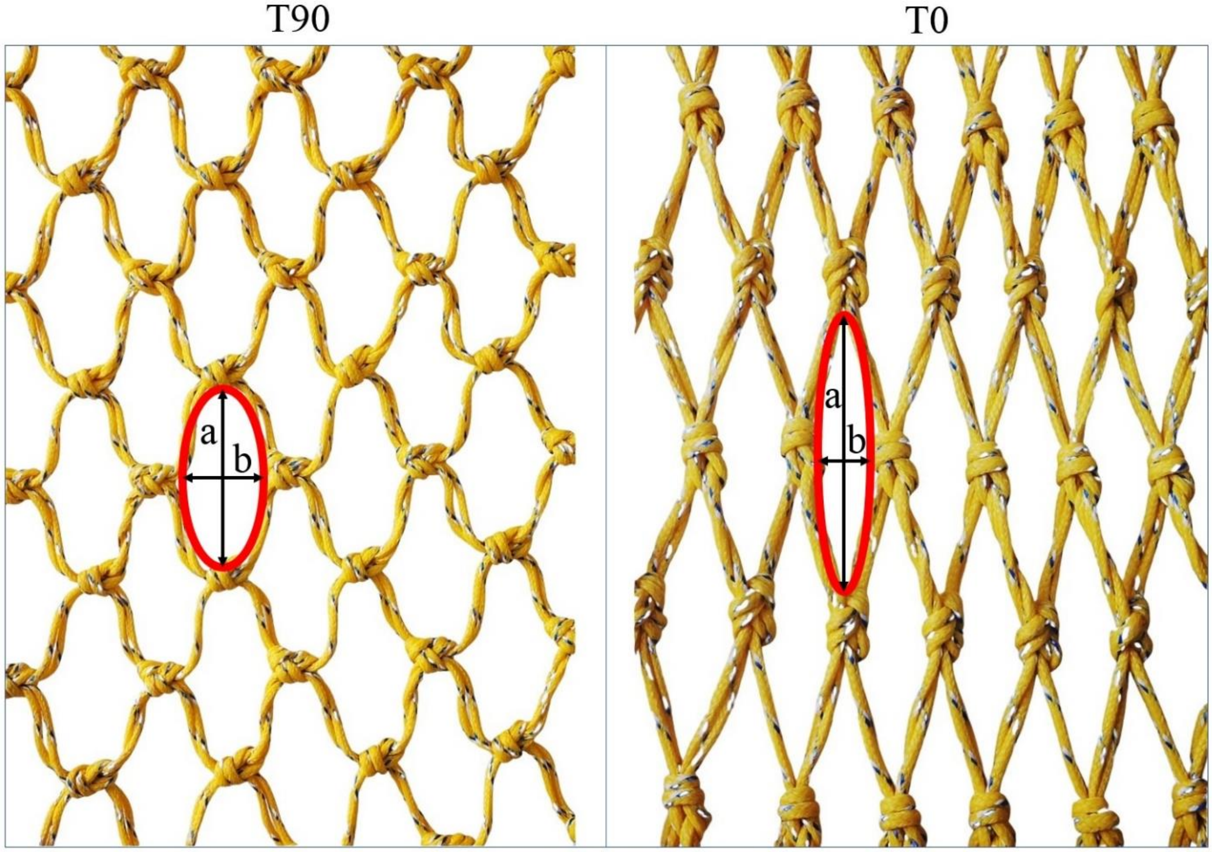

Figure 5.2. Mesh shape fitted with an ellipse. The letter a indicates the length of major axis of the fitted ellipse; b the minor axis.

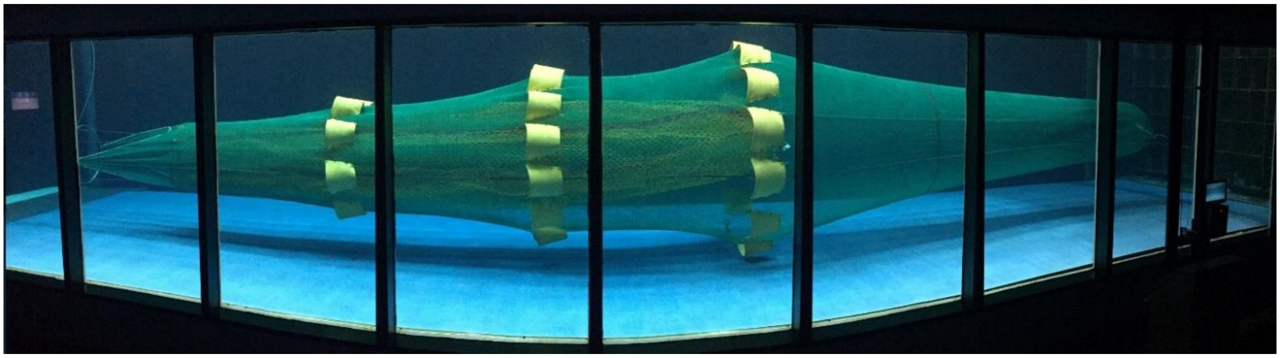

Figure 5.3. Codend with cover shown in the flume tank, St. John's, NL, Canada.

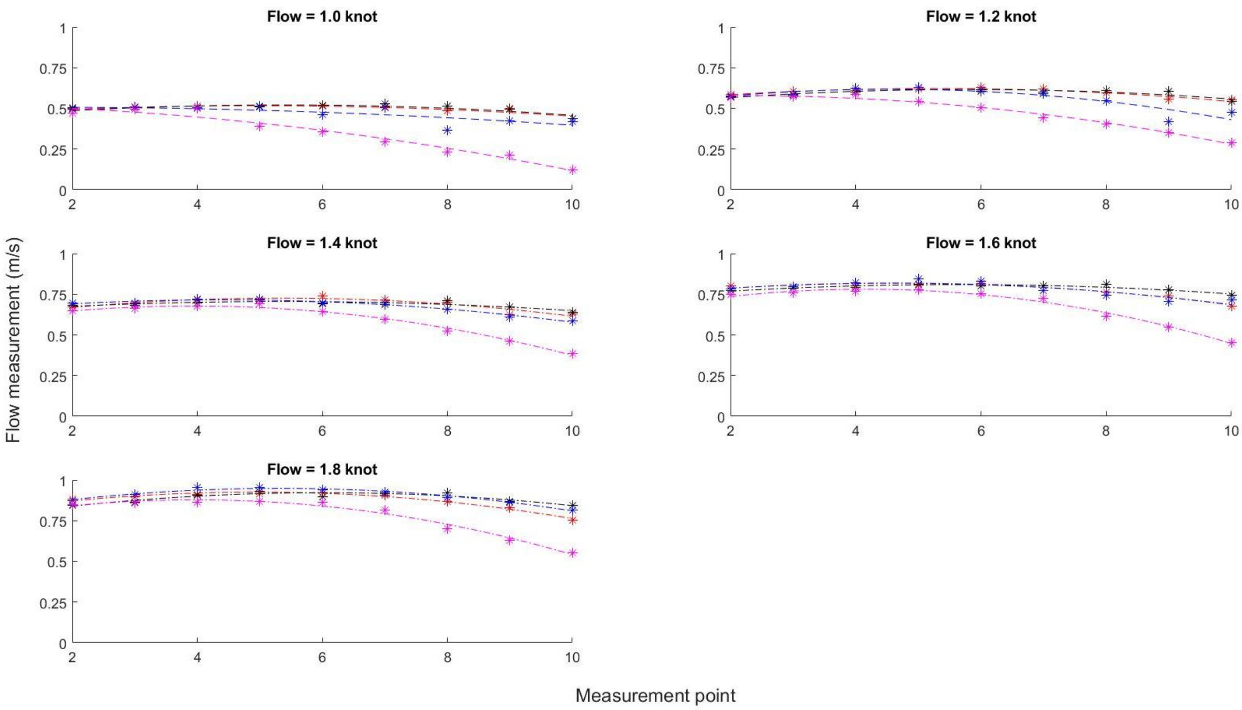

Figure 5.4. The flow velocity through the centre of each codend, where the dashed line is the model and the stars are the recorded values. Magenta represents the T0 (90 mm) codend, red T90 (90 mm), black T90 (100 mm), and blue T90 (110 mm).

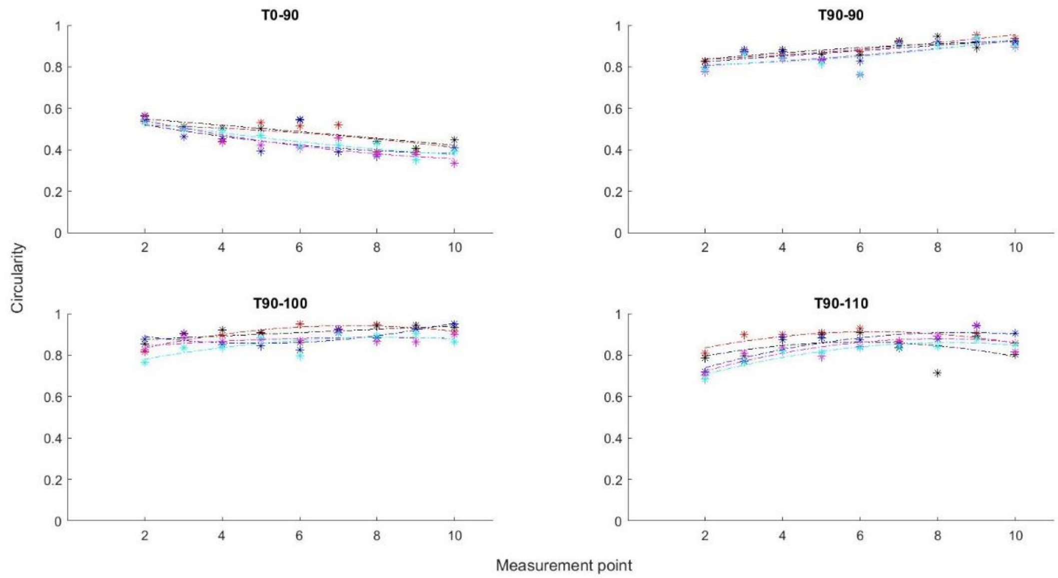

Figure 5.5. Mesh circularity from the begining to terminal end of each codend, where the dashed line is the model and the star is the mean. The colour indicates the towing speed: red is 1.0 knot, black 1.2, blue 1.4, magenta 1.6, and cyan 1.8 knot.

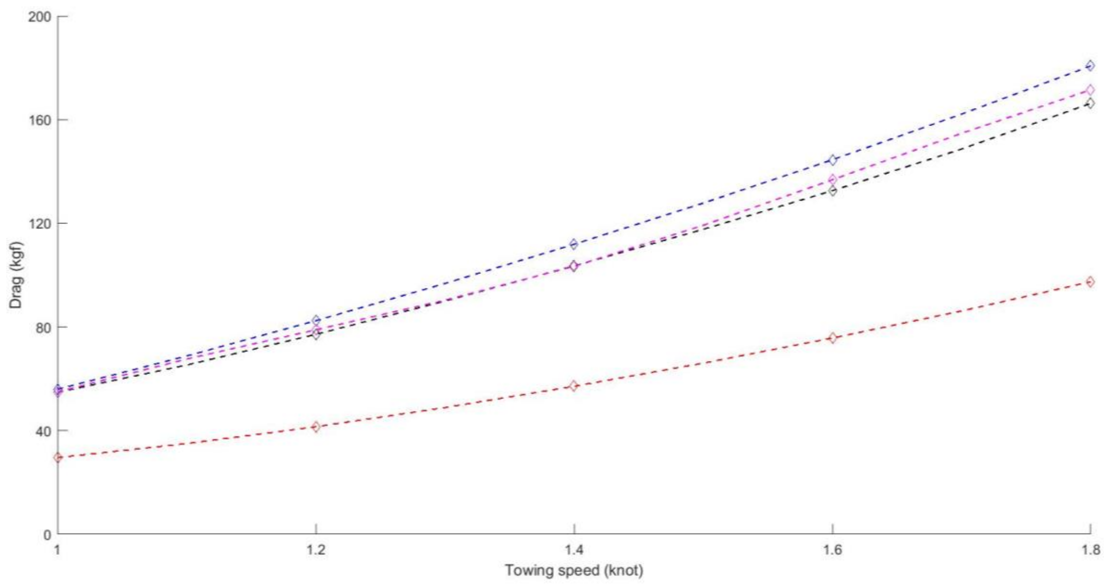

Figure 5.6. Total drag of each codend with simulated catch. The diamond points show the mean value of measured drag; dashed line indicates the fitted model under different towing speeds. The colour indicates the codend type: red is T0 codend, black T90 (90 mm), blue T90 (100 mm), and magenta T90 (110 mm) codend.

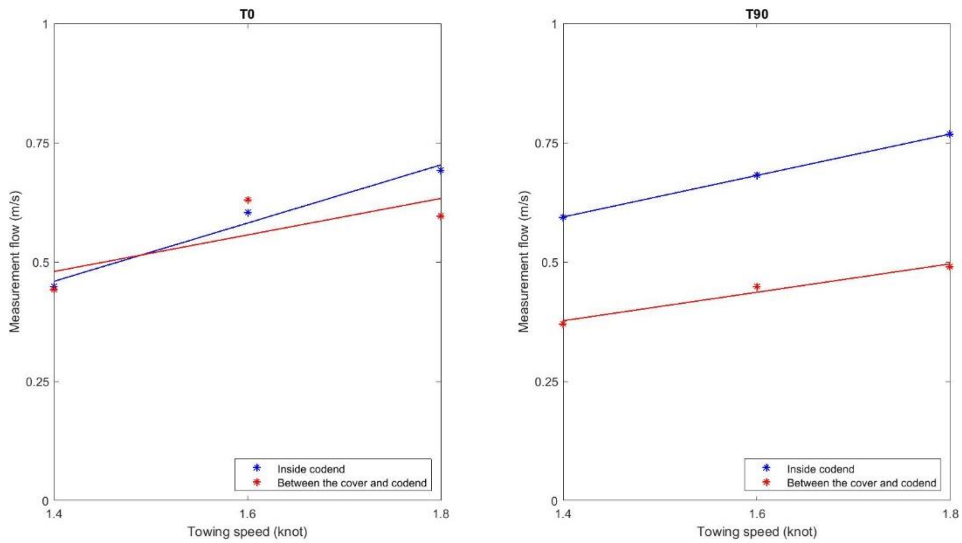

Figure 5.7. The flow velocity around each codend with cover net attached, where the blue star represents the measured flow inside each codend, and the red star represents the measured flow between the cover and codend. Solid lines represent the fitted linear regression curve.

CHAPTER 6. Summary and Recommendations

6.1 Overview of Thesis

In this thesis I have investigated various modifications to the codends of bottom trawls with the aim of improving the size selectivity of northern shrimp and redfish fisheries in the North Atlantic. Chapter 1 outlined the background to the target species and fisheries. In Chapter 2, the size selectivity of traditional T0 and experimental codends (T45 and T90) were investigated and compared using data from coastal shrimp fisheries in Iceland. Then, the size selection properties of a traditional (knotted) codend and experimental (knotless) codend were investigated through sea trials in an Icelandic redfish fishery (Chapter 3). In Chapter 4, the size selectivity of T0 and T90 codends with different mesh sizes were investigated in eastern Canada. In Chapter 5 I examined and compared the hydrodynamic performance of codends used in Chapter 4 with flume tank testing. Finally, Chapter 6 of this thesis summarizes the studies, discusses the research limitations and provides recommendations for further research.

6.2 Major Findings and Significance

The experiments conducted in this thesis have made contributions to research on reducing bycatch and improving size selectivity in northern shrimp and redfish fisheries, as well as to the provision of some directions for future research. Firstly, my results demonstrate that the T90 and T45 codends tested in Chapter 2 are more effective than the T0 codend at reducing the catch of undersized northern shrimp within certain length ranges. The study provides potential solutions (using T90) to reducing the bycatch in Iceland northern shrimp fisheries. Since discarding of undersized shrimp is prohibited in Iceland, using the T90 codend would enable fishers to use their individual quotas (IQ's) more efficiently.

Secondly, although the knotless codends evaluated in Chapter 3 did not improve selectivity, reporting the findings is meaningful from both the scientific and the fishing industry viewpoint, because they enhance our understanding of fishing gear selectivity and reduce the risk of testing the same design concepts in the future. Moreover, the findings from Chapter 3 provide a useful contribution to the literature on size selectivity in redfish fisheries.

The findings from Chapter 4 clearly demonstrate that the traditional (regulated) codend currently used by Canada's east coast fishing industry (Unit 1) has a poor size selectivity. My results showed that it captured greater than 97% of redfish over all of the length classes observed. My results also reveal that T90 codends can improve size selectivity in which large proportions of undersized fish can be successfully released, reducing unintended fishing mortality of juvenile redfish. This study contributes to the development of selective redfish fishing gears and, where applicable, future policies on the management of redfish fisheries in Canada.

Finally, the differences in selectivity between T0 and T90 codends described in Chapter 4 can be explained in part by their difference in hydrodynamic performance. In Chapter 5, I investigated their hydrodynamic performance through controlled laboratory testing in a flume tank. The T90 codends exhibited high flow velocities inside the codend and better mesh opening than the T0 codend at the rear end of the codend. Although some researchers have conducted simulation work in relation to the net performance (e.g., Priour, 2001; Herrmann and O'Neill, 2006; Herrmann et al., 2009), testing the full-scale nets and comparing the results, particularly with T90 codends, in highly novel. As a result, the findings should enhance our knowledge of the hydrodynamic performance of T0 and T90 codends and are significant for understanding the mechanism affecting codend selectivity. Using the flume tank in this manner significantly increases the originality of my research and thesis.

6.3 Limitations of My Approach

The covered codend method (Wileman et al., 1996) was used to estimate codend size selectivity in all sea trials described in Chapter 2, 3, and 4. Although using the cover is a common approach to studying selectivity (e.g., Wileman et al., 1996; Madsen et al., 2001; He, 2007), the effects of a cover on a codend and therefore its selectivity are not well understood. The estimated selectivity properties of each tested codend may be biased if the cover net has a masking effect on the codend. Furthermore, the mesh size of the cover is generally smaller than the codend but not small enough to retain all the escaped individuals from the codend. The number of small individuals is therefore limited, which affects the reliability of the selectivity curve at smaller animal sizes (left side of the curve). The CIs of the selectivity curves are wide for small individuals with few numbers; the accuracy of the selectivity curves within these length ranges is uncertain in Chapter 2. A similar situation occurred in Chapters 3 and 4: the number of redfish retained in the cover net is low for individuals smaller than 13 cm. The codend selectivity is also uncertain for fish within these ranges (Chapters 3 and 4). Another possible reason for the lack of small individuals retained in the cover is the fished population structure. However, either the population structure or the cover net may account for the uncertainty of the estimated selectivity.

Codend selectivity described in Chapter 4 is based on a limited number of sea trials, fishing areas, and towing times. Although forty-five hauls were carried out in different fishing locations, the sampled area accounted for a small part of fishing grounds in the Gulf of St. Lawrence. The usability indicators which depend on the fished population may be biased if a high degree of spatial variability exists in population size structure. The resulting usability interpretations may be different if additional fishing areas are included. Finally, the long-term effects of codend modifications on size selectivity are unknown, even though the findings demonstrate that the changes to the nets are effective at reducing the undersized bycatch (Chapters 2 and 4). Application of these findings to commercial fishing practices and related management policies should be done with caution. The assessment and prediction of the impacts of these codend modifications to the selectivity require long-term and practical fishing and biological data.

The premise of size selective fishing, whether for shrimp or redfish, is based on the simple conservation objective of minimizing fishing mortality on non-targeted (undersized) animals. By escaping from the bottom trawl, these juvenile fish are able to grow and contribute to the productivity of the stock. Maximizing the potential for survival of these escaping individuals is important for fulfilling this purpose (Chopin et al., 1996; Heino and Godø, 2002; Condie et al., 2014). If the mortality of escaped northern shrimp or redfish is proportionately lower for the experimental codends than the traditional codends, then the use of these designs (see Chapters 2, 3, and 4) to improve codend selectivity will indeed produce long-term benefits. However, if the escaped individuals suffer proportionately higher mortality, then the conservation objective will not be met and the benefits not realized. This brings me to the next limitation of this thesis – due to limited time and funding, I did not conduct survival experiments on the escaping animals. I assume their survival is comparable to the traditional codends, but was unable to verify under the current scope of this thesis.

Finally, the controlled laboratory conditions used in the flume tank (Chapter 5) are admittedly biased and do not completely simulate real-world fishing conditions. The simulated catch placed in the codend was much smaller than a typical catch size observed at sea. Measurements of codend drag were therefore smaller than the actual values expected at sea, and are supposed to increase as the catch accumulates in the codend (O'Neill et al., 2005). The mesh opening and net geometry may also differ if the drag and resulting twine tensions change (O'Neill et al., 2005). Maximum towing speed simulated in the flume tank (1.8 kt) was also lower than typical towing speeds for redfish at sea (2.5 kt). Taken together, these two biases (catch size and towing speed) may explain differences between what I observed in the flume tank and what could be expected at sea. Therefore, the results of this chapter must be interpreted comparatively and may not be a good indicator of at-sea fishing performance.

6.4 Recommendations for Further Research

Despite the limitations discussed above, the research conducted in this thesis has suggested some useful results and conclusions that could be employed to understand and improve codend size selectivity. However, it has also identified several areas in which further research would be beneficial for improving size selectivity and for achieving sustainable development of northern shrimp and redfish fisheries in the North Atlantic.

The areas of further research are suggested as following:

1. Investigate the effects of a cover net on codend performance including flow, mesh opening, net shape etc. as well as the resulting selectivity of the codend. This task is important since the covered codend method (Wileman et al., 1996) was applied in all of the sea trials conducted in this thesis. Somewhat surprising, very little is known about the effect of covers on codend performance, despite their widespread use in selectivity experiments. I propose flume tank testing, mathematical simulation, and field observations as fruitful pathways for understanding the effects of cover nets.
2. Repeat the experiments in Chapters 3 and 4 to increase replicates and to test the nets on additional fishing grounds. Increasing the sampling ratio and towing stations would help improve the reliability of the estimated selectivity curves. Also, repeating the sea trials on different fishing grounds would increase the generality of the findings, especially the usability indicators.

3. Evaluate the codends used in Chapter 4 under real-world commercial fishing conditions. I propose collaborating with fishers to test the codends with longer tow durations than those used in this thesis. For example, up to 1 or 2 hours in tow duration. Testing the codends in this manner may provide insights into any practical challenges not foreseen or encountered during this thesis. Also, as individuals in fishery grow in size, fewer legal sized will escape the T90 codend.
4. Conduct additional field work using the T90 codends in Chapter 4 to better understand the 'meshed fish' phenomenon. Although there were generally few fish stuck (or meshed) in the codend during my sea trials, meshed redfish has been reported as a problem in trawl fisheries (Isaksen and Valdemarsen, 1986; ICES 2012). These meshed fish block available meshes, decreasing escape rates and affect codend selectivity (Pol et al., 2016; Brčić et al., 2019). This problem should be further investigated to determine whether it is size-dependent.
5. Conduct video observations of northern shrimp and redfish escaping through codend meshes. This has been shown to be useful in documenting, especially for redfish, the depth at which fish choose to escape the codend (Pol, 2017). Preliminary evidence suggests that redfish may delay escaping until haul-back, which could negatively affect survival. Building on the work of Pol (2017) with camera observations in the Canadian fishery would be beneficial.
6. Evaluate the survival rate of escaped northern shrimp and redfish from the codend. Selective fishing gears should be used not only to reduce the bycatch but maximize the survival rate of escapees. The escaped individuals, especially the juvenile, contribute to the fish stocks if they survive the capture and escape

process (DeAlteris and Reifsteck, 1993; Ordines et al., 2006). Investigating the survival rate is therefore significant for the sustainable development of the fishery.

7. Development of species selective technologies that could catch different species of redfish. Since *S. mentella* and *S. fasciatus* have similar morphological characteristics, it is difficult to imagine sorting them mechanically with grids/grates. However, behavioural reactions within a trawl are known to vary across species (Winger et al., 2010), opening an interesting avenue for future research. The use of underwater cameras inside the trawl, for example, could potentially reveal species-specific differences in behaviour that could be used to help separate the species.
8. Expand the experiment in Chapter 5 to evaluate the hydrodynamic performance of full-scale codends under similar conditions with the field work (Chapter 4). Assuming relevant modifications to the flume tank were possible, it would be beneficial to increase the experiment towing speed to the one used in commercial fishing, as well as match the simulated catch size with the actual fishing catch. This would address some of the limitations of my approach (see section 6.3).
9. Expand the experiment in Chapter 5 to collect additional parameters to those collected in my thesis (i.e., water flow, mesh opening, and drag). For example, documenting the dynamic behaviour (Druault and Germain, 2016) of the codends at different towing speeds could be useful. These results could be compared to mathematical simulations and at-sea underwater camera observations.
10. The hydrodynamic performance of T0 and T90 codends in Chapter 5 are compared using a flume tank. Further research might compare the results with

codends made of T45 netting. Testing the T45 codend described in Chapter 2 would be beneficial for explaining the selectivity difference among the codends with different mesh orientation.

11. Conduct an in-depth exploration of the flow field within codends, especially T45 and T90 codends for which there is no published literature. Further research might use Particle Image Velocimetry techniques (e.g., Pichot et al., 2009) to accurately characterize the three-dimensional flow profile. These findings could help fishing gear designers/engineers better understand the mechanisms behind codend selectivity.
12. A final but important question is how other parts of a bottom trawl affect the hydrodynamic performance of the fishing system and the resultant selectivity. Although the codend is the research focus in Chapter 5, other parts of a bottom trawl may also affect its hydrodynamic performance (Ferro and O'Neil, 1994). Further research might test the effects of bridles, otter boards, net wing, net belly, etc. on the performance.

6.5 Conclusion

This thesis has investigated the size selectivity of several codend designs (knotless netting, T0, T45 and T90) for northern shrimp and redfish fisheries in North Atlantic waters as well as the hydrodynamic performance of the codends (T0 and T90) using a flume tank. Many of the methods are novel and provide a foundation for future selectivity and engineering research. The results are informative and may help industry improve sustainable fishing practices and management bodies introduce effective technical measures to achieve conservation objectives. However, the results are not just locally relevant. Given the widespread distribution of northern shrimp and redfish in the North Atlantic, this thesis also offers significant contributions to other regions, including Russia, Denmark, USA, Greenland, Iceland, Norway, etc.

In summary, the findings from this thesis confirm the importance of codend design on the size selectivity of bottom trawls. Changes in mesh size and mesh orientation in particular, were shown to significantly affect the size selectivity of northern shrimp (Iceland) and redfish (Iceland and Canada). These results could prove helpful in the pursuit of sustainable fisheries, whereby smaller undesirable or non-targeted animals can be released from codends during towing operations, preventing their unnecessary capture and mortality.

6.6 References

Brčić, J., Herrmann, B., Masanovic, M., Krstulovic Sifner, S., Baranovic, M., Škeljo, F. 2019. Mesh sticking probability in fishing gear selectivity: Methodology and case study on Norway lobster (*Nephrops norvegicus*) and mantis shrimp (*Squilla mantis*) in the Mediterranean Sea creel fishery. Mediterr. Mar. Sci., 20, 487–495.

Chopin, F., Inoue, Y., Arimoto, T., 1996. Development of a catch mortality model. Fish Res., 25, 377-382.

Condie, H.M., Grant, A., Catchpole, T.L., 2014. Incentivising selective fishing under a policy to ban discards; lessons from European and global fisheries. Mar. Policy, 45, 287-292

DeAlteris, J.T., Reifsteck, D.M., 1993. Escapement and survival of fish from the codend of a demersal trawl. ICES Mar. Sci. Symp., 196, 128-131.

Druault, P., Germain, G., 2016. Analysis of hydrodynamics of a moving trawl codend and its fluttering motions in flume tank. Eur. J. Mech.-B/Fluid., 60, 219-229.

Ferro, R.S.T., O'Neill, F.G., 1994. An overview of the characteristics of twines and netting that may change codend selectivity. ICES C.M. 1994/35p.

Heino, M., Godø, O.R., 2002. Fisheries-induced selection pressures in the context of sustainable fisheries. Bull. Mar. Sci., 70, 639-656.

He, P., 2007. Selectivity of large mesh trawl codends in the Gulf of Maine I: Comparison of square and diamond mesh. Fish. Res., 83, 44-59.

He, P., 2010. Behavior of marine fishes: capture processes and conservation challenges. Wiley-Blackwell, Ames, USA. 375p.

Herrmann, B., Krag, L.A., Frandsen, R.P., Madsen, N., Lundgren, B., Stæhr, K.J., 2009. Prediction of selectivity from morphological conditions: methodology and a case study on cod (*Gadus morhua*). Fish. Res., 97, 59-71.

Herrmann, B., O'Neill, F.G., 2006. Theoretical study of the influence of twine thickness on haddock selectivity in diamond mesh cod-ends. Fish. Res., 80, 221-229.

ICES, 2012. Report of the ICES-FAO Working Group on Fishing Technology and Fish Behaviour (WGFTFB). ICES C.M. SSGESST:07, 214p.

Isaksen, B., Valdemarsen, J.W., 1986. Selectivity experiments with square mesh codends in bottom trawl. ICES C.M. 1986/B:28.

Madsen, N., Hansen, K.E., Moth-Poulsen, T., 2001. The kite-cover: a new concept for covered codend selectivity studies. Fish Res., 49, 219-226.

Ordines, F., Massutí, E., Guijarro, B., Mas, R., 2006. Diamond vs. square mesh codend in a multi-species trawl fishery of the western Mediterranean: effects on catch composition, yield, size selectivity and discards. Aquat. Living Resour., 19, 329-338

O'Neill, F.G., Knudsen, L.H., Wileman, D.A., McKay, S.J., 2005. Cod-end drag as a function of catch size and towing speed. Fish. Res., 72, 163-171.

Pichot, G., Germain, G., Priour, D., 2009. On the experimental study of the flow around a fishing net. Eur. J. Mech. B/Fluid., 28, 103-116.

Pol, M.V., Herrmann, B., Rillahan, C., He, P., 2016. Impact of codend mesh sizes on selectivity and retention of Acadian redfish *Sebastes fasciatus* in the Gulf of Maine trawl fishery. Fish. Res., 184, 54-63.

Pol, M.V., 2017. Establishing a sustainable Acadian redfish trawl fishery in the Gulf of Maine: a conservation engineering approach. PhD thesis, University of Massachusetts Dartmouth, Maine. 167p.

Priour, D., 2001. Introduction of mesh resistance to opening in a triangular element for calculation of nets by the finite element method. Commun. Numer. Meth., 17, 229-237

Wileman, D.A., Ferro., R.S.T., Fonteyne, R., Millar, R.B., 1996. Manual of methods of measuring the selectivity of towed fishing gears. ICES Coop. Res. Rep., No 215, 126p.

Winger, P.D., Eayrs, S., Glass, C.W., 2010. Fish behaviour near bottom trawls. *In:* Behavior of Marine Fishes: Capture Processes and Conservation Challenges. Edited by P. He. Blackwell Publishing. pp. 67-103.